AD-A093 754 RAND CORP SANTA MONICA CA F/G 7/4
AB INITIO CONFIGURATION INTERACTION CALCULATIONS ON THE STATES --ETC(U)
SEP 80 K A WOLF
UNCLASSIFIED RAND/P-6535 NL

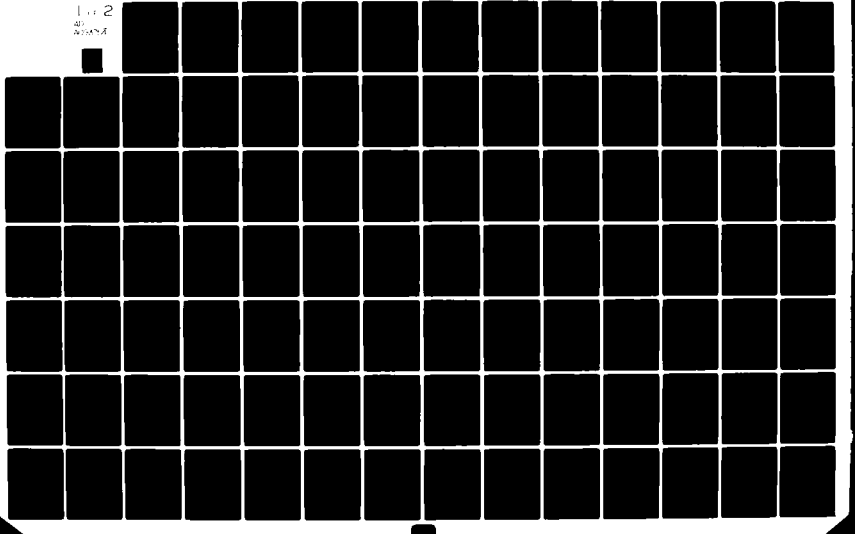

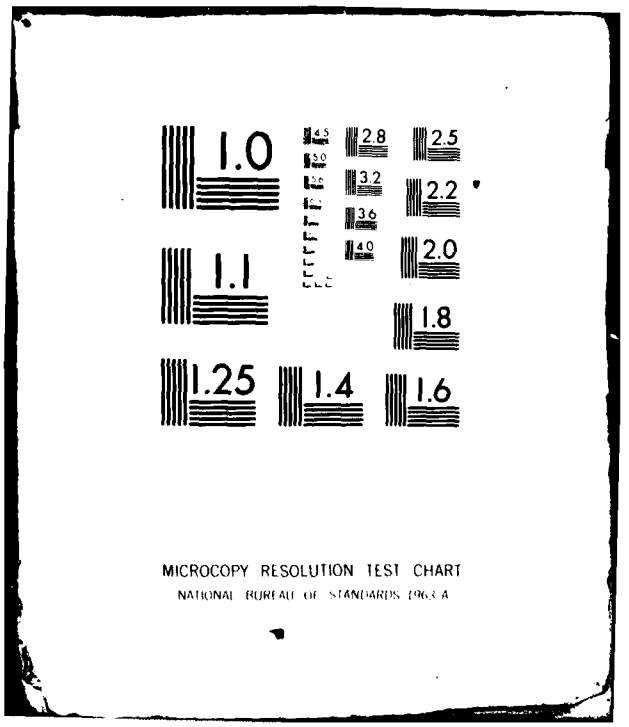
1.0
1.1
1.25
1.4
1.6
1.8
2.0
2.2
2.5
2.8
3.2
3.6
4.0
4.5
5.0
MICROCOPY RESOLUTION TEST CHART
NATIONAL BUREAU OF STANDARDS 1963 A

AB INITIO CONFIGURATION INTERACTION CALCULATIONS ON THE STATES OF HF^-

Kathleen A. Wolf

September 1980

P-6535

The Rand Corporation
Santa Monica, California 90406

AB INITIO CONFIGURATION INTERACTION CALCULATIONS ON THE STATES OF HF(-)

Kathleen A. Wolf

September 1980

P-6535

TABLE OF CONTENTS

LIST OF TABLES

LIST OF FIGURES

INTRODUCTION

The principles that form the basis of all quantum mechanics were first introduced in 1926 by Schroedinger.[1] Since that time these principles have been extended to become the framework of the theory used today. Although the simplicity of the theory cannot be questioned, practical implementation of the basic concepts has often proven difficult. For certain applications, including the hydrogen atom as well as other one electron systems, the Schroedinger Theory allows exact analytic solution. For larger systems, approximations are necessary.

The first approximation that is generally incorporated into the Schroedinger Theory is known as the Born Oppenheimer Approximation.[2] The use of this approximation allows the separation of electronic and nuclear motions. Further simplification can be achieved through a method for dealing with the electron-electron interaction potential. This approach was first suggested by Hartree,[3] and was subsequently extended by Fock[4] to include exchange effects. In molecular orbital theory, an electron orbital is replaced by a one-electron wave function delocalized over the whole molecule. This concept, together with the Pauli principle[5] and the work of Hartree and Fock allow the wavefunction to be expressed in a single Slater[6] determinant. In minimizing

the energy of the determinant through the Variation Principle, a set of integrodifferential equations called the Hartree-Fock equations are obtained. These equations must be solved iteratively, and the lowest energy single determinant wavefunction that can be constructed is known as the Self-Consistent Field (SCF) wavefunction. The Roothaan equations[7] provide the means of translating the integrodifferential equations into algebraic form. The approach allows application of the SCF method to molecules where linear combinations of atomic orbitals (LCAO) are assumed to represent the molecular orbitals.

The difference between the Hartree-Fock energy for a single determinant wave function and the true energy is known as the correlation energy. The magnitude of this energy can be quite large even for small molecules, and the technique most commonly used to calculate the correlation energy is Configuration Interaction (CI). This method involves expanding the electronic wavefunction to include a linear combination of all possible products of Slater determinants. CI is best described as the calculation of the optimum linear combination based on the variational approach of Ritz.[8] Although the CI technique can be used in principle for diverse chemical problems, in practice full solution of the CI problem is severely limited. Fortunately, it is possible to obtain relatively good accuracy by limiting the full problem

to a subset of the full determinental basis. Indeed a reasonable estimate of the significant corrections to the SCF basis is possible if the space includes only single and double excitations.[9]

Full solution of most problems at the double excitation level is still prohibitive, and techniques for further optimizing the choice of configurations must be utilized. The CI method used in this work is based on the fact that in any system, there will be a small number of configurations which dominate the final wavefunction. These configurations are identified and all other configurations are ranked according to their interaction with the small group of important configurations using Raleigh Schroedinger Perturbation Theory. The configurations that interact most strongly are treated exactly while the remaining configurations are treated as a perturbation. It is this technique of solving only a subset of the entire problem exactly that makes CI calculations on medium-sized molecules possible.

Chapter I of this work provides some detail on the historical development of Configuration Interaction. The specific method of CI used to obtain the results of the applications presented here is described in Chapter II.

In Chapter III, theoretical and experimental considerations central to the examination of compound states of polar molecules are discussed. Compound states are formed

when an incident electron interacts with a molecule. The electron is temporarily captured in the neighborhood of the molecules and the resulting complex is known as a negative ion or resonance state. In the lower energy region, polar molecules can form resonances that are largely dipole-supported. At somewhat higher energies, traditional valence-type resonances occur. At still higher energies, the incident electron occupies a Rydberg orbital of the neutral excited molecule, giving rise to a Feshbach state. In Chapter III, the general background information on the various types of compound states is presented. In addition, the theoretical basis for the actual binding of an electron by a polar molecule is considered.

In Chapter IV, the results of CI calculations on the lower energy (< 9 eV) negative ion states of HF^- are presented. We find that the lowest HF^- state lies below the ground state of HF at all internuclear distances and is therefore capable of binding an electron. Because the calculated binding energy is less than the error inherent within the method used in the calculations, it cannot be stated with certainty that there is a bound state of HF^-. The minimum dipole concept indicates that a stable negative ion state will be formed if the dipole moment of the neutral molecule exceeds 1.625 D. The HF molecule, with an experimental dipole moment of 1.82 D,

is thus expected to support a bound state. When nuclear considerations are taken into account, the minimum dipole moment for binding an electron is increased slightly. Our calculated dipole moment for HF is 2.01D, higher than the experimental value by a few tenths of a Debye. The fact that we find HF^- to be slightly bound is not unexpected, but is also not sufficient proof that the lowest HF^- state is truly bound.

The results of the calculated potential curves for four other HF^- states are also presented in Chapter IV. The lowest three of these states are formed by occupying a Rydberg orbital with the additional electron; the extra electron occupies a valence orbital in the fourth state. Since experimental evidence on these states of HF^- is virtually nonexistence, it is not clear whether or not they are resonances. Nevertheless, we present qualitative arguments that support the assignment of resonance character to all four states.

A detailed examination of the higher energy (9-14 eV) Feshbach states of HF^- is presented in Chapter V. We first discuss the results of CI calculations on the excited states of the neutral molecule, HF. The results of these calculations agree well with the available experimental data. We have performed CI calculations on the Feshbach states of HF^- which are formed by the attachment of an additional electron to the excited states

of the netural molecule. We find evidence of one attractive state with features that agree well with the experimental observations.

There is no doubt that the results of the studies presented in Chapters IV and V clearly illustrate the utility of the CI method for detailed examination of the compound states of polar molecules. The work is also significant for two further reasons. First, a good explanation of the observed experimental features of the HF^- negative ion states is provided. Second, the results predict certain unobserved experimental features and serve as a guide for both experimentalists and theoreticians for further investigation of HF^- in particular, and other polar molecules in general.

References

1. E. Schroedinger, Ann. Physik. 79, 361, 489, 734 (1926).
2. M. Born and J.R. Oppenheimer, Ann. Physik. 84, 457 (1927).
3. D.R. Hartree, Proc. Camb. Phil. Soc. 24, 89, 111 (1928).
4. V. Fock, Z. Physik. 61, 126 (1930) and 62, 795 (1930).
5. W. Pauli, Z. Physik. 43, 601 (1927).
6. J.C. Slater, Phys. Rev. 34, 1293 (1929).
7. C.C.J. Roothaan, Rev. Mod. Phys. 23, 69 (1951) and 32, 179 (1960).
8. W. Ritz, J. Reine Angew. Math. 135, 1 (1909).
9. A. Pipano and J. Shavitt,

CHAPTER I

HISTORICAL BACKGROUND

The solution of virtually all chemical problems involving atomic and molecular structure is based on the Schrodinger Equation:[1]

$$H\Psi = E\Psi \tag{1.1}$$

H, the Hamiltonian operator, represents the total energy of a system. It is specified by summing the contributions to the Kinetic Energy (T) and the Potential Energy (V). Solutions are obtained in the form of eigenvalues describing the energy of each state of the system. For molecules consisting only of the lighter atoms, spin-orbit coupling and relativistic effects can be reasonably neglected. With this in mind, the Kinetic and Potential Energy Operators in atomic units* can be expressed as

$$T = \sum_A -\frac{\nabla_A^2}{2M_A} + \sum_a -\frac{\nabla_a^2}{2} = T_N + T_E \tag{1.2}$$

$$V = \sum_{A>B} \frac{Z_A Z_B}{r_{AB}} + \sum_{Ab} -\frac{Z_A}{r_{Ab}} + \sum_{a>b} \frac{1}{r_{ab}} \tag{1.3}$$

$$= V_N + V_{EN} + V_{EE}$$

---

* In this system of units, $\hbar$, the mass of the electron, and the electronic charge are unity. The unit of length is the bohr (1 bohr = $.52918 \times 10^{-8}$ cm), while the unit of energy is the hartree (1 hartree = 27.205 eV).

where the Nuclear contributions are denoted as A, B and the electronic contributions by a, b. M_A is the mass of nucleus A, and Z_A is the charge of nucleus A. T_N and T_E represent the nuclear and electronic kinetic energy respectively. V_{NN} describes the repulsion between the nuclei, V_{EE} is the repulsion between electron pairs, and V_{EN} is the electrostatic attraction of all nuclei for all electrons.

The Hamiltonian operator can thus be written

$$H = T_N + T_E + V_{NN} + V_{EN} + V_{EE} \qquad (1.4)$$

Specifying the operator for a given system is straightforward. Solution of the eigenvalue problem of Equation (1.1) is more difficult, and has been accomplished exactly in only two instances, those of the hydrogen atom and the hydrogen molecule ion. For systems with more than one electron, adoption of the Born Oppenheimer Approximation[2] leads to a simplification of the problem. This approximation is based on the premise that the nuclei, having mass far greater than that of the electrons, move much more slowly than the electrons. Thus, at any instant, the motion of the electrons is the same as if the nuclei were in a fixed position in space. When the nuclei are in fixed positions, $T_N = 0$, V_{NN} = constant, and the Hamiltonian can be written

$$H_E = T_E + V_{EN} + V_E + V_{NN} \qquad (1.5)$$

where H_E now represents the electronic Hamiltonian.

Equation (1.5), in which the kinetic energy of the nuclei has been set equal to zero, is the electronic Hamiltonian. It can be solved for any fixed geometry of the nuclei, and when solutions are obtained for a range of nuclear coordinates, a potential surface is defined. The energy eigenvalues for each point on the potential surface can then be used for solution of the nuclear wave functions and the total energy.

For the remainder of this work, we will devote our attention to the solution of equation (1.5). Although nuclear motion has indeed been found to play an insignificant part in some chemical problems, it is more important in certain others. In the binding of electrons to polar molecules, for example, it has been found that including consideration of vibration does not alter the conclusions on stability of negative ions.[3] In contrast, the conditions for binding an electron are altered slightly when rotation is taken into account.[4]

The Born Oppenheimer Approximation considerably simplifies the Schroedinger Equation. Nevertheless, it is still too complex to allow complete solution of most practical problems, and further approximation is necessary. Over the years, Molecular Orbital Theory has emerged as the most useful approximation for understanding most molecular systems.

The Variation Principle[5] states that if Ψ is any well behaved function that satisfies the boundary conditions of a problem, then

$$\int \Psi^* H_E \Psi d\tau \geq E_o \qquad (1.6)$$

where E_o is the true value of the lowest energy eigenvalue of H_E. The "best" set of Ψ's for solving equation (1.6) is that which provides the lowest energy. The true energy can only be obtained by using the exact wavefunction, Ψ, which would require an infinite set of functions. In practice, it has been found that linear combinations of atomic orbitals (LCAO) centered on each atom form a reasonable approximation to the true wavefunction in molecules. These one-electron functions are known as Molecular Orbitals (MO's).

The simplest approximate wave function for an N-electron system is the product of N one-electron basis functions first introduced by Hartree.[6]

$$\Psi(1...N) = \phi_1(1)\phi_2(2)...\phi_N(N) \qquad (1.7)$$

The $\phi(N)$ are products of a space component and a spin component, α or β.[7] The additional requirement that the product wave functions must be antisymmetric to the exchange of any pair of electrons leads to the expression of the wavefunction in the form of a Slater determinant.[8]

$$\Psi = \frac{1}{\sqrt{N!}} \begin{vmatrix} \phi_1(1)\phi_1(2).....\phi_1(N) \\ \phi_2(1)\phi_2(2).....\phi_2(N) \\ \vdots \quad\quad \vdots \quad\quad \vdots \\ \phi_N(1)\phi_N(2).....\phi_N(N) \end{vmatrix} \qquad (1.8)$$

This wave function, called the Hartree-Fock wave function, is the "best" function that can be constructed by assigning each electron to a separate orbital.

In minimizing the energy of equation (1.6), a set of integrodifferential equations called the Hartree-Fock equations are derived. The true Hamiltonian and wave function involve the coordinates of all N electrons, while the Hartree-Fock Hamiltonian is a one electron operator. The Hartree-Fock equations are

$$H^{eff}(1)\phi_p(1) = \varepsilon_p\phi_p(1) \qquad (1.9)$$

where ε_p is the orbital energy. The Hartree-Fock Hamiltonian can be written

$$H^{eff} = -\sum_a \frac{\nabla_a^2}{2} - \sum_{Aa} \frac{Z_A}{r_{Aa}} + \sum_i J_i - \sum_i K_i \qquad (1.10)$$

The first term is the operator for the kinetic energy of each electron; the second term is the potential energy operator for the attraction between each electron and the nuclei. The Coulomb operator, J_i, is the operator representing the electrostatic repulsion between each

electron and all other electrons. It has the form

$$J_i\phi_j = \phi_j \int \phi_i^* \frac{1}{r_{ab}} \phi_i d\tau \qquad (1.11)$$

The fourth term, K_i, known as the Exchange Operator, has no simple physical interpretation, but arises from the requirement of antisymmetry of electrons to exchange. It can be written

$$K_i\phi_j = \phi_i \int \phi_i^* \frac{1}{r_{ab}} \phi_j d\tau \qquad (1.12)$$

The Hartree-Fock equations must be solved iteratively. Generally, an initial guess provides a set of initial wave functions, which in turn lead to an improved potential. This improved potential is then used to obtain improved wave functions. The process is repeated until the energy reaches a reasonable stability. The Hartree-Fock energy is

$$E_{HF} = 2 \sum_i \varepsilon_i - \sum_i \sum_j (2 J_{ij} - K_{ij}) \qquad (1.13)$$

The Hartree-Fock equations can be solved in closed form only for a limited number of systems. Numerical integration provides fairly accurate results for atoms,[9] while for molecules, analytic basis functions are generally employed. The self-consistent-field (SCF) wave function is the lowest energy single determinant wave function that can be constructed within a finite basis.

The analytic approach developed by Roothaan,[10] involves expanding the orbitals as a complete set of basis

functions, f_k. That is,

$$\phi_i = \sum_k C_{ik} f_k \qquad (1.14)$$

Substitution of this expression into equation (1.9) gives

$$\sum_k C_{ik} H^{eff} f_k = \varepsilon_i \sum_k C_{ik} f_k \qquad (1.15)$$

Multiplication by f_j^* and subsequent integration leads to

$$\sum_k C_{ik} (H_{jk}^{eff} - \varepsilon_i S_{jk}) = 0 \qquad j=1,2,... \qquad (1.16)$$

where

$$H_{jk}^{eff} = \int f_j^* H^{eff} f_k d\nu \qquad (1.17)$$

and

$$S_{jk} = \int f_j^* f_k d\nu \qquad (1.18)$$

Equations (1.16) are a set of simultaneous linear homogeneous equations in the unknown coefficients, C_{ik}. In order to obtain a nontrivial solution,

$$\det (H_{jk}^{eff} - \varepsilon_i S_{jk}) = 0 \qquad (1.19)$$

must be satisfied. Equations (1.16) must be solved iteratively since H_{jk}^{eff} depends on the orbitals ϕ_i, which in turn depend on the coefficients C_{ik}. The advantage of this approach is that it reduces the eigenvalue problem to a matrix problem.

In molecular systems, the choice of a set of basis

functions, the f_k of equation (1.14), is extremely important. These basis functions are generally centered on each atom, but effectively span the appropriate molecular space. Exponential functions of the form

$$Nr^{n-1} e^{-\alpha r} Y_{\ell}^{m}(\theta,\phi) \qquad (1.20)$$

are known as Slater-type orbitals.[11] N is a normalization constant, n is the principal quantum number, and α is the screening parameter. Slater orbitals are useful for many applications, but they do not possess the proper number of radial nodes and therefore do not provide a good representation of the inner part of the orbital. In addition, for large molecular calculations, they are not economically practical because of the difficulty in solving the two electron integrals.

In contrast, these same integrals can be evaluated relatively easily if Gaussian functions are used. These functions are of the form

$$Mx^{a}y^{b}z^{c}e^{-\beta r^{2}} \qquad (1.21)$$

where the x, y, z represent the angular dependence, and a, b, and c are integers. These functions are less appropriate for describing molecular systems than Slater type functions. Frequently, however, the description may be improved by contracting several Gaussians together to act as one function. In spite of the fact

that greater accuracy can almost universally be obtained from the use of Slater-type Orbitals, Gaussians have received wide use because of the relative ease of the two-electron integral evaluation.

The smallest basis set that can be used for any system is a minimum basis set. In these cases, either Slater type Orbitals or contractions of three Guassians are generally employed. For the oxygen atom, for example, a minimum basis set would include 1s, 2s, and 2p functions. Since the calculated energies obtained from the minimum basis sets are usually rather far above the Hartree-Fock energies, larger basis sets are often utilized. One type of basis set, the double zeta, contains twice as many functions as the minimum basis. Any basis set larger than the double zeta is an extended basis. Extended basis sets comprised of primitive Gaussian functions can require an often prohibitive amount of time for solution of the SCF equations, and may not lead to convergence of the energy. To ameliorate this problem, contracted gaussians[12] or linear combinations of gauassians with fixed coefficients are frequently used.

A further step for improvement in molecular description can be obtained by inclusion of polarization functions.[13] These are functions of higher ℓ value than required by any atom in the molecule. For the H_2 molecule, for example, a polarization function would be

a p function. Many properties of chemical interest, including dissociation energies and dipole moments, can be reliably calculated only if polarization functions are included.

Regardless of the size or type of basis set, the Hartree-Fock approximation neglects an important contribution to the total energy. The correlation energy, or the energy of the instantaneous repulsions between pairs of electrons, is the difference between the Hartree-Fock and the exact energy of a system. In spite of the fact that this energy represents only a small percentage of the total energy (less than 1 percent for lighter atoms[14]), its absolute magnitude may be as high as 10 eV. The Hartree-Fock energy is particularly inadequate when calculating potential curves of small molecules where the correlation may vary considerably as the molecule is stretched.

The most frequently used technique for dealing with the problem of electron correlation is Configuration Interaction (CI). The earliest calculations of this type were performed in 1927,[15] and were necessarily limited to very small systems. With the advent of the computer, the ability to handle larger systems, atoms and their negative ions,[16] as well as small molecules,[17] was established. The advantage of the CI method lies in its simplicity and universal applicability. It can be

used to calculate ground and excited state energies for molecules, atoms, negative ions, or transition complexes.

In addition to the Hartree-Fock orbitals, there are an infinite number of other orbitals that are eigenfunctions of H_{eff} for any atom or molecule. These additional orbitals can be used to construct configurations other than the Hartree-Fock configuration. With the inclusion of all configurations formed from an infinite number of orbitals, the Schroedinger Equation can be solved exactly. In practice, of course, a complete set of these configurations cannot be used and the problem is generally truncated at some reasonable level.

The C.I. wave function has the form

$$\psi = \sum_n C_n \phi_n \qquad (1.22)$$

where the ϕ's are an orthonormal set of n-electron configurations. Equation (1.22) is a linear variation function, and the coefficients C_i are determined to minimize the energy. Application of the variation principle leads to the determinantal equation

$$(\underset{\sim}{H} - E\underset{\sim}{1})\underset{\sim}{C} = 0 \qquad (1.23)$$

where the E are the eigenvalues and the C's are the matrix of eigenvectors. The matrix element H represents the interaction between two determinants or configurations, D_p and D_q

$$H_{pq} = \int D_p H D_q d\tau \qquad (1.24)$$

In a particular CI calculation, if N configurations are included, the N energies or eigenvalues will be obtained in the solution of equation (1.24). A set of coefficients, C_n, which define the CI wave function is associated with each energy.

The solution of equation (1.24) is greatly simplified by the fact that the matrix elements H_{pq} between two configurations p and q of different symmetry are identically zero. Moreover, an additional simplification results from the expression of these matrix elements as the sum of integrals in the orthonormal one electron basis. It can be written in terms of the one-electron operator of the Hamiltonian,

$$h_{ij} = \int \phi_i^*(a) \{-\frac{\nabla_a^2}{2} - \sum_A \frac{Z_A}{r_{aA}}\} \phi_j(a) d\tau \qquad (1.25)$$

and the two-electron Hamiltonian,

$$V_{ijkl} = \int \phi_i^*(b) \phi_j(b) \{\frac{1}{r_{ab}}\} \phi_k^*(a) \phi_l^*(a) d\tau_a d\tau_b \qquad (1.26)$$

The determinants of equation (1.24) may be equivalent or they may differ in occupation by one or more spin orbitals. In the case where the determinants are identical, the matrix element between them is

$$H_{mm} = \sum_i^{\substack{OCC \\ SO}} h_{ii} + \frac{1}{2} \sum_{ij}^{\substack{OCC \\ SO}} (V_{iijj} - V_{ijji}) \qquad (1.27)$$

For the case where the determinants differ by the occupation of one spin orbital (i>j),

$$H_{mm} = h_{ij} + \sum_{k}^{OCC\ SO} (V_{ijkk} - V_{ikkj}) \qquad (1.28)$$

Occupations which differ by two spin orbitals can be represented as

$$H_{mn} = (V_{ijkl} - V_{ilkj}) \qquad (1.29)$$

If the two determinants differ by more than two spin-orbitals, equation (1.24) is identically zero, which significantly reduces the potential size of the calculation. Nevertheless, within any basis set larger than a minimum basis, CI calculations even for small molecules can be extremely large. It is therefore important to identify techniques for further simplifying the problem.

One traditional method for limiting the size of a CI calculation is the frozen-core approximation. This method involves freezing the occupation of the M.O.'s that play a neglgible part in contributing to the energy ot the desired property. For example, in calculating the transition energy from the ground to an excited state of the CO molecule, the 1s M.O.'s of carbon and oxygen might be dropped from consideration. They contribute very little to the energy difference, since they are basically atomic in nature. In cases of this type, where the M.O.'s

dropped from consideration have only a trivial effect on the results, the frozen core approximation is justified. Alternatively, attempts to separate the sigma and pi space of certain molecules using this approximation have been unsuccessful.[18] It has been found, for example, that the correlation from the sigma space contributes unequally to the pi states of some systems. Therefore, both parts of the space must be included to obtain reasonable results.

Another method of limiting the CI problem is to restrict the number of configurations. Generally, a particular state is dominated by only a few main configurations which together comprise more than 90 percent of the final wavefunction. The only configurations which interact directly with the dominant configurations are those that differ by two or fewer occupations. Those configurations differing by more than two occupations interact directly with the corrections, but only indirectly with the dominant configurations. In a study of the BH_3 molecule,[9] only a few triple and quadruple excitations from the ground state were found to contribute to the final wave function. Indeed, it is common practice in CI calculations to include only single and double excitations from the dominant configurations.

Other techniques for reducing the size of the CI problem focus on simplifying the construction and diagonalization of the Hamiltonian matrix. One method

that handles the problem indirectly is based on selection of a small subspace of the full matrix for diagonlization.[20] The remaining space is treated as a perturbational sum. The threshold for selection, based on the interaction with a few dominant configurations, is varied. The total energies obtained by varying the threshold can be extrapolated to obtain the energy of the full space. A second method for limiting the problem involves the direct calculation of only the diagonal matrix elements and a small strip of the full matrix.[21]

Another technique for reducing the problem to manageable proportions is described in the next chapter. This method was used to obtain the results of the studies presented in Chapters IV and V. It involves a partitioning of the Hamiltonian so that direct diagonalization can be avoided and, in addition, presents an efficient method for calculating matrix elements. The full details of this technique are presented in references 22 and 23.

References

1. E. Schroedinger, Annal. Physik, 79, 361, 489, 734 (1926), Phys. Rev. 28, 1049 (1926).
2. M. Born and J.R. Oppenheimer, Annal. Physik, 84, 457 (1927).
3. O.H. Crawford, Mol. Phys. 20, 585 (1971).
4. O.H. Crawford, J. Chem. Phys. 66, 4068 (1977).
5. I.N. Levine, Quantum Chemistry, Vol. I, Quantum Mechanics, and Molecular Electronic Structure, Allyl and Bacon, Boston, 1970, p. 184.
6. For a review see D.R. Hartree, Repts. Prog. Phys. 11, 113 (1946-7).
7. W. Pauli, Z. Physik, 43, 601 (1927).
8. J.C. Slater, Phys. Rev. 35, 210 (1930).
9. D.R. Hartree, The Calculations of Atomic Structures, John Wiley and Sons, New York, 1957.
10. L.C.J. Roothaan, Rev. Mod. Phys. 23, 69 (1951).
11. J.C. Slater, Phys. Rev. 36, 57 (1930).
12. E. Clementi and D.R. Davis, J. Comput. Phys. 2, 223 (1967).
13. R.K. Nesbet, Rev. Mod. Phys. 32, 272 (1960).
14. P.O. Lowdin, Adv. Chem. Phys. 2, 207 (1959).
15. E.A. Hylleras, Z. Physik, 48, 469 (1928).
16. S.F. Boys and V.E. Price, Phil. Trans. Roy. Soc. (London), A246, 451 (1954).

17. S.F. Boys, G.B. Cook, C.M. Reeves, I. Shavitt, Nature, 178, 1207 (1956).

18. S.D. Peyerimhoff, R.J. Buenker, W.E. Kramer, and H. Hsu, Chem. Phys. Lett. 8, 129 (1971).

19. A. Pipano and J. Shavitt, Int. J. Org. Chem. 2, 741 (1968).

20. R.J. Buenker and S.D. Peyerimhoff, Theor. Chim. Acta, 35, 33 (1974) and 39, 217 (1975).

21. Z. Gershgorn and I. Shavitt, Int. J. Org. Chem. 2, 75. (1968).

22. R.W. Wetmore and G.A. Segal, Chem. Phys. Lett. 36, 478 (1975).

23. G.A. Segal, R.W. Wetmore and K. Wolf, Chem. Phys. 30, 296 (1978).

CHAPTER II

METHOD

The construction and diagonalization of the matrices necessary for the solution of the CI problem for small and medium sized molecules (> 20 M.O.'s) is prohibitive. Various techniques for truncating the space so that full solution can be avoided have already been mentioned. The purpose of this chapter is to describe one such technique which has been used with considerable success in numerous cases.

The method described here relies on the fact that for most chemical systems of interest, there exists a small set of configurations that together dominate the CI wavefunction. This set of configurations is called the core. All remaining configurations, deemed the tail, have a less significant contribution to the final wavefunction. The main configurations can be identified either through a preliminary calculation or by scanning the CI matrix diagonal for the terms of lowest energy. These configurations can be gathered together to form the nucleus of the calculation. The interaction of all remaining configurations with those of the nucleus is then tested using Raleigh Schroedinger Perturbation theory. The configurations which interact strongly with the nucleus are identified and grouped with the nucleus to

complete the core. Other configurations which interact less strongly are also grouped together, in this case to form the tail.

These basic concepts suggest a partitioning of the matrix eigenvalue problem as first proposed by Lowdin.[1] If the core is denoted by H_{aa} and the tail by H_{bb}, this can be expressed

$$\begin{vmatrix} H_{aa} & H_{ab} \\ H_{ba} & H_{bb} \end{vmatrix} \begin{vmatrix} C_a \\ C_b \end{vmatrix} = \omega \begin{vmatrix} C_a \\ C_b \end{vmatrix} \tag{2.1}$$

where C_a and C_b represent the coefficients. This matrix equation can be reformulated into two simultaneous equations in two unknowns.

$$\underset{\sim}{H}_{aa}\ \underset{\sim}{C}_a + \underset{\sim}{H}_{ab}\ \underset{\sim}{C}_b = \omega\ \underset{\sim}{C}_a \tag{2.2}$$

$$\underset{\sim}{H}_{ba}\ \underset{\sim}{C}_a + \underset{\sim}{H}_{bb}\ \underset{\sim}{C}_b = \omega\ \underset{\sim}{C}_b \tag{2.3}$$

Solving for C_b in equation (2.3), and substitution of the result into equation (2.2) leads to

$$\underset{\sim}{H}_{aa}\ \underset{\sim}{C}_a + \underset{\sim}{H}_{ab}\ [\omega \underset{\sim}{I} - \underset{\sim}{H}_{bb}]^{-1}\ \underset{\sim}{H}_{ba}\ \underset{\sim}{C}_a = \omega \underset{\sim}{C}_a \tag{2.4}$$

where the term $\underset{\sim}{H}_{ab}\ [\omega \underset{\sim}{I} - \underset{\sim}{H}_{bb}]^{-1}\ \underset{\sim}{H}_{ba}$ corresponds to a kind of optical potential.

Although equation (2.4) reduces the diagonalization problem to the size of the core block, H_{aa}, evaluation of the inverse term is still at least as difficult as the original diagonalization. The inverse matrix will

always exist and can be made diagonally dominant provided that all terms of H_{bb} whose diagonal elements, h_{bb}, lie close to ω are placed in the core block, H_{aa}. Assuming this to be the case, the inverse can then be expressed in the following manner.

$$[\omega \underset{\sim}{I} - H_{bb}]^{-1} = D^{-1} + D^{-1}OD^{-1} + D^{-1}OD^{-1}OD^{-1} + \cdots$$

where O represents the off-diagonal terms

$$O = [\underset{\sim}{H}_{bb} - h_{bb}\underset{\sim}{I}] \tag{2.6}$$

and D^{-1} is the inverse diagonal

$$D = [\omega \underset{\sim}{I} - h_{bb}\underset{\sim}{I}] \tag{2.7}$$

Substitution of equation (2.5) into equation (2.4) leads to

$$\underset{\sim}{H}_{aa}\underset{\sim}{C}_a + \underset{\sim}{H}_{ab}D^{-1}\underset{\sim}{H}_{ba}\underset{\sim}{C}_a + \underset{\sim}{H}_{ab}\underset{\sim}{D}^{-1}\underset{\sim}{O}\underset{\sim}{D}^{-1}\underset{\sim}{H}_{ba}\underset{\sim}{C}_a + \underset{\sim}{H}_{ab}\underset{\sim}{D}^{-1}\underset{\sim}{O}\underset{\sim}{D}^{-1}\underset{\sim}{O}\underset{\sim}{D}^{-1}\underset{\sim}{H}_{ba}\underset{\sim}{C}_a + \cdots = \omega \underset{\sim}{C}_a \tag{2.8}$$

Although this expansion is energy dependent through the terms in ω, the dependence arises only in the diagonal terms, D. Diagonalization of the H_{aa} block can provide an estimate, ω_o, of the true eigenvalue, ω. The diagonal can again be expanded, this time in terms of the difference between the approximate and the true eigenvalue, $\Delta\omega$. Thus,

$$\underset{\sim}{D}^{-1}(\omega) = \underset{\sim}{D}^{-1}(\omega_o) \sum_{n=0}^{\infty} (\underset{\sim}{D}^{-1}(\omega_o)\Delta\omega)^n \tag{2.9}$$

Substituting this result into equation (2.8) gives

$$\{\underset{\sim}{H}_{aa} + \underset{\sim}{H}_{ab}[\underset{\sim}{D}^{-1}(\omega_o) + \underset{\sim}{D}^{-1}(\omega_o)\underset{\sim}{\underset{\sim}{O}}\underset{\sim}{D}^{-1}(\omega_o) + \cdots]\underset{\sim}{H}_{ba}$$

$$+ \underset{\sim}{H}_{ab}[\underset{\sim}{D}^{-2}(\omega_o)\Delta\omega + \underset{\sim}{D}^{-2}(\omega_o)\underset{\sim}{\underset{\sim}{O}}\underset{\sim}{D}^{-1}(\omega_o)\Delta\omega$$

$$+ \underset{\sim}{D}^{-1}(\omega_o)\underset{\sim}{\underset{\sim}{O}}\underset{\sim}{D}^{-2}(\omega_o)\Delta\omega + \cdots]\ \underset{\sim}{H}_{ba} + \ldots\}\omega\underset{\sim}{C}_a = \omega\underset{\sim}{C}_a \tag{2.10}$$

The advantages of equation (2.10) are more readily apparent if it is written in another way

$$[\underset{\sim}{H}_{aa} + \sum_{n=0}^{\infty} \underset{\sim}{V}_{aa}^{(n)} \Delta\omega^n]\ \underset{\sim}{C}_a = \omega\underset{\sim}{C}_a \tag{2.11}$$

In equation (2.11), the dominant contributions to the final wavefunction, and those terms that interact with them strongly, together form H_{aa}. This subspace can be treated fully by exact diagonalization. All other terms, which interact less significantly, can be treated simply as a potential, $V(\omega)$. Equation (2.11) could, in principal be solved iteratively for a complete solution to the problem. Fortunately, reasonable accuracy in the solution of most problems can be attained without full solution by truncation of the potential. Close examination of equation (2.8) reveals that the terms have a one-to-one correspondence with successively higher Brillouin-Wigner Perturbation corrections. The term, $H_{ab}D^{-1}H_{ba}C_a$ is related to the second order Brillouin-Wigner perturbation

correction; the next term is related to the third order correction, and so on. Tests performed on small, medium, and large matrices indicate that for most practical problems, sufficient accuracy can be achieved by retention of corrections through second order.[3] It is this result that makes the approach of value for the large scale CI calculations described in Chapters IV and V.

The method is pictorially described in Figure II-1 and can be summarized as follows. The configurations which are most important to a particular calculation are identified and gathered together in the upper left hand corner of the core block, H_{aa}. The interaction of each of the configurations in the nucleus with all other configurations is evaluated and becomes part of H_{ab}. Using Raleigh-Schroedinger Perturbation Theory, the most important of the remaining configurations are gathered together with the nucleus to complete H_{aa}, the core block. The interaction of these configurations in the core block with all other configurations forms the balance of H_{ab}. The remaining configurations form the tail, H_{bb}. The H_{aa} block is then diagonalized to provide an initial guess for the energy. The potential function is evaluated, and finally, the full problem is solved through iteration. In addition to providing a unique solution for solving the eigenvalue problem, the method used in this work also includes techniques for simplifying

calculation of the matrix elements, the other time-consuming step in a CI calculation. A complete description of the approach can be found in references 2 and 3.

References

1. P.O. Lowden, Adv. Chem. Phys. 2, 207 (1959).

2. G.A. Segal and R.W. Wetmore, Chem. Phys. Lett. 36, 478 (1975).

3. G.A. Segal, R.W. Wetmore and K. Wolf, Chem. Phys. 30, 296 (1978).

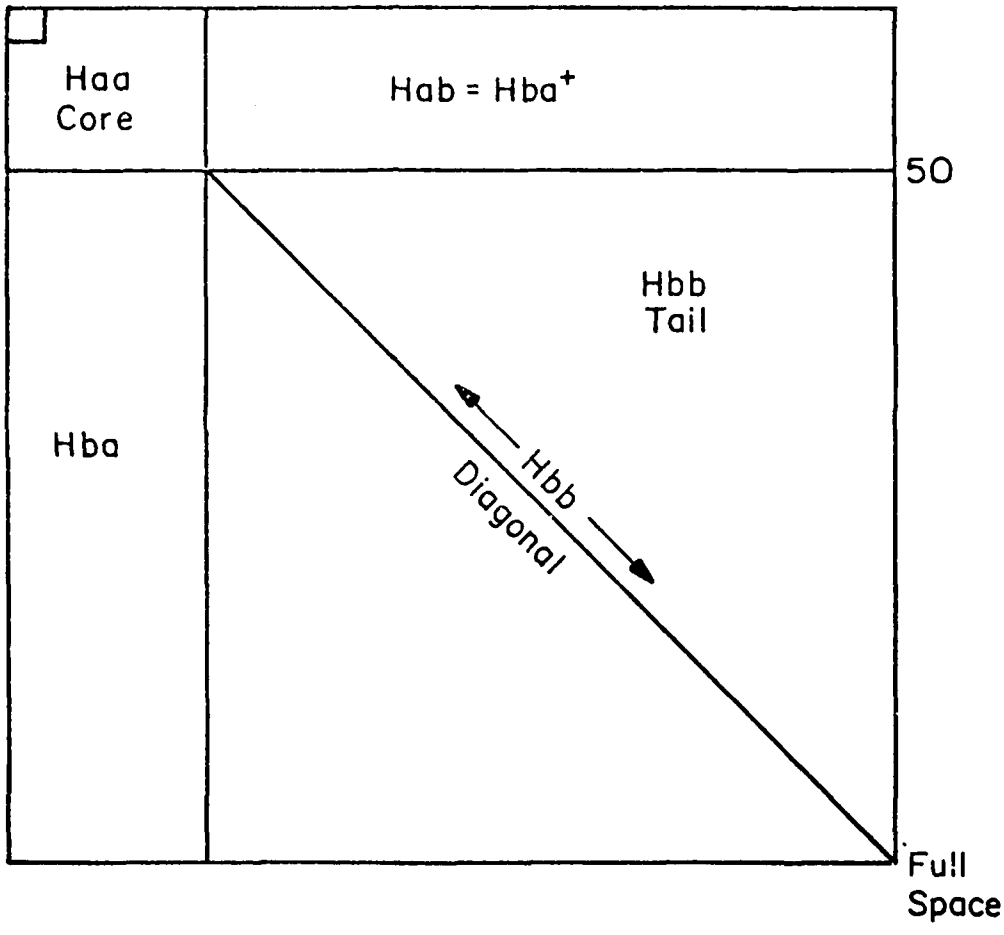

Fig. II-1--Partitioning of the Hamiltonian Matrix

CHAPTER III

RESONANCES OF POLAR MOLECULES

In recent years, the electron scattering and binding properties of polar molecules have been the subject of considerable interest. A number of interesting effects result from the very long-range interaction between a molecule with a permanent dipole moment and a charged particle. The Configuration Interaction Method described in the last chapter has been used with considerable effectiveness to study the binding and scattering characteristics of one such polar molecule, hydrogen fluoride. The results of this study are presented in Chapter IV for the lower energy region (< 9 eV) and Chapter V for the higher energy range (9 to 14 eV). Before moving to this discussion, however, a basic understanding of the nature of compound states is useful. It is the purpose of this chapter to provide some general background on negative ion resonances.

A compound state is formed by the interaction of an incident electron with a target molecule. The incident electron is temporarily captured within the neighborhood of the molecule and a complex, called a temporary negative ion or a resonance, is formed. The term resonance implies a definite energy, and sharp structure is observed in the cross section. The first evidence on the existence

of compound states appeared in 1921, but it was not until the 1960's that the resonance model was applied to molecules.[1]

Molecular compound states have lifetimes in the range of 10^{-10} to 10^{-15} sec. The lifetime τ can be described as

$$\tau = \frac{\hbar}{\Gamma} \qquad (3.1)$$

where Γ is the width. These states decay by the emission of an electron into various final states where they can be detected experimentally. The decay channels include rotational, vibrational, and electronic excitation, elastic scattering and dissociative attachment, to name a few.

A shape or single particle resonance is formed when an electron is trapped in the potential or behind the centrifugal barrier of the molecular state. These types of resonances occur at energies below about 10 eV and have been observed in H_2, D_2, O_2, HD, N_2, NO, and CO.[1] Core excited resonances, which occur at energies above 10 eV, consist of a "hole" in one of the normally occupied orbitals of the molecule and two "particles" in normally unoccupied orbitals. The excited neutral molecule is called the parent of the negative ion state, while the positive ion is referred to as the grandparent. Core excited resonances that lie below their parent are entitled Feshbach resonances. They have lifetimes that are long compared to a vibrational period and can

therefore give rise to band structure. The two outer electrons are held in Rydberg orbitals which lie far from the ion core and as a result, these bands exhibit vibrational structure similar to the grandparent.

Single Particle Resonances

In recent years, low energy electron impact experiments have revealed pronounced structure in the vibrational excitation cross sections of polar molecules.[2-4] Within about 0.5 eV of threshold, the observed cross sections are larger by 10 to 100 times than would be predicted by the Born approximation. That is, these very large cross sections cannot be simply attributed to collisional momentum transfer. The sharp peaks are rather the result of pronounced distortion of the incident electron by the potential well of the target molecule. The resonances that arise from the interaction are dominated by very few partial waves and the symmetry of the resonant state is reflected in the angular dependence of the cross section.

There has been considerable interest in the question of whether or not a neutral polar molecule is capable of binding an electron to form a stable negative ion state. Several authors[5-10] have shown that the electric dipole field of such a molecule can bind an electron if the dipole moment is greater than 1.625 D. To understand

this result we can consider the scattering of an electron by a point dipole. In a polar molecule with electric dipole moment μ and an electron at distance r, the potential is given by:

$$V = -\frac{e\mu}{r^2}\cos\theta \tag{3.2}$$

where θ represents the angle between the vectors μ and r. Schroedinger's equation becomes

$$\left[\nabla^2 + \frac{2m_e}{\hbar^2}\left(\frac{e\ \cos\theta}{r^2}\right) + E\right]\ \psi(r) = 0 \tag{3.3}$$

Setting

$$k^2 = \frac{2m_e eE}{\hbar^2} \tag{3.4}$$

and the dimensionless dipole moment,

$$\mu_o = \frac{2\mu}{ea_o} = \frac{2m_e\mu}{\hbar^2} \tag{3.5}$$

where a_o is the bohr radius, equation (3.3) takes the simple form

$$\left[\nabla^2 + \frac{\mu_o\cos\theta}{r^2} + k^2\right]\ \psi(r) = 0 \tag{3.6}$$

Separation of equation (3.6) in terms of spherical coordinates leads to equations in the three variables R, θ, Φ.

$$\left[\frac{d^2}{dr^2} + \frac{2}{r}\frac{d}{dr} + k^2 - \frac{A}{r^2}\right] R(r) = 0 \qquad (3.7)$$

$$\left[-\frac{1}{\sin\theta}\frac{d}{d\theta}\sin\theta\frac{d}{d\theta} + \frac{M^2}{\sin^2\theta} - \mu_o\cos\theta - A\right]\theta(\theta) = 0 \qquad (3.8)$$

and

$$\left[\frac{d^2}{d\phi^2} + M^2\right]\Phi(\phi) = 0 \qquad (3.9)$$

where A is a separation constant and M, an integer. For the limiting case, as $E \to 0$, equation (3.7) becomes

$$\left[\frac{d^2}{dr^2} + \frac{2}{r}\frac{d}{dr} - \frac{A}{r^2}\right] R(r) = 0 \qquad (3.10)$$

A stationary solution of equation (3.10) takes the form $R(r) \sim r^{s}$.[12] Substitution of this solution leads to

$$S(S+1) - A = 0 \qquad (3.11)$$

Solutions with $A \leq 1/4$ have the form

$$R(r) = \frac{B}{r^{|s|}} \qquad (3.12)$$

where B is a constant. Solutions with $A > \frac{1}{4}$ take the form

$$R(r) \propto r^{-1/2}\cos(A-1/4)^{1/2}\log r \qquad (3.13)$$

It should be noted that equation (3.13) produces an infinite number of zeros and thus an infinite number of nodes, while equation (3.12) leads to only one node.

We now return to equation (3.8). For M = 0, the solutions are

$$\Phi(\theta) = \sum_{\ell} c_{\ell} P_{\ell}(\cos\theta) \tag{3.14}$$

the Legendre Polynomials. Substitution of these solutions into equation (3.8) leads to

$$\left\{\mu_o \frac{\ell}{2\ell-1} C_{\ell-1} + C_\ell \ell(\ell+1) - C_\ell A + \mu_o \frac{(\ell+1)}{(2\ell+3)} C_{\ell+1}\right\} = 0 \tag{3.15}$$

where the ℓ are integers ≥ 0. When A = 1/4, equation (3.15) can be written

$$\left[\frac{\ell}{(2\ell-1)} b_{\ell-1} + \frac{1}{\mu_o(MIN)} \ell(\ell+1) b_\ell + \frac{1}{4\mu_o(MIN)} b_\ell + \frac{(\ell+1)}{(2\ell+3)} b_{\ell+1}\right] = 0 \tag{3.16}$$

where $\mu_o(MIN)$ is the minimum dipole moment. For this case, and for A < 1/4, there are no negative energy levels and therefore no bound states. Alternatively, when A > 1/4, there are an infinite number of negative energy levels, and thus an infinite number of bound states.

The implications of this result are interesting. The case where $A \leq 1/4$, since it has no zeros, corresponds to the state with E=0, the lowest level. As $E \to 0$, the negative ion becomes degenerate with the neutral molecule, and the state for the case where A = -1/4 has the minimum dipole moment for binding. Both analytic and numerical techniques have been employed to determine the value of

$\mu_0(min)$ in equation (3.16). The solutions lead to the conclusion that when the dipole moment is less than 1.625 D, there are no bound states, while for a dipole moment greater than this value, an infinite number of bound states exist.

Although the critical value of the dipole moment for binding an electron has the value 1.625 D in the conventional Born-Oppenheimer treatment, this result is modified to some extent with the inclusion of the rotational degrees of freedom of the nuclei. To account for rotation, the Hamiltonian for a symmetric rigid rotor would contain the term $\frac{\hbar^2\hat{j}^2}{2I}$ where $h^2\hat{j}^2$ is the operator for the square of the angular momentum and I is the moment of inertia. This term does not contribute to the ground state energy of the neutral system. However, when an extra electron is present, the interaction of this electron with the added term in the Hamiltonian acts to raise the energy of the ground state of the ion relative to neutral system.[13] This follows from the fact that the rotational angular momentum of the dipole and the orbital angular momentum of the incident electron are coupled to give the total angular momentum which is conserved. The result is that some or all of the bound states of the electron are moved to the continuum. The exact value of the minimum dipole for binding varies, depending on the values of I and the

internuclear distance in the molecule. However, no binding is found to occur for dipole moments less than about 2D. The stationary dipole has a very small electron affinity when the dipole is less than 2D. For dipole moments in the range of about 2.1 to 2.3 D, the electron affinity is much larger. When the effect of rotation is included, only one bound state is supported for a dipole moment of 2 D. For higher values of the dipole moment, two or more bound states exist.

The effects of molecular vibration on the binding of polar molecules have also been investigated.[14] As long as the dipole moment of interest is the average of the dipole moment over the ground state vibration, the minimum dipole moment for binding is not altered, except in cases where exothermic dissociative attachment can occur.

There is some indication that induced dipole forces are a very important contribution to the energy of the weakly bound electron, even for systems with larger permanent dipole moments. Garrett suggests that a strongly polar molecule with a dipole moment greater than about 4D will almost surely form a stable negative ion. For molecules with dipole moments in the range of 2 to 3.5 D, a negative ion with binding energy greater than 0.01 eV will be formed if the polarizability is between 20 and 40 a_o^3 (3 and 6 $\mathring{A}^3$).[15]

As a test of the minimum dipole moment concept, ab initio studies of the electron affinities of polar molecules with various dipole moments have been performed.[16-18] One source of difficulty in calculations of this type is the lack of accuracy in the computed dipole moments. Even with wavefunctions of near Hartree-Fock quality, calculated dipole moments are generally higher than the experimental values by several tenths of an eV. Because of the strong dependence of the electron affinity on the dipole moment when the dipole moment is close to the critical value, it might be thought that calculations of this type are not particularly useful. This, however, is not the case. Ab initio techniques, while they cannot provide completely accurate binding energies or predictions of binding, can indeed serve as at least a qualitative guide on the binding capabilities of polar molecules.

One group in particular has performed ab initio calculations on several polar molecules including LiH^-,[17,18] NaH^-,[17,18] BeO^-,[17] LiF^-,[17] and $LiCl^-$.[16,17] The results of these theoretical studies were used, together with the available experimental data, to assess the validity of the simple fixed finite dipole model for predicting binding. The technique used in these investigations is straightforward. Hartree-Fock calculations were performed for the negative ions listed above. Special attention was paid to choosing an adequate basis set for each

particular anion. Diffuse functions with optimized exponents were added to the electro-positive atom to permit the extra electron to attach to the positive end of the polar molecule. The difference between the Hartree-Fock energies of the neutral molecule and the negative ion give the electron affinity. The orbital energy for the lowest unoccupied orbital (LUMO) for the neutral molecule in the Hartree-Fock calculation can be used to estimate the magnitude of the binding capability. A negative orbital energy implies a stable negative anion will be formed, while a positive orbital energy implies that the neutral molecule is not capable of binding an electron. This is simply Koopman's Theorem Approximation.

For LiH, BeO, NaH, and LiF with respective dipole moments of 5.88D, 7.41D, 6.98D, and 6.33D, negative orbital energies were obtained. This is not surprising, since all of these molecules have dipole moment significantly in excess of the minimum dipole moment for binding. Unfortunately comparison of the ab initio results with experiment is not possible since the energies for binding an electron to these molecules have not yet been determined. One molecule for which the experimental binding energy has been measured is LiCl,[19] which has a dipole moment of 7.13 D. The calculated binding energy for this molecule of 0.54 eV[17] compares rather well with the experimental value of 0.61 eV. From this example, the

only case where an experimental binding energy is available, we can conclude that ab initio studies are capable of providing fairly accurate values for binding energies.

Jordan et al. discuss in detail the limitations of their method for calculating exact binding energies.[17,18] The Hartree-Fock calculations neglect two very important contributions to the binding energy: orbital relaxation and correlation corrections. In the calculations, the electron affinity was calculated by taking the difference between the Hartree-Fock energies of the neutral molecule and the anion. The binding energy of 0.54 eV for LiCl cited above was obtained in this manner.

To derive estimates of the contributions not included in the Hartree-Fock technique, Jordan et al. utilized the Equation of Motion (EOM) Method. In this method, electron affinities are calculated directly without the need for performing calculations on both the neutral molecule and its anion. The electron affinity attained using this method inherently includes the second order correlation and orbital relaxation corrections as well as the third and higher order corrections to the Koopman's Theorem estimates.[15] The difference between the orbital energy of the LUMO of the neutral molecule in the Hartree-Fock calculations and the electron affinities from the EOM calculations is thus the orbital relaxation and correlation corrections. For the molecules LiH, LiF, BeO, and NaH,

the binding energies obtained through the EOM calculations indeed give a larger value for the binding energy than those obtained through the Hartree-Fock calculations. For LiCl, for example, the binding energy obtained through the EOM method is higher by 0.13 eV than that obtained from the Hartree-Fock calculations.

Jordan et al.[17] maintain that the orbital relaxation and correlation effects would be expected to be small in the case of LiCl. This follows from the fact that the additional electron is located primarily behind the electropositive atom in a molecular orbital that is largely nonbonding in nature. This nonbonding MO does not correlate strongly with the other electrons in the molecule. The good agreement between the calculated binding energy and the experimental data certainly support this interpretation. The contributions not included in the Hartree-Fock calculations are included in configuration interaction calculations. As we shall see in Chapter IV, CI techniques have been applied with considerable success to determine the binding energy of HF. This molecule has a dipole moment of 1.82 D, only slightly larger than the minimum dipole for binding and, as such, is an excellent candidate for investigation.

The calculated results for LiCl suggest that rather good agreement between ab initio studies and experiment for binding energies is possible. The investigations on

LiCl also provide the oportunity to evaluate the capabilities of the fixed finite dipole model in predicting binding energies. Jordan and Luken have examined the accuracy of the dipole model in some detail.[18] For a molecule with a dipole moment of 7.2 D (the dipole moment of LiCl), the model predicts a binding energy of 0.08 eV. This is well below the experimental binding energy of 0.6 eV, and poses serious questions about the applicability of the model. Jordan and Luken attribute at least part of the discrepancy to what can be called penetration effects. In the Lithium atom, the 2s electron is "pulled in". That is, the 2s electron penetrates the 1s shell and is permitted to feel the nuclear charge of +3. The fixed finite dipole model fails to account for this behavior. If the ground state of the dipole model is correlated with the negative ions of molecules, incorrect nodal behavior is predicted. One must instead correlate the negative ions with the first excited state of the dipole model. Correlation with this state, however, leads to an underestimate of the binding energy of a real molecule. From the LiCl study, it can be concluded that although the simple dipole model may be of some qualitative use, its ability to predict binding energies of real molecules appears somewhat limited. In Chapter IV, where we examine the binding capability of HF, this has important implications. The binding energy of HF

as predicted by the dipole model is on the order of 10^{-5} eV, while our calculations indicate the binding energy to be higher by several orders of magnitude.

Core-Excited Resonances

Core-excited resonances, as mentioned earlier, are characterized by two electrons in normally unoccupied MO's and a "hole" in a normally occupied MO. When these negative ion resonances lie below the excited state of the parent or neutral excited molecule, they are known as Feshbach states and the parents are said to exhibit a positive electron affinity. The binding energy of a Feshbach state is defined as the difference in energy between the positive ion state and the negative ion state formed by adding two outer electrons to the positive ion core.

The primary experimental means of detecting Feshbach states is electron transmission spectroscopy. This technique involves measurement of the unscattered transmitted current as a function of electron energy when monoenergetic electrons are accelerated into a collision chamber filled with the target gas. Experimental results are generally presented with the ordinate representing the derivative of the transmitted current and the abscissa, the electron energy. In many cases, sharp structure which mimics the vibrational spacing of the grandparent

state is observed.

Core-excited resonances of atoms have been studied extensively, particularly those of the rare gases.[20] These resonances have also been detected in many diatomic molecules.[21] In principle, a core-excited state of a molecule may consist of an electron temporarily bound either to a valence or Rydberg excited state. Only the Rydberg excited states, however, lead to negative ion states that have a positive electron affinity for a fixed internuclear separation in the Franck-Condon region. Thus for Rydberg excited states, sharp resonances which lie somewhat below the Rydberg excited states are expected. The vibrational spacing of the resonances should be similar to that of the grandparent, since the two excited electrons reside rather far from the positive ion core and therefore perturb it only slightly.

In many cases, vibrational progressions overlap leading to confusion in identification. A further complication is that the width of a core-excited resonance can change due to the opening of a new decay channel. If, for example, the new decay channel is a repulsive negative ion state, vibrational progressions may be observed only for a limited number of levels; that is, the vibrational progression may partially predissociate. This situation can arise from an avoided crossing between two states of the same symmetry. As we shall see in Chapter V, this

explanation may apply to an experimental observation where only one vibrational level is excited in a study of the Feshbach states of HF^-.

References

1. G.J. Schulz, Rev. Mod. Phys. 45, 423 (1973).
2. K. Rohr and F. Linder, J. Phys. B: Atom. Molec. Phys. 9, 2521 (1976).
3. K. Rohr, J. Phys. B: Atom. Molec. Phys. 10, 1175 (1977).
4. K. Rohr, J. Phys. B: Atom. Molec. Phys. 11, 1849 (1978).
5. M.H. Mittleman and V.P. Myerscough, Phys. Lett. 23, 545 (1966).
6. J.E. Turner and K. Fox, Phys. Lett. 23, 547 (1966).
7. O.H. Crawford and A. Dalgarno, Chem. Phys. Lett. 1, 23 (1967).
8. W.B. Brown and R.E. Roberts, J. Chem. Phys. 46, 2006 (1967).
9. O.H. Crawford, Proc. Phys. Soc. London, 91, 279 (1967).
10. J.M. Levy-Lebbond, Phys. Rev. 153, 1 (1967).
11. 1.625 D = 0.639 ea where 1 D = 10^{-18} esu cm.
12. L.D. Landau and E.M. Lifshitz, Quantum Mechanics, (Pergammon Press, London), 1958, p. 119.
13. W.R. Garrett, Chem. Phys. Lett. 5, 393 (1970).
14. O.H. Crawford, Mol. Phys. 26, 139 (1973).
15. W.R. Garrett, J. Chem. Phys. 69, 26251 (1978).
16. K.M. Griffing, J. Kenney, J. Simons, and K.D. Jordan, J. Chem. Phys. 63, 4073 (1975).

17. K.D. Jordan, K.M. Griffing, J. Kenney, E.L. Andersen and J. Simons, J. Chem. Phys. 64, 2760 (1976).

18. K.D. Jordan and W. Luken, J. Chem. Phys. 64, 2760 (1976).

19. J.L. Carlsten, J.R. Peterson and W.C. Lineberger, Chem. Phys. Lett. 37, 5 (1976).

20. L. Sanche and G.J. Schulz, Phys. Rev. A, 5, 1672 (1972).

21. L. Sanche and G.J. Schulz, Phys. Rev. A, 6, 69 (1972).

CHAPTER IV
CONFIGURATION INTERACTION CALCULATIONS ON THE RESONANCE STATES OF HF^-

Introduction

In the last chapter, a review of the theory of resonances of polar molecules was given. In this chapter, we present the results of ab initio calculations on one such molecule in the low energy region. Before describing these results, however, it will be useful to summarize a few pertinent concepts.

The electron scattering and electron binding properties of polar molecules have recently been the topic of considerable experimental and theoretical attention. The very long range interaction potential for a charged particle and a molecule with a permanent dipole moment leads to interesting effects. It has been demonstrated by a number of researchers[1-4] that the electric dipole field can support an infinite number of bound states if the dipole moment is greater than 1.625 D.[5] For a dipole moment less than this value, no bound states exist. Other work has shown that if a molecular system is treated dynamically by calculating non-Born-Oppenheimer rotational degrees of freedom, the number of bound states is finite.[6] For the non-stationary dipole, the critical dipole for binding an electron is from 10-30% greater than 1.625 D.[7]

There is also an indication that induced dipole forces make very important contributions to the energies of weakly bound electrons, even for systems with larger permanent dipole moments. Garrett suggests that a strongly polar molecule with a dipole greater than about 4 D will surely form a stable negative ion. For a molecule with a dipole moment in the range of 2 to 3.5 D, a negative ion with binding energy greater than 0.01 eV will be formed, if the polarizability is from 20-40 a_o^3 (3-6 $\AA^3$).[8]

Ab initio calculations have been performed on several polar molecules. Based on the premise that the electron affinity may be reliably estimated by the negative of the orbital energy of the lowest unoccupied molecular orbital (LUMO) of the neutral molecule, a series of ionic molecules have been investigated. For LiH, LiF, LiCl, NaH, NaF, NaCl, BeO, MgO, LiCN, LiNC, LiOH, and $LiCH_3$ which have dipoles ranging from 4.6 to 9.5 D, the calculated electron affinities were between 0.2 to 0.7 eV.[9] Another examination of the nonionic molecules, $(HF)_2$, HCN, HNO_3, CH_3CN, H_2O, and HF indicates stable anions for the first four are formed, while they are not for H_2O and HF.[10] Since the first four of these molecules have dipole moments greater than about 3.5 D, they would be expected to form stable negative ions. In spite of the fact that the calculated dipole moments of HF and H_2O are stated to be too high by 0.5 D (and thus larger than the critical value

by more than 0.8 D), the study finds no stable anion for the two molecules.[10]

The HF molecule has a dipole moment of 1.82 D,[11] just slightly greater than that necessary to bind an electron. Studies of the negative ion states of this molecule are of importance both because of the minimum dipole concept, and because of the recent interest in resonant states of polar molecules in general. We have performed extensive configuration interaction calculations on the lower energy states of HF^-. Although the molecule has not been widely studied, the available experimental and theoretical data are summarized below.

Experimental studies of *HF* have traditionally been difficult because of the corrosive effect of the vapor on the surfaces of optical components. Nevertheless, a few relevant studies have been performed.

(a) Dissociative Attachment

$$e^- + HF \rightarrow F^- + H$$

The onset for F^- formation is reported to have a threshold of 1.88 eV and a maximum at 4 eV.[12] The dissociation energy of HF is 6.1 eV[13] (D_o = 5.84 ± .01 eV) while the electron affinity of F is 3.448 ± .005 eV.[14] The thermodynamic limit, therefore, requires an appearance potential of 2.65 eV. The observed threshold of 1.88 eV implies that F^- is formed as soon as is thermodynamically possible.

(b) Associative Detachment

$$F^- + H \rightarrow HF(v,j) + e^-$$

This process is fast and occurs at a rate close to the Langevin rate constant with no temperature dependence. This implies little or not activation energy for the process and an attractive potential energy curve.[15]

(c) Vibrational Excitation

$$e^- + HF \rightarrow e^- + HF(v,j)$$

In each final vibrational state, a large (10^{-15} cm^2), sharply peaked cross section is observed at threshold.[16] A cross section of this magnitude was also observed for HCl. The cross section of both molecules have a maximum of much larger width which decreases monatonically thereafter. Since the cross sections are isotropic in the regions of the peaks, they do not result from electron-dipole long range interactions (direct vibrational excitation). The spectra presented by Rohr and Linder indeed indicate a very pronounced maximum for HCl in the region of about 2 to 3 eV. For HF, however, this second maximum is hardly discernible. It is therefore questionable whether these data support the existence of a broad maximum in the case of HF, although they clearly do for HCl.

Theoretical studies of HF^- are rather more prevalent than experimental investigations, but are nevertheless far from complete. Two ab initio calculations on the

ground state of $HF(^1\Sigma^+)$ and the ground state of $HF^-(^2\Sigma^+)$ find the HF^- state repulsive for all values of internuclear separation.[17,18] Bondebey et al., however, point out that the exclusion of diffuse functions from the basis set necessarily leads to a "diabatic" potential curve.[18] Since diffuse functions were not employed in either calculation, the fact that the negative ion state was found to be repulsive is not surprising. Although the two studies do agree qualitatively, one[17] finds the crossing of the $HF^-(^2\Sigma^+)$ potential with that of the $HF(^1\Sigma^+)$ at 3.9 bohr, while the other claims it to occur at 2.7 bohr.[18] In contrast to this finding, two other studies[19,20] reach an alternative conclusion. Both of the latter calculations find the $HF^-(^2\Sigma^+)$ ground state bound for a considerable range of R.

The fundamental approach to the calculation of resonances is the stabilization method.[21] Using square integrable (Gaussian) functions and Configuration Interaction, we have performed extensive CI calculations on the ground state of HF and the states of HF^- lying below about 9 eV. Since the procedure involves representing the limit of HF plus an electron at infinite separation within a basis set of functions of finite extent, it is necessary to establish each stable root as a resonance, and not simply as an artifact of the calculation. The results of this study provide an interpretation for the

experimentally observed features and clearly resolve the disagreement arising from the conclusions of previous theoretical calculations. Certain of the results also allow prediction of some characteristics not yet measured experimentally.

Techniques like those employed here were used successfully in an earlier study of HCl.[22] Although there are similarities between the states of HCl^- and HF^-, there are also important differences, and throughout this chapter we will refer to the previous work on HCl for comparison. We begin with a brief description of the computational method, then present the results for all calculated states, discuss the evidence of resonance character in the calculated negative ion states, and finally, examine the capability of the HF molecule to bind an electron.

Method

The atomic orbital basis set was chosen to be sufficiently flexible to represent both HF and HF^- for a range of internuclear distances. A Dunning basis the (9S/5P) primitive gaussian basis of Huzinaga,[23] contracted to (3S/2P) proved adequate, while the hydrogen was represented by the Dunning (2S) basis.[24] In addition to these functions, uncontracted Gaussian Rydbergs functions of exponent 0.036 and 0.0066, and P functions of exponent

0.074, 0.029 and 0.0054 were added to F. Finally, a P type polarization function of exponent 0.9 was added to hydrogen and a d type, of exponent 1.15, to fluorine. The complete atomic orbital basis set is shown in Table IV-1.

The SCF wave functions and energy for HF were calculated within this basis set. Of the 31 molecular orbitals comprising the basis, only one, that of lowest energy, was dropped from consideration in the CI calculations. Table IV-2 provides a list of the molecular orbitals and their eigenvalues. In the second column of this table, the M.O. identification system used in the text is given. The total SCF energy of HF at its equilibrium internuclear distance is -100.04905 a.u., which can be compared with the near Hartree-Fock value of -100.0705 a.u.[25]

The SCF virtual orbitals of HF were assumed to form an adequate basis for CI calculations on HF^-. This is justified by previous work on HCl,[22] which confirms the accuracy of this assumption. The SCF virtual orbitals of HF are eigenfunctions of the full n electron HF potential including its permanent dipole moment. Since, in a case of this type, the scattering is long range, the target molecule is relatively little perturbed by the scattering event. Consequently, the HF virtual orbitals are a good representation of the natural orbitals of HF^-.

Indeed, as we shall see later, this is generally verified by the dominance in the final CI wave functions by a single configuration.

Configuration Interaction calculations were performed for the ground states of HF and HF^-, as well as the excited states of HF^-. The HF^- states were described by populating the appropriate HF virtual orbital with a single electron. In general, one or more seed configurations were selected to represent a given state of interest. All single and double hole particle excitations relative to these few seed configurations were then generated to form the CI space. Solution of the CI problem was accomplished by the partitioning technique which was discussed in Chapter II.

Results and Discussion

Full CI calculations on HF and HF^- were carried out at a number of internuclear distances. Depending upon the particular state, full calculations were performed at more than one internuclear distance including 1.5 bohr, 1.732 bohr (equilibrium), 2.0 bohr, 2.5 bohr, 3.0 bohr, 4.0 bohr, 5.0 bohr, and 7.0 bohr. The potential curves resulting from these calculations are displayed in Figure IV-1, and their energies at the various internuclear distances are presented in Table IV-3. We will first describe the general procedure used in all calculations

and then discuss the results for each specific state separately.

General Procedure

In a study of this type, two important concepts must be considered. First, at any particular point on the potential surface, the HF and HF^- calculations must be balanced with respect to one another. This will allow reasonable interpretation of results involving the relative location of the HF and the HF^- states. Second, the calculations must permit proper dissociation behavior for the HF and the HF^- ground states, independent of one another. This second consideration is important for insuring confidence in the absolute results.

At the equilibrium internuclear distance, the HF ground state is dominated by the configuration $1\sigma^2 2\sigma^2 3\sigma^2 1\pi^4$, while the dominant configuration of the lowest HF^- state ($1^2\Sigma^+$) is $1\sigma^2 2\sigma^2 3\sigma^2 1\pi^4 4\sigma$. The higher HF^- Σ^+ states result from promotion of the additional electron to the higher Σ^+ molecular orbitals. At 7.0 bohr, which we use to represent the dissociation limit, the molecular orbital picture has altered considerably. The molecular orbital designated at 1π now falls lower in energy than the 3σ molecular orbital. Thus, at 7.0 bohr, the ordering of the occupied M.O.'s is $1\sigma^2 2\sigma^2 1\pi^4 3\sigma^2$.

The 3σ M.O., at this large distance, is composed of contributions from the H 1s and the F p_σ atomic orbitals. The 4σ M.O. is simply the antibonding complement to the 3σ M.O., and is only slightly higher in energy. The HF molecule which dissociates to $H(^2S) + F(^2P)$, is represented at 7.0 bohr by a linear combination of three electron configurations. The first is $1\sigma^2 2\sigma^2 1\pi^4 3\sigma^2$, the SCF base. The second, $1\sigma^2 2\sigma^2 1\pi^4 3\sigma 4\sigma$, contains one electron each in the bonding and antibonding H-F M.O.'s. The third, $1\sigma^2 2\sigma^2 1\pi^4 4\sigma^2$, has both electrons in the antibonding H-F M.O. In the case of HF^-, one electron already occupies the antibonding H-F M.O. Thus the $1^2\Sigma^+$ HF^- state, which dissociates to $H(^2P) + F^-(^1S)$, is represented simply by a linear combination of the two configurations $1\sigma^2 2\sigma^2 1\pi^4 3\sigma^2 4\sigma$ and $1\sigma^2 2\sigma^2 1\pi^4 3\sigma 4\sigma^2$. A higher HF^- state, the $5^2\Sigma^+$ given in Figure IV-3 is one of the states leading to the limit $H^-(^1s) + F(^2p)$. This latter state is presented by the same two electron configurations as the $1^2\Sigma^+$ HF^- state, this time, with opposite signs.

For the dissociation behavior of HF and HF^- to be adequately represented, this picture must be taken into account in the CI calculations. A proper calculation for HF must include all single and double excitations generated from three configurational bases, $1\sigma^2 2\sigma^2 1\pi^4 3\sigma^2$, the SCF base, as well as $1\sigma^2 2\sigma^2 1\pi^4 3\sigma 4\sigma$ and $1\sigma^2 2\sigma^2 1\pi^4 4\sigma^2$, the two configurations representing the H-F bond. For both the

$1^2\Sigma^+$ and the $5^2\Sigma^+$ states at 7.0 bohr, generation of all single and double excitations from the two configuration bases, $1\sigma^2 2\sigma^2 1\pi^4 3\sigma^2 4\sigma$ and $1\sigma^2 2\sigma^2 1\pi^4 3\sigma 4\sigma^2$ is adequate for decribing dissociation.

With the dissociation limit requirements in mind, the structure of the calculations for shorter internuclear separations is defined. At the equilibrium internuclear distance, the dominant contribution to the wavefunction is the SCF base. Although, at this point, the two additional bases used to generate configurations do not contribute as heavily to the wavefunction as at 7.0 bohr, they must be included to insure balance across the potential surface. Thus, at 1.732 bohr, the calculations on HF consisted of all single and double excitations from the SCF base in addition to two bases, $1\sigma^2 2\sigma^2 3\sigma 1\pi^4 10\sigma$ and $1\sigma^2 2\sigma^2 1\pi^4 10\sigma^2$. At this shorter distance, the 10σ M.O. has essentially the same character as the 4σ M.O. at 7.0 bohr. For the lowest state of HF^-, the bases included $1\sigma^2 2\sigma^2 3\sigma^2 1\pi^4 4\sigma$ and $1\sigma^2 2\sigma^2 1\pi^2 4\sigma 10\sigma^2$. At intermediate points on the potential surface, the calculations were performed in an analogous manner. Generally, in the HF calculations, all single and double excitations were generated from three bases, the SCF base, the base representing the configuration contributing most strongly to the wavefunction (a double excitation from the SCF base), and one other base representing a sort of "cross term"

(a single excitation from the SCF base). For the lowest HF^- state, two generating bases were used at each point. The first was formed by placing the additional electron in the lowest unoccupied molecular orbital of the SCF base for HF. The second was the same doubly excited configuration used in the HF calculations. Table IV-3 presents the configuration bases used at various distances for HF and the lowest HF^- state.

The higher states of HF^- were treated in the same manner as the $1^2\Sigma^+$ HF^- state, with the extra electron simply occupying successively higher Σ^+ molecular orbitals. The procedure resulted in a total space of about 8,400 configurations for the HF calculations. The HF^- calculations generally included between 11,000 and 13,000 total configurations. This procedure resulted in a reasonable balance in correlation energy between the HF ground state and the HF^- Rydberg states. At the equilibrium internuclear separation, the correlation energy of the HF^- states should be slightly greater than that of the HF ground state. The presence of the extra electron leads to a small polarization contribution to the energy, in addition to the correlation energy itself. We indeed find the correlation energy of all HF^- states to be slightly greater than that of HF.

HF $(1^1\Sigma^+)$. This state is described by the configuration $1\sigma^2 2\sigma^2 3\sigma^2 1\pi^4$ which represents about 99% of the

final wavefunction at the equilibrium internuclear separation. It goes smoothly to the limits $H(^2S) + F(^2P)$ with a calculated dissociation energy of 6.02 eV which can be compared to the experimental value for D_e of 6.1 eV.[13]

HF⁻ ($1^2\Sigma^+$). The $1^2\Sigma^+$ state was generated through occupation of M.O. 6, an S type Rydberg function. At the equilibrium nuclear separation, this configuration represents 99% of the total wavefunction. It has already been mentioned that, at larger internuclear distances, this HF^- state leads to the limit $H(^2S) + F^-(^1S)$. The state is clearly bound with respect to these limits, at least qualitatively confirming the results of two previous calculations,[19,20] and refuting those of two others.[17,20] This finding also agrees with the dissociative attachment results which indicate the state to be attractive into the autodetaching region. The calculated electron affinity of HF at 7.0 bohr is 3.17 eV which agrees rather well with the experimental electron affinity for F of 3.45 eV.[14]

It should be noted from Figure IV-1 and the values of Table IV-3 that the $1^2\Sigma^+$ state of HF^- appears to be bound at all distances relative to the HF ground state, implying a positive electron affinity of 0.010 eV for HF. This is in contrast to the results of earlier study on HCl, where the $1^2\Sigma^+$ state of HCl^- was found to lie about 0.12 eV above the HCl ground state.[22] The unbound nature

of the HCl^- state is not unexpected, however, since the dipole moment of HCl (1.1 D) is well below the critical dipole moment for binding an electron. We return later to a complete discussion of the bound or unbound nature of the $1^2\Sigma^+$ HF^- after presenting the results of the other calculated HF^- states.

$\underline{HF^- (2^2\Sigma^+)}$. This state occurs at the equilibrium internuclear distance through occupation of M.O. 9, essentially a Pσ Rydberg function. This configuration has a weight of 99% in the final CI wavefunction at 1.732 bohr. At this same distance, the state lies only 0.32 eV above the $1^2\Sigma^+$ HF^- ground state and corresponds to the $2^2\Sigma^+$ mimic state of HCl.[22]

$\underline{HF^- (3^2\Sigma^+)}$. The $3^2\Sigma^+$ state results from occupation of M.O. 10, also a Pσ type Rydberg function at the equilibrium internuclear distance. It, like the lower HF^- states, comprises 99% of the final CI wavefunction. This state lies about 1.7 eV above HF at equilibrium, and corresponds to a state in HCl^-, the $A^2\Sigma^+$, that was not considered to be a resonance.

$\underline{HF^- (4^2\Sigma^+)}$. This state occurs at equilibrium through occupation of M.O. 13, principally an S type Rydberg function. It lies about 2.3 eV above the HF ground state. This state, like the $3^2\Sigma^+$ state just discussed, is analogous in occupation to a second state of HCl^-, the $B^2\Sigma^+$, that was not considered to have resonance character.[22]

HF$^-$ ($5^2\Sigma^+$). The $5^2\Sigma^+$ state results from the occupation of M.O. 14 at equilibrium, largely an S type function. It is more radially contracted than the lower energy M.O.'s and corresponds in character to the $3^2\Sigma^+$ state of HCl$^-$ which is responsible for the broad resonance observed in the HCl vibrational excitation spectrum.[16] At the equilibrium internuclear distance, this state lies well above the ground state of HF, at about 6.7 eV. At longer distances, it crosses the repulsive $7^2\Sigma^+$ HF$^-$ state which will be discussed shortly.

HF$^-$ ($6^2\Sigma^+$). The $6^2\Sigma^+$ state occurs at the equilibrium internuclear distance through occupation of M.O. 17 a $p\sigma$ type M.O. which is valence in character. At short distances, this state also crosses the repulsive $7^2\Sigma^+$ state. We have indicated only a portion of this curve in Figure IV-1.

HF$^-$ ($7^2\Sigma^+$). This state is one of the Feshbach states of HF$^-$ and is considered in more detail in the next chapter. It crosses the $6^2\Sigma^+$ at about 9.7 eV and the $5^2\Sigma^+$ at approximately 7.3 eV. At 7.0 bohr, the $7^2\Sigma^+$ state (which has now become the $5^2\Sigma^+$ state) leads, together with the $4^2\pi$ state discussed below, to the limit $H^-(^1S) + F(^2P)$. We have indicated the adiabatic curves in Figure IV-1 for the crossings of this state with the $5^2\Sigma^+$; for its crossing with the $6^2\Sigma^+$ state we show the diabats. From the crossing of the $7^2\Sigma^+$ and the $5^2\Sigma^+$ states

we would predict H^- production to have a vertical onset with a maximum about 7.3 eV above the HF ground state.

In HCl^-, the situation is somewhat different. In this case, H^- production, which occurs at about 6.9 eV, results from a crossing of two $^2\Sigma^+$ states, only one of which corresponds in electron configuration to the two HF^- states.[22] The ascending state of HCl^- is a Σ^+ state lying above the broad resonance state in energy. The ascending state of HF^-, the $5^2\Sigma^+$ is the state that would lead to experimental observation of a broad resonance. The broad resonance in HF^- lies much higher in energy than the broad resonance in HCl^- by some 3.7 eV. It is therefore reasonable to assume that the $5^2\Sigma^+$ HF^- state is responsible for H^- production.

<u>HF^- ($3^2\pi$)</u>. This state occurs at the equilibrium internuclear distance through occupation of the π M.O.'s 15 and 16. It is shown in Figure IV-2 simply because it crosses the $4^2\pi$ state. There are two π states that lie lower in energy than the $3^2\pi$ formed by occupation of M.O.'s 7 and 8 ($1^2\pi$) and M.O.'s 11 and 12 ($2^2\pi$). Although we have not performed full CI calculations on these states, initial single configuration calculations indicate that the $1^2\pi$ lies between the $1^2\Sigma^+$ and the $2^2\Sigma^+$ and the $2^2\pi$ lies between the $3^2\Sigma^+$ and the $4^2\Sigma^+$.

<u>HF^- ($4^2\pi$)</u>. This state, together with the $7^2\Sigma^+$ state, leads to the limit $H^-(^1S) + F(^2P)$ at 7.0 bohr, It, like the

$7^2\Sigma^+$ HF^- state, is a Feshbach state of HF^-. It has an avoided crossing with the $3^2\pi$ state at shorter internuclear distances, indicated adiabatically in Figure IV-1.

The $4^2\pi$ HF^- state corresponds in electron configuration to the $^2\pi$ state of HCl^- shown in Figure II of reference 22. In the dissociative attachment of HCl^-, the $^2\pi$ state produces a second overlapping, gaussian shaped peak at 9.2 eV.[22] In HF^-, the $4^2\pi$ state could lead to a similar peak that would lie at about 10.2 eV.

Table IV-5 summarizes the results of the calculations and also presents the existing experimental data for comparison. We also show our estimates of certain experimental parameters and suggest the type of experimental investigation that might be used to determine them.

Limits

In this study, we have performed full CI calculations on the states leading to three limits: $H(^2S) + F^-(^1S)$, $H(^2S) + F(^2P)$, and $H^-(^1S) + F(^2P)$. With the aid of a simple MO picture, it is clear that the limits are produced by the states so indicated.

One state, the $1^2\Sigma^+$ state, leads to the limit $H(^2S) + F^-(^1S)$. At 7.0 bohr, the final wavefunction of this state is dominated by two electron configurations, $1\sigma^2 2\sigma^2 1\pi^4 3\sigma^2 4\sigma$ and $1\sigma^2 2\sigma^2 1\pi^4 3\sigma 4\sigma^2$ with signs that are in-phase with one another. At the true limit, these

configurations would have exactly equal weighting. At large distances, the 3σ M.O. is the bonding combination of the H 1s AO and the F pσ AO; the 4σ is essentially its antibonding complement. The linear combination of the two configurations in terms of the F pσ AO and the H 1s AO leads to equal weighting of $(H_{1s} + F_{p\sigma})^2$ $(H_{1s} - F_{p\sigma})$ and $(H_{1s} + F_{p\sigma})$ $(H_{1s} - F_{p\sigma})^2$. Upon expansion and summation of the two terms, we obtain H_{1s} $F^-_{p\sigma}$, which simply represents an H atom and an F^- atom.

Two states, the $5^2\Sigma^+$ and the $3^2\pi$, lead to the limit $H^-(^2S) + F(^2P)$ at 7.0 bohr. The $5^2\Sigma^+$ at long internuclear distances is largely composed of two configurations, $1\sigma^2 2\sigma^2 1\pi^4 3\sigma 4\sigma^2$ and $1\sigma^2 2\sigma^2 1\pi^4 3\sigma^2 4\sigma$. These are the same two configurations as those representing the $1^2\Sigma^+$ state. In this case, however, the configurations have signs that are out-of-plase with one another. Expansion of the configurations in terms of the A.O.'s leads to the occupation H^-_{1s} $F_{p\sigma}$ which represents an H^- atom and an F atom. The $3^2\pi$ state, at large internuclear separations is dominated by the configuration $1\sigma^2 2\sigma^2 1\pi^3 3\sigma^2 4\sigma^2$. Expansion of this configuration in terms of the A.O.'s also leads to the occupation H^-_{1s} $F_{p\sigma}$. From this simple M.O. picture, it is reasonable to assume that the $4^2\pi$ and the $7^2\Sigma^+$ HF^- states indeed lead to the limit $H^-(^1S) + F(^2P)$.

The $H(^2S) + F(^2P)$ limit is produced by two states. One of these states is the $HF(^1\Sigma^+)$ ground state discussed

earlier. The other, a $^1\pi$ state, is an excited state of HF considered in detail in the next chapter.

Other States

In initial single excitation calculations we observe three states, A, B and C, which fall between the limits $H(^2S) + F^-(^1S)$ and $H(^2S) + F(^2P)$ at 7.0 bohr. Two other states, the $5^2\Sigma^+$ and the $3^2\pi$, as already indicated, also fall within this energy region and lead to the limit $H^-(^1S) + F(^2P)$. The simple M.O. picture presented earlier supports the fact that these two states indeed lead to the $H^-(^1S) + F(^2P)$ limit. Of the three other states falling within the same energy region two, A and B, are Σ^+ states, while the third, C, is a π state.

The electron configurations contributing to the A and B states are $1\sigma^2 2\sigma^2 1\pi^4 3\sigma 4\sigma n6$, where $n \geq 5$. When $n > 5$, the $n\sigma$ M.O.'s are dominated by A.O. contributions either from $F_{p\sigma}$ or F_s. Formulation of these electron configurations in terms of the A.O.'s leads to $(H_{1s} + F_{p\sigma})(H_{1s} - F_{p\sigma})F^*$, where F* represents an excited $F_{p\sigma}$ or F_s AO. Expansion of the configurations produces terms in F^{--}. To our knowledge, F^{--} is not known to exist and we can only conclude that the states leading to the F^{--} limits also do not exist.

A similar situation arises in the case of the $c^2\pi$ state. A full CI calculation at 7.0 bohr places this

state between the $H^-(^1S)$ + $F(^2P)$ and the $H(^2S)$ + $F(^2P)$ limits in energy. The state is dominated by the electron configuration $1\sigma^2 2\sigma^2 1\pi^4 3\sigma 4\sigma 2\pi$. Expansion of this configuration in terms of the AOs again yields terms in F^{--}. We therefore feel that all three states are not real. All other states lie above the $H(^2S) + F(^2P)$ limit in energy and can probably be assumed to be real.

Comparison with HCl^-

In light of the current HF^- study, we have reviewed the results of the earlier study on HCl^-[22] for comparative purposes. Several points are of particular interest. First, the $1^2\Sigma^+$ state of HF^- is found to be bound by some 0.01 eV, while the $1^2\Sigma^+$ state of HCl^- lies above the HCl ground state. The unbound nature of the lowest HCl^- state is reasonable, given that the dipole moment of HCl is much less than that required for binding an electron.

The second point of interest involves the higher $^2\Sigma^+$ states of HCl^- and HF^-. In the HCl study, only those states that could be experimentally reported were calculated. Two states of HCl^-, the $A(^2\Sigma^+)$ and $B(^2\Sigma^+)$, that lie in energy between the reported $2^2\Sigma^+$ and $3^2\Sigma^+$ states were therefore not investigated. The states of HF^- corresponding to these two HCl^- states are the $3^2\Sigma^+$ and the $4^2\Sigma^+$. On the basis of the appearance of plots

of the density functional against distance from the HCl molecule, the two HCl^- states were not considered to be resonances.[22] We now question this conclusion. The plots of these states, when compared with those of the $3^2\Sigma^+$ and $4^2\Sigma^+$ HF^- states, do not seem to differ significantly. In the next section we return to this general point with a discussion of the difficulty of distinguishing those HF^- states that have resonance character from those which are simply continuum functions.

The final issue of importance in the comparison of HF^- and HCl^- involves the $2^2\Sigma^+$ and $3^2\Sigma^+$ HCl^- states and their counterparts, the $2^2\Sigma^+$ and the $5^2\Sigma^+$ states of HF^- In the work on HCl^-, these states were stated to merge with the continuum at longer internuclear distances. From the results of a series of single configuration CI calculations, it now appears that these states can still be followed at very large separations after an intermediate region of confusion. This is gratifying since the $2^2\Sigma^+$, $3^2\Sigma^+$, $4^2\Sigma^+$, and $5^2\Sigma^+$ HF^- states also remain relatively pure in calculations of this type to 7.0 bohr. This suggests that the behavior of the $^2\Sigma^+$ states of HCl^- and those of HF^- is similar.

One further difference should be noted. The $3^2\Sigma^+$ HCl^- valence state responsible for the broad resonance observed in the vibrational excitation spectrum has a minimum approximately 2.3 eV above the ground state of

HCl. According to Domcke and Cederbaum,[30] the half width of this state is 2.3 eV. In HF^-, the state corresponding to the $3^2\Sigma^+$ HCl^- state is the $5^2\Sigma^+$ which lies about 6 eV above the HF ground state. This is far higher in energy than the HCl^- state. The HF^- state was not observed in the vibrational excitation experiment of Rohr and] Linder.[16] This is not surprising, however, since the reported energy range extended only to about 3 eV. The results of Domcke and Cederbaum in the case of HF^- would require the state to have a half width of about 6 eV, which seems excessive.[30]

Proof of Resonance Character

A resonance or a temporary negative ion state is formed by the interaction of a target molecule with an incident electron. The electron is temporarily captured within the neighborhood of the molecule. The attachment of the electron can occur at a definite energy in which case, sharp structure is observed in the cross section. These states have a lifetime, τ, of between 10^{-10} and 10^{-15} sec where $\tau = h/\Gamma$ with Γ representing the width of the state. Experimental study of these states is possible when they decay into inelastic channels (rotational and vibrational excitation, electronic excitation, dissociative attachment, and so on). When the cross section is dominated by inelastic processes, then the

resonance contribution can be observed without interference from the direct scattering mechanism.

In addition to examining the energy dependence of the cross section, experimentalists can also observe the angular dependence of the cross section for the purpose of studying resonances. In studies of this type, the angular distribution can be uniquely determined through comparison of symmetries of the initial, resonant, and final state. When the resonant state is expanded in terms of spherical harmonics, the contribution from the lowest allowed value of ℓ predominates. In heteronuclear diatomic molecules, mixtures of these waves, called partial waves, are possible. It has been demonstrated[31] that pure partial waves of $p\sigma$ or $p\pi$ symmetry exhibit characteristic p wave shapes leading to a minimum in the cross section at 90° Pure waves of $d\sigma$, $d\pi$, or $d\delta$ symmetry alternatively produce a maximum at 90°. Mixtures of partial waves are also possible in heteronuclear molecules.

Theoretical methods for determining whether or not a state is a resonance have also been developed. In the original stabilization method,[21] frequently used for this purpose, heavy weights of a single or few configurations were used as a criterion to identify stable roots. These calculations, however, were generally performed on molecules without permanent dipole moments, so that no dominant fields were present. It is our experience, in the case

of molecules with permanent dipole moments[22] that purity of the vector is not particularly useful for establishing stability. In Configuration Interaction calculations on the negative ion states of these molecules, all states seem to give relatively pure CI vectors which represent successive Rydberg states in the field of a dipole.

One study on the states of LiF^- utilizes orbital amplitude plots for qualitative speculation on the character and width of states thought to be resonances.[32] In our earlier work on HCl^-, resonance character was attributed by the appearance of "stability" with the addition of very diffuse functions to the original basis set.[22] This approach was based on the assumption that the relative purity of the CI vectors indicates that the MO occupied by the scattered electron is a fair approximation to the natural orbital of the electron. A graph of the density functional of this MO plotted against distance for each state with and without addition of the diffuse functions provided qualitative "proof" of resonance character. States that are attempting to place the scattered electron at infinity appear increasingly sinusoidal with increasing flexibility of the basis set. Alternatively, those states possessing resonance character seem to show a high probability of the electron in the area of the target with sinusoidal behaviour at longer distance.

Another recent study,[33] which is also based on the assumption that calculated energy values for stable resonances will show only small changes with basis set variation, has adopted a somewhat different approach. Rather than enlarging the basis set, the study rather recommends varying the basis set continuously. This involves, for example, going from an original basis, $\alpha_i = \alpha_o \delta^i$ to a shifted basis, $\alpha_i = \alpha_o \delta^{i+1}$. For a stable eigenvalue, avoided crossings will appear.

Based on the previous work, we employed basically two general techniques for investigating the resonance character of each particular HF^- state. It was assumed throughout that the M.O. produced in an SCF calculation is a good representation of the natural orbital of the scattered electron. Thus MOs 6, 9, 10, 13 and 14 are reprsentative of the $1^2\Sigma^+$, $2^2\Sigma^+$, $3^2\Sigma^+$, $4^2\Sigma^+$ and $5^2\Sigma^+$ HF^- states respectively. The first technique simply involves comparison of the SCF energy and the M.O. eigenvalues in an altered bases set to those in the original basis set. If an M.O. indeed represents a resonant state, then the energy (eigenvalue) would be expected to remain relatively constant. The second technique consists of adding basis functions to the original basis set and visually observing the density of the M.O. This was accomplished by plotting, in confocal elliptical coordinates, the variation of the density functional with

distance from the two-center target molecule. We plot $\psi^2(\mu^2-\nu^2)\ D^3/8$, where μ and ν are functions of two coordinates x and y against the coordinate along the internuclear axis, x. The F atom lies at x=0 and the H atom is located a distance D(1.732 bohr) from the F atom in the positive x direction. The five variations of the original basis set which were considered are described in Table IV-6.

Table IV-7 presents the SCF eigenvalues for the M.O.'s of Σ^+ symmetry resulting from the original basis set (basis set #1) and the varied basis sets (basis set #2 through basis set #5). The first variation we will consider is the addition of very diffuse functions. In basis set #2, an s function with exponent 0.001 was added to fluorine. In basis set 3#, this function and an additional p function with the same exponent were added to fluorine. Since the added functions are much more diffuse than any contained within the original basis set, it would be expected that new M.O.'s would appear, with eigenvalues lower than those of the M.O.'s in the original basis set. The results of the SCF calculations indeed verify this. In basis set #2, the new M.O. falls much lower in energy and is dominated by the added function. Adding both S and P functions, as in basis set #3, creates two new M.O.'s of Σ^+ symmetry which also fall below the energy of the M.O.'s in the original basis set.

From the data for basis sets #2 and #3 in Table IV-6 and IV-7, we clearly observe the stability of the SCF energy and of the energy of the individual M.O.'s in the original basis set. For example, the eigenvalue of M.O. 6 in the original basis set changes by only about 0.002 A.U. (0.06 eV) in basis set #2, and by only slightly more, 0.003 (0.08 eV), in basis set #3. The change in eigenvalue for M.O. 6 on moving to the augmented basis sets is, in fact, the largest change in eigenvalue for any of the M.O.'s. This is to be expected since the added diffuse functions interact most strongly with the lowest lying M.O. These data indicate strongly that, since the energy of any given M.O. varies by at most, 0.08 eV, energy stability of all states considered here is preserved upon variation of the basis set.

In addition to the energy stability criteria, we have also made use of a technique used previously[22] for examining the change in appearance of the M.O.'s on moving to the augmented basis set. A graph of the density functional of the M.O. with distance along the internuclear axis provides an adequate two dimensional picture of each state. Figures IV-2 through IV-6 present these plots for M.O.'s 6, 9, 10, 13 and 14 respectively. Each state is shown for the original and the two augmented basis sets. The change in scale on the ordinate for the various M.O.'s should be noted. Figure IV-7 presents the

one additional Σ^+ M.O. created in basis set #2 and Figures IV-8 and IV-9 show the two additional M.O.'s formed in basis set #3. In each of these plots, the fluorine atom is at the zero point of the abcissa with the hydrogen 1.73 bohrs in the positive direction.

The character of the M.O.'s of the original basis set changes very little upon addition of the very diffuse functions, as illustrated by the plots. For an M.O. which is attempting to place the scattered electron at infinity, the density plots should show the electron density moving to further distances from the molecule. In none of the plots presented here, does this seem to occur. Rather, the addition of the more flexible functions appears to tighten the main peaks in each case. Comparison of the density plots of the states considered to be resonances with those for the M.O.'s formed with the addition of the more flexible functions points to an important difference. The newly formed M.O.'s appear to be a clear attempt to place the electron at infinity, since they show the bulk of their electron density at very large distance from the target.

The second variation we consider is the addition of diffuse functions to the original basis set. In basis set #4, two s and two p functions with exponents 0.003 and 0.006 were added, this time to the hydrogen atom. This addition resulted in three new Σ^+ M.O.'s between M.O. 6 and M.O. 14, and one new Σ^+ M.O. below M.O. 6 in

M.O. 14, and one new Σ^+ M.O. below M.O. 6 in energy. Upon addition of these functions, the SCF energy was lowered by only 0.00005 a.u. (.001 eV). The largest variation in eigenvalue is observed for M.O. 13 for which the energy increased by about 0.03 a.u. (0.85 eV). Basis set #5 represents the addition of both very diffuse and diffuse functions to the original basis sets. The SCF energy, in this case, was lower by 0.00008 a.u. (.002 eV) than the SCF energy of the original basis set. The M.O. that was again most affected by the changes was M.O. #13. The eigenvalue of this M.O. changed by some 0.04 a.u. (1.12 eV).

The density plots for the M.O.'s of basis sets #4 and #5 are presented in Figures IV-10 through IV-14 together with those of the original basis set for comparison.

In both basis set #4 and basis set #5, the new M.O.'s fall below M.O. 10 in energy. We should therefore expect that the M.O.'s most perturbed by the augmentation would be M.O. 6 and M.O. 9. Figures IV-10 through IV-14 indeed show this to be the case. The curves of Figure IV-10 illustrate that M.O. 6 may not be a resonance. Addition of diffuse functions causes the main peak to move much farther from the molecule, behavior that is not expected in a resonance. We have considered the possibility that these M.O.'s of basis sets #4 and #5 thought

to be the same as M.O. 6 in the original basis set have not been correctly assigned. If, instead the M.O.'s with eigenvalue 0.01225 a.u. of basis set #4 and eigenvalue of 0.00967 a.u. of basis set #5 in Table IV-7 are assigned, we obtain the density functionals of Figure IV-15. This alternative assignment supports the attribution of resonance character to M.O. 6. In basis sets #4 and #5, the main peak is in approximately the same location as it was in basis set #1. Although in the two altered basis sets, density is building at longer range, this is not unexpected for a resonance when diffuse functions are introduced. M.O.'s 9, 10, 13, and 14 as shown in Figure IV-11 through IV-14 also changed minimally upon introduction of the additional functions.

We have examined numerous other basis set additions that are not presented here. New functions of both diffuse and valence character were added to both H and F. In all cases, the M.O.'s of the original basis set with which the added functions interacted strongly were the most affected by the additions. This suggests that altering the basis set and observing little change in the appearance of the M.O. is not a sufficient criterion for judging resonance character. Our experience indicates that the appearance of any M.O. can be changed considerably simply by judicious choice of additional functions. Further studies of this type on molecules

with known resonances are necessary to establish definitive criteria for assignments of resonance character.

The Bound State

Because the bound or unbound nature of the lowest HF state is a subject of much debate, we sought to better understand the results of our calculations by further investigation. The resonances of HF^- that result from the addition of one electron to a Rydberg orbital of HF arise primarily from the permanent and induced dipolar forces. The $1^2\Sigma^+$ HF^- state is one such resonance, as mentioned earlier. In the HF molecule, for which the permanent dipole moment is only slightly greater than that necessary for binding an electron, the binding energy is undoubtedly extremely small. In C.I. calculations of the type described here, the error in energy may be as high as 0.1 eV. This is a factor of 10 larger than the binding energy we calculate (0.01 eV). Because this is so, our results do not show unequivocally that HF is capable of binding an electron.

One method of investigating the reliability of the calculated results is to consider the forces contributing to the bound nature of a state. One of these forces is the permanent dipole moment. A calculation performed for HF at the equilibrium internuclear distance at the CI level yielded a value of 2.01 D for the dipole moment which

is well above the experimental value of 1.82 D. The other factor contributing to the forces generated in the molecule is the polarizability. The experimental value of this variable for HF is about 16.6 a_o^3 (2.5 $\AA^3$).[29] According to reference 8, a molecule with a permanent dipole moment as low as 2D and an average molecular polarizability of between 20 and 40 a_o^3 should have the capability to bind an electron by 0.01 eV. This result also allows rotation of the molecule which contributes positively to the energy of the negative ion. The CI calculations used in this work do not include the effects of rotation. Our calculated dipole moment of 2.01 D, together with the experimental polarizability of 16.6 a_o^3 implies that our calculations should find HF bound by something less than 0.01 eV. Our calculated electron affinity (0.01 eV), given the inherent inaccuracy of the method, seems to be at least of the proper order of magnitude. Unfortunately, because the value obtained for the electron affinity is so close to zero, it cannot be stated with certainty from the results of the calculations that the HF^- state is bound.

Another method of testing the bound or unbound nature of the state was employed. This technique involved augmenting the original basis set with a diffuse s function of exponent .001 on the H atom. In the SCF calculation, the new Σ^+ molecular orbital fell energetically

below the molecular orbital occupied by the single electron in the original $1^2\Sigma^+$ HF^- state. Table IV-8 presents the eigenvalues and total SCF energy for the original and altered basis set at 1.732 bohr. CI calculations were then performed for HF^- at the equilibrium internuclear separation within the new basis set. In the first calculation, the additional electron occupied the original M.O. (the LUMO + 1). In the second calculation, the additional electron occupied the new Σ^+ M.O. (the LUMO). In the third calculation, the HF ground state was calculated within the new basis set. Table IV-9 gives the results of these calculations and, for comparison, the results of the CI calculations in the original basis set.

In the altered basis, the HF ground state falls below the original HF ground state by 0.005 eV. The HF^- state with the extra electron occupying the new Σ^+ M.O. lies below the new HF ground state by 0.168 eV. The HF^- state with the extra electron occupying the original Σ^+ M.O. now lies above the new HF ground state by 0.046 eV. Since the original and new HF ground state energies differ by only 0.005 eV, the HF^- $1^2\Sigma^+$ state remained constant in energy to within 0.051 eV.

The implications of this exercise are important. It may be that the functions necessary for properly describing the HF^- ground state were not included in the original basis set. The additional flexibility of the

basis set achieved through the addition of a diffuse function may in fact provide the true picture of an unbound HF^- ground state. The results are simply not definitive regarding the bound nature of the $1^2\Sigma^+$ HF^- state. It could be that, since the energy of the original state rose above the HF ground state after augmentation of the basis set, the state is not bound. Indeed, this is probably so. Whether or not the HF molecule can, in reality, bind an electron is not in question. Theory has shown that it is certainly possible. Our calculated dipole moment exceeds the experimental value by some 0.2 D. This fact makes it more likely that the results of our calculations will lead to a bound HF^- state. That we find a bound state within our original basis set is therefore not surprising. Although our results do not allow an unequivocal conclusion on the bound or unbound nature of HF, they are significant for at least two other reasons. First, we have illustrated through extensive CI calculations that, within a basis set that includes diffuse functions, the HF molecule can probably bind an electron if the calculated dipole moment is as high as 2.0 D. We cannot speculate on what the results would be if the dipole moment were lower. The second reason for the importance of these calculations lies in the fact that they provide guidance for other ab initio studies. Polar molecules with

permanent dipole moments slightly in excess of HF should certainly be the subject of further investigation.

Conclusions

The calculated potential curves presented in this work are in good agreement with the existing experimental data. Moreover, some of the results of the study are useful for guidance in future experimental investigations. It appears that the computational techniques employed in this study are effective for theoretical study of the negative ion states of polar molecules.

The presence of a permanent dipole moment in HF gives rise to presumed resonances that cannot be intuited from the separated atom limits. That all the states described here are in fact resonances cannot be proven definitively. Nevertheless, the technique we have utilized for probing the problem providesat least a strong indication that the states of HF^- indeed possess resonance character.

Whether or not the $1^2\Sigma^+$ HF^- state is bound also cannot be unequivocally determined from this study. We find this state bound by only 0.010 eV, a value which is small compared with the accuracy of the calculational procedure. We can only conclude with certainty that the $1^2\Sigma^+$ state of HF^- lies extremely close in energy to the HF ground state and is therefore either slightly bound or slightly unbound.

References

1. M.H. Mittleman and V.P. Myerscough, Phys. Lett. 23, 545 (1966).
2. J.E. Turner and K. Fox, Phys. Lett. 23, 547 (1966).
3. W.B. Brown and R.E. Roberts, J. Chem. Phys. 46, 2006 (1967).
4. O.H. Crawford, Proc. Phys. Soc. 91, 279 (1967).
5. μ = 1.625 D = 1.625 debye, where 1 D = 10^{-18} esu cm.
6. W.R. Garrett, Mol. Phys. 20, 751 (1971).
7. W.R. Garrett, Phys. Rev. A3, 961 (1971).
8. W.R. Garrett, J. Chem. Phys. 69, 2621 (1978).
9. Jordan and Wendolowski, paper given, ref. 13.
10. K.D. Jordan and J.J. Wendoloski, Chem. Phys. 21, 145 (1977).
11. R. Weiss, Phys. Rev. 113, 659 (1963).
12. D.C. Frost and C.A. McDowell, J. Chem. Phys. 29, 503 (1958).
13. J. Berkowitz, W.A. Chupka, P.M. Guyon, J.H. Holloway, and R. Spoler, J. Chem. Phys. 54, 5165 (1971).
14. R.S. Berry and C.W. Reimann, J. Chem. Phys. 38, 1440 (1963).
15. F.C. Fehsenfeld et al., J. Chem. Phys. 58, 5841 (1973).
16. K. Rohr and F. Linder, J. Phys. B, Atom. MOlec. Phys. 9, 2521 (1976).

17. H.H. Michels, F.E. Harris and J.C. Browne, J. Chem. Phys. 48, 2821 (1968).

18. V. Bondybey, P.K. Pearson and H.F. Shaefer III, J. Chem. Phys. 57, 1123 (1972).

19. A.W. Weiss and M. Krauss, J. Chem. Phys. 52, 4363 (1969).

20. W.M. Hartmann, T.L. Gilbert, K.A. Kaiser and A.C. Wahl, Phys. Rev. B, 2 1140 (1970).

21. H.S. Taylor and A. Hazi, Phys. Rev. A, 14, 2071 (1976).

22. E. Goldstein, G.A. Segal and R.W. Wetmore, J. Chem. Phys. 68, 271 (1978).

23. S. Hazinaga, J. Chem. Phys. 42, 1293 (1969).

24. T.H. Dunning and P.J. Hays, "Modern Theoretical Chemistry", Volume 3, H.F. Shaefer Ed., Plenum Press, New York, N.Y. (1977).

25. A.D. McLean and M. Yoshimine, J. Chem. Phys. 47, 3256 (1967).

26. G.A. Segal and R.W. Wetmore, Chem. Phys. Lett. 32, 556 (1975).

27. G.A. Segal and R.W. Wetmore, Chem. Phys. Lett. 36, 478 (1975).

28. G.A. Segal, R.W. Wetmore and K.A. Wolf, Chem. Phys. 30, 269 (1977).

29. J.O. Hirschfelder, C.F. Curtiss and R.B. Bird, Molecular Theory of Gases and Liquids (John Wiley and Sons, New York, 1954).

30. W. Domcke and L.S. Cederbaum, to be published.

31. F.H. Read, J. Phys. B1, 893 (1968).

32. W.J. Stevens, J. Chem. Phys., to be published.

33. A. Macias and A. Riera, J. Sociela Chemica Italiana, 108, 329 (1978).

AD-A093 754 RAND CORP SANTA MONICA CA F/G 7/4
AB INITIO CONFIGURATION INTERACTION CALCULATIONS ON THE STATES --ETC(U)
SEP 80 K A WOLF
UNCLASSIFIED RAND/P-6535 NL

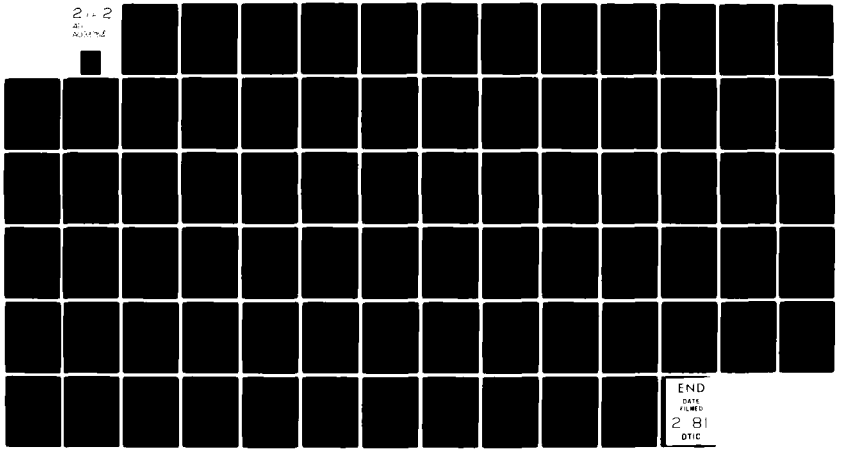

END
DATE FILMED
2 81
DTIC

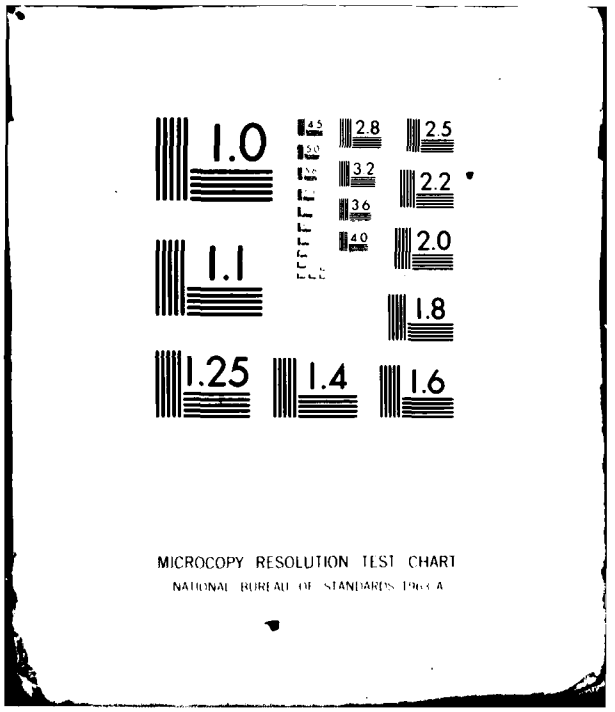
1.0
1.1
1.25
1.4
1.6
1.8
2.0
2.2
2.5
2.8
3.2
3.6
4.0
4.5
5.0
MICROCOPY RESOLUTION TEST CHART
NATIONAL BUREAU OF STANDARDS 1963-A

Table IV-1

Gaussian Basis Set

Fluorine		Hydrogen	
ξs	[5s]	ξs	[2s]
9995.0	0.001166	13.36	0.032828
1506.0	0.008870	2.013	0.231204
350.3	0.042380	0.4538	0.817226
104.1	0.142929		
34.84	0.355372	0.1233	1.000000
12.22	0.462085		
4.369	0.140848		[1p]
12.22	-0.148452	1.000000	1.000000
1.208	1.05527		
0.3634	1.000000		
0.036	1.000000		
0.0066	1.000000		
ξp	[5p]		
44.36	0.020876		
10.08	0.130107		
2.996	0.396166		
0.9383	0.620404		
0.2733	1.000000		
0.074	1.000000		
0.029	1.000000		
0.0054	1.000000		
ξd	[1d]		
1.15	1.000000		

Table IV-2

SCF Results for HF (R = 1.732 bohr)

M.O.	Text Notation	Symmetry	Eigenvalue (a.u.)
1	1σ	Σ^+	-26.29879
2	2σ	Σ^+	-1.60169
3	3σ	Σ^+	-0.76886
4	1π	π	-0.65063
5		π	-0.65063
6	4σ	Σ^+	0.00696
7	2π	π	0.01335
8		π	0.01335
9	5σ	Σ^+	0.01511
10	6σ	Σ^+	0.06850
11	3π	π	0.07965
12		π	0.07965
13	7σ	Σ^+	0.09187
14	8σ	Σ^+	0.26703
15	4π	π	0.30504
16		π	0.30504
17	9σ	Σ^+	0.32973
18	10σ	Σ^+	0.92540
19	11σ	Σ^+	1.33003
20	5π	π	1.34772
21		π	1.34772
22	12σ	Σ^+	1.71036
23	6π	π	1.84189
24		π	1.84189
25	13σ	Σ^+	2.75878
26	1Δ	Δ	2.91399
27		Δ	2.91399

Table IV-2 (continued)

M.O.	Text Notation	Symmetry	Eigenvalue (a.u.)
28	7π	π	3.35095
29		π	3.35095
30	14σ	Σ^+	4.17831
31	15σ	Σ^+	5.65648

Total Energy: -100.04905 a.u.

Nuclear Repulsion Energy = 5.19630 a.u.

Total Electronic Energy = -105.24535 a.u.

Table IV-3

Calculated CI Energy Points [a]

		1.5 bohr	1.732 bohr	2.000 bohr	2.5 bohr	3.0 bohr	4.0 bohr	5.0 bohr	7.0 bohr
HF	$1^1\Sigma^+$	0.771	0.010	0.346	2.056	3.644	--	5.932	6.025
HF^-	$1^2\Sigma^+$	0.739	0	0.246	1.661	2.311	--	2.782	2.852
	$2^2\Sigma^+$	1.088	0.324	0.510	2.114	4.559	--	--	--
	$3^2\Sigma^+$	2.526	1.698	1.776	2.626	4.841	--	--	--
	$4^2\Sigma^+$	3.038	2.298	2.662	4.423	6.277	--	--	--
	$5^2\Sigma^+$	8.105	6.736	5.869	6.078	7.693	5.819	--	--
	$6^2\Sigma^+$	--	--	8.811	10.324	--	--	--	--
	$7^2\Sigma^+$	--	13.611	11.338	8.726	--	--	--	--
	$3^2\pi$	8.808	8.117	--	9.952	--	5.824	--	5.626
	$4^2\pi$	--	10.209	8.701	7.230	--	--	--	--

Table IV-3 (continued)

[a] Relative to HF^- at equilibrium, E = 2727.440 eV.

Table IV-4

Configuration Bases for the Ground States of HF and HF^-

R (bohr)	HF	HF^-
1.5	$1\sigma^2 2\sigma^2 3\sigma^2 1\pi^4$ $1\sigma^2 2\sigma^2 3\sigma 1\pi^4 10\sigma$ $1\sigma^2 2\sigma^2 1\pi^4 10\sigma^2$	$1\sigma^2 2\sigma^2 3\sigma^2 1\pi^4 4\sigma$ $1\sigma^2 2\sigma^2 1\pi^4 4\sigma 10\sigma^2$
1.732	$1\sigma^2 2\sigma^2 3\sigma^2 1\pi^4$ $1\sigma^2 2\sigma^2 3\sigma 1\pi^4 10\sigma$ $1\sigma^2 2\sigma^2 1\pi^4 10\sigma^2$	$1\sigma^2 2\sigma^2 3\sigma^2 1\pi^4 4\sigma$ $1\sigma^2 2\sigma^2 1\pi^4 4\sigma 10\sigma^2$
2.0	$1\sigma^2 2\sigma^2 3\sigma^2 1\pi^4$ $1\sigma^2 2\sigma^2 3\sigma 1\pi^4 8\sigma$ $1\sigma^2 2\sigma^2 1\pi^4 8\sigma^2$	$1\sigma^2 2\sigma^2 3\sigma^2 1\pi^4 4\sigma$ $1\sigma^2 2\sigma^2 1\pi^4 4\sigma 8\sigma^2$
2.5	$1\sigma^2 2\sigma^2 3\sigma^2 1\pi^4$ $1\sigma^2 2\sigma^2 3\sigma 1\pi^4 6\sigma$ $1\sigma^2 2\sigma^2 1\pi^4 6\sigma^2$	$1\sigma^2 2\sigma^2 3\sigma^2 1\pi^4 4\sigma$ $1\sigma^2 2\sigma^2 1\pi^4 4\sigma 6\sigma^2$
3.0	$1\sigma^2 2\sigma^2 1\pi^4 3\sigma^2$ $1\sigma^2 2\sigma^2 1\pi^4 3\sigma 4\sigma$ $1\sigma^2 2\sigma^2 1\pi^4 4\sigma^2$	$1\sigma^2 2\sigma^2 1\pi^4 3\sigma^2 4\sigma$ $1\sigma^2 2\sigma^2 1\pi^4 3\sigma 4\sigma^2$
5.0	$1\sigma^2 2\sigma^2 1\pi^4 3\sigma^2$ $1\sigma^2 2\sigma^2 1\pi^4 3\sigma 4\sigma$ $1\sigma^2 2\sigma^2 1\pi^4 3\sigma$	$1\sigma^2 2\sigma^2 1\pi^4 3\sigma^2 4\sigma$ $1\sigma^2 2\sigma^2 1\pi^4 3\sigma 4\sigma^2$

Table IV-4 (continued)

R (bohr)		
7.0	$1\sigma^2 2\sigma^2 1\pi^4 3\sigma^2$ $1\sigma^2 2\sigma^2 1\pi^4 3\sigma 4\sigma$ $1\sigma^2 2\sigma^2 1\pi^4 4\sigma^2$	$1\sigma^2 2\sigma^2 1\pi^4 3\sigma^2 4\sigma$ $;\sigma^2 2\sigma^2 1\pi^4 3\sigma 4\sigma^2$

Table IV-5

Summary of Observed and Calculated Results

	Observed	Calculated	Suggested Experiment
HF^- $1^2\Sigma^+$	> 1.88	-0.01	
HF^- $5^2\Sigma^+$	--	5.87	Vibrational Excitation
HF^- $5^2\Sigma^+$	--	7.3	Electron Impact
HF^- $4^2\pi$	--	10.2	
F^- + H	--	2.9	
F + H^-	--	7.3	Dissociative Attachment
Electron Affinity F	3.45	3.17	
Dissociation Energy HF	6.1	6.02	

Table IV-6

Original and Altered Basis Set Description

Basis Set #	Variation	SCF Total Energy (au)
1	Original	-100.04905
Very Diffuse		
2	Original + ξ = .001	
	F(s)	-100.04905
3	Original + ξ = .001	
	F(s,p)	-100.04906
Diffuse		
4	Original + ξ = .006, .003	
	H(s,p)	-100.04911
Diffuse + Very Diffuse		
5	Original + ξ =.006, .003, .002, .001	
	H(s) + = .006, .003 H(p)	-100.04913

Table IV-7

Σ^+ M.O. SCF Eigenvalues for Original and Altered Basis Sets

M.O. #	Basis Set 1	2	3	4	5
1	-26.29879	-26.29880	-26.29881	-26.29709	-26.29788
2	-1.60169	-1.60170	-1.60171	-1.60113	-1.60143
3	-0.76886	-0.76887	-0.76887	-0.76834	-0.76858
			0.00093		0.00077
		0.00121	0.00274	0.00217	0.00337
6	0.00696	0.00924	0.00977	0.00615	0.00647
				0.01225	0.00967
					0.01978
9	0.01511	0.01592	0.01735	0.02001	0.02196
				0.02161	0.02242
				0.03603	0.04617
10	0.06850	0.06967	0.07051	0.08117	0.08168
13	0.09187	0.09396	0.09437	0.12321	0.13316
14	0.26703	0.26782	0.26847	0.27758	0.27779

Table IV-8

SCF Energy and Eigenvalues for Original and Altered Basis Sets (au)

	Original Basis Set	Altered Basis Set
SCF Energy	-100.04905	-100.04905
Eigenvalues		
New M.O.	--	+0.00114
Original M.O.	+0.00696	+0.00936

Table IV-9

CI Energy within the Original and Altered Basis Set (eV)

	Original Basis Set	Altered Basis Set
HF Ground State Energy	-2727.430	-2727.435
HF^- State Energy (New M.O.)	--	-2727.603
HF^- State Energy (Original M.O.)	-2727.440	-2727.389

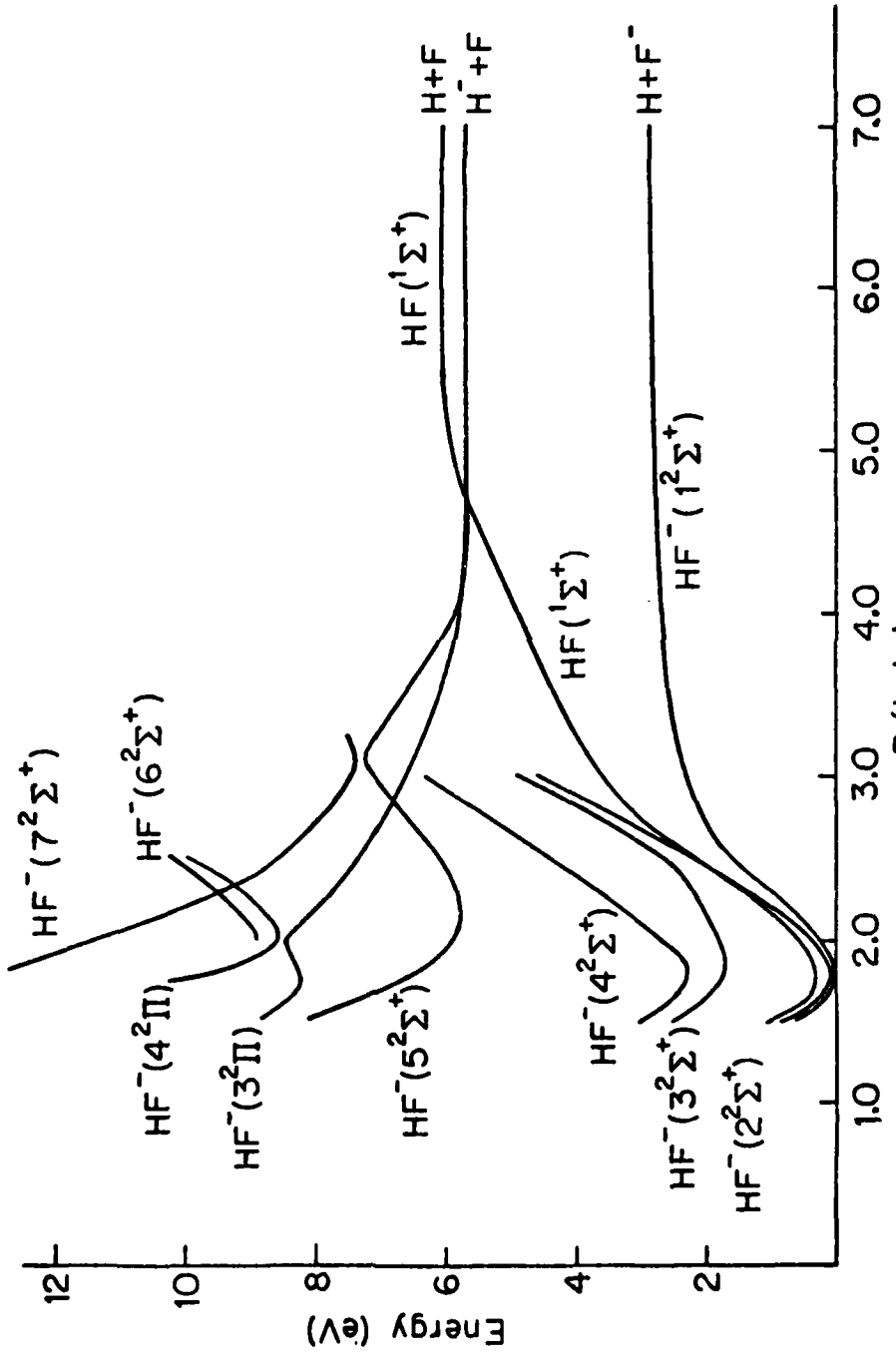

Fig. IV-1--Gaussian Basis Set

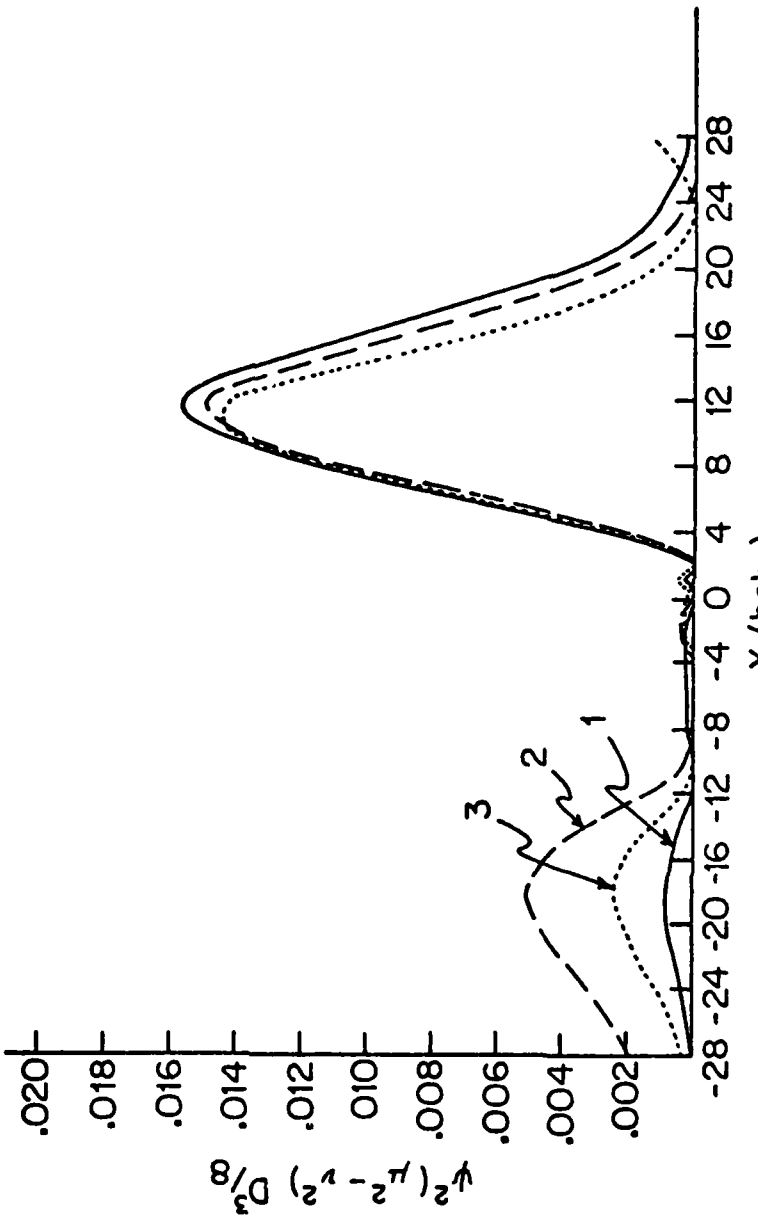

Fig. IV-2--M.O. 6 -- Basis Sets 1, 2 and 3

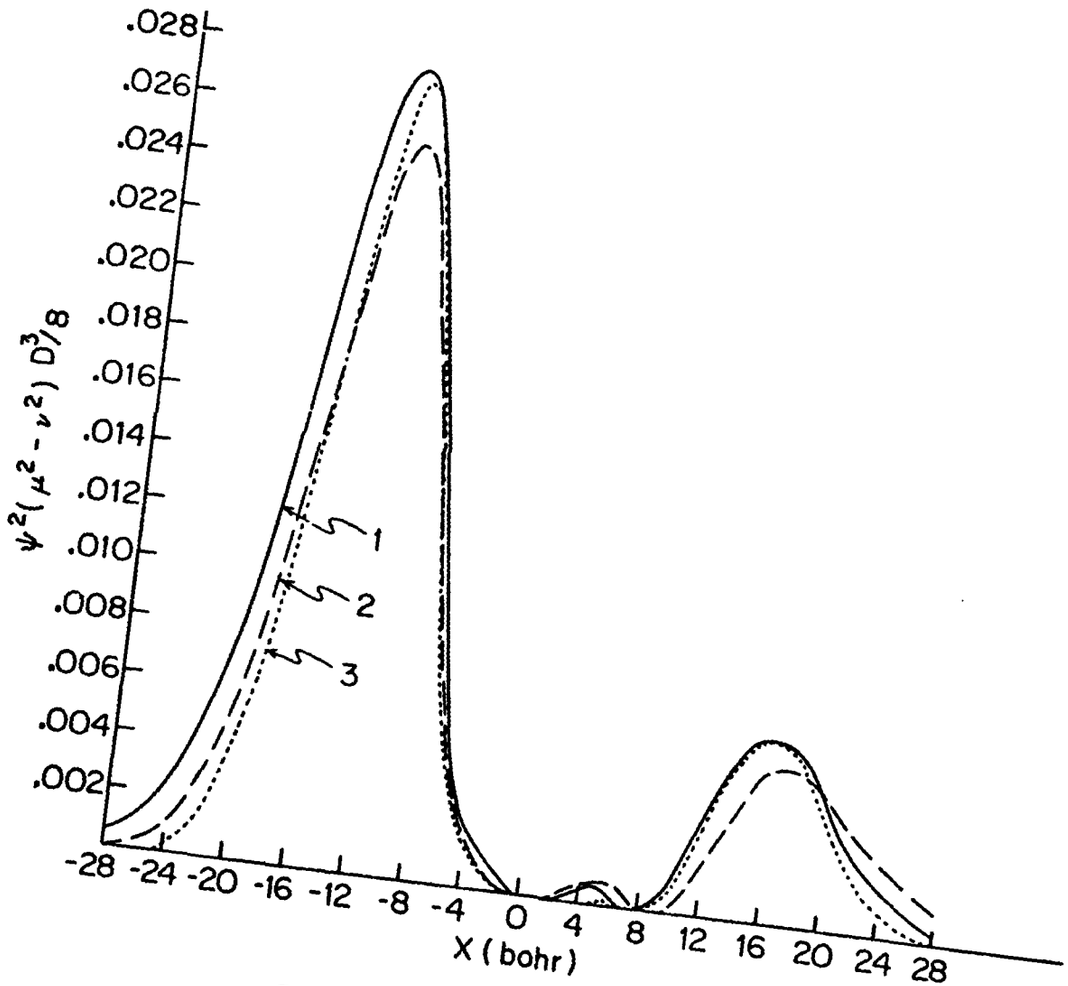

Fig. IV-3--M.O. 9 -- Basis Sets 1, 2 and 3

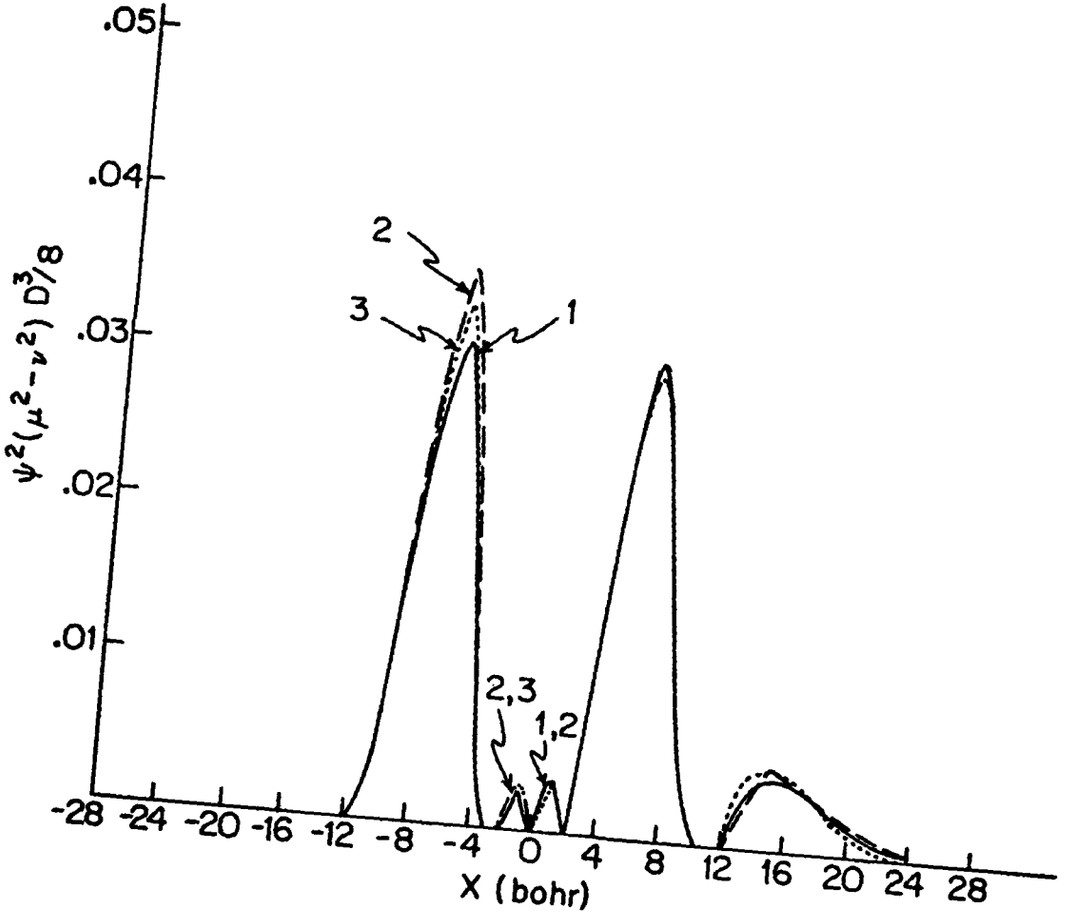

Fig. IV-4--M.O. 10 -- Basis Sets 1, 2 and 3

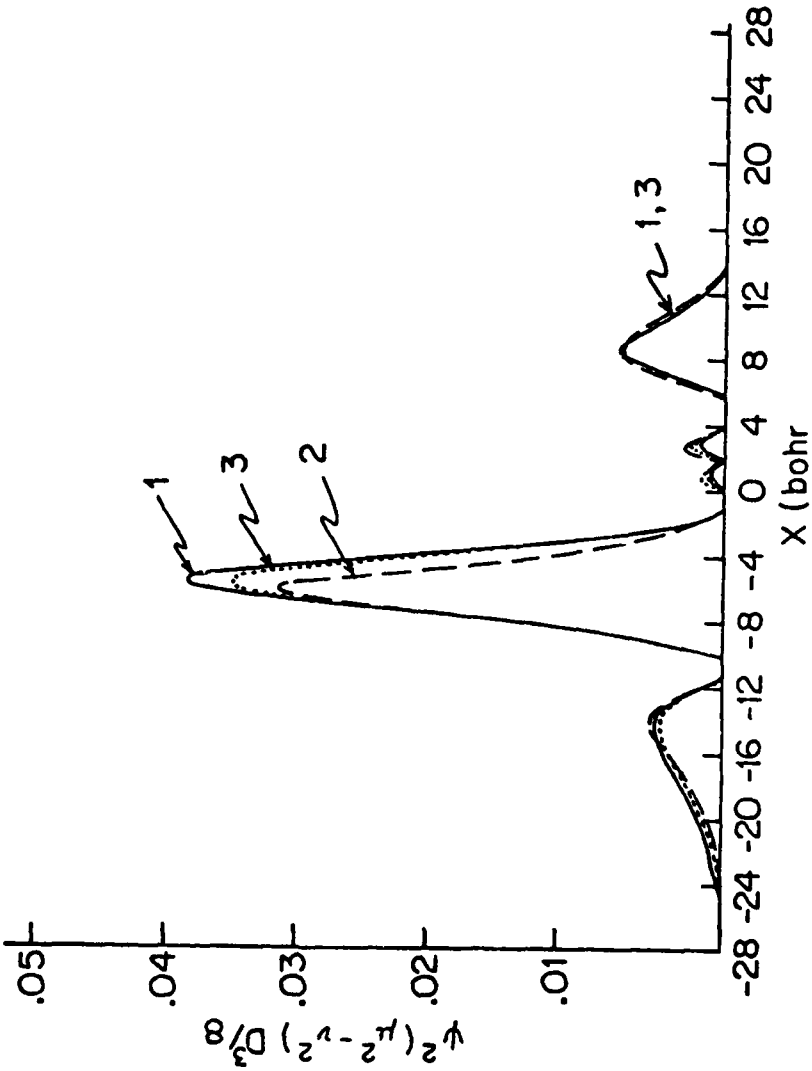

Fig. IV-5--M.O. 13 -- Basis Sets 1, 2 and 3

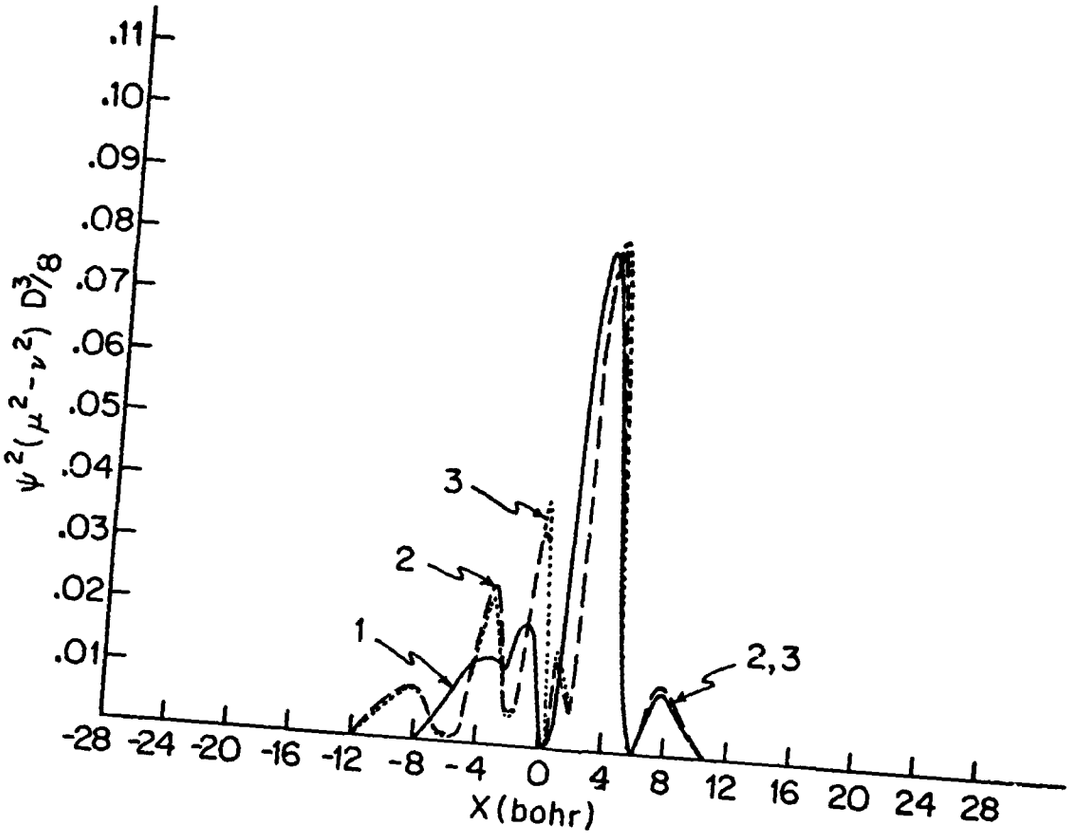

Fig. IV-6--M.O. 14 -- Basis Sets 1, 2 and 3

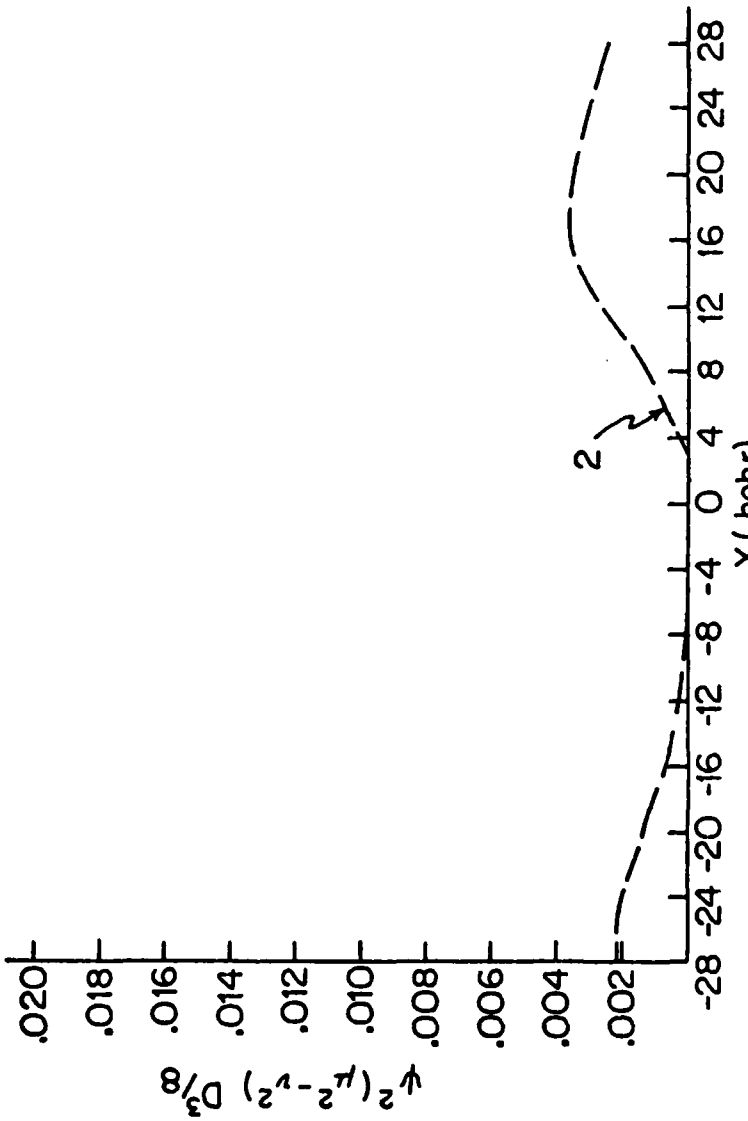

Fig. IV-7--New M.O. -- Basis Set 2

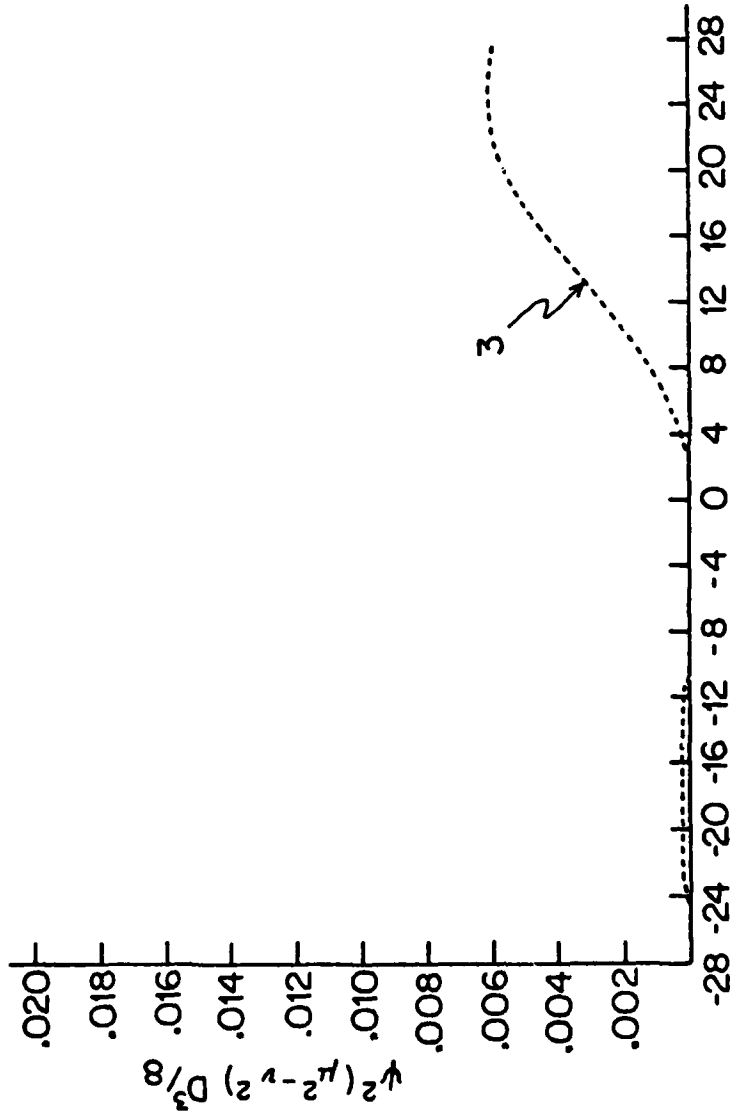

Fig. IV-8--New M.O. 1 -- Basis Set 3

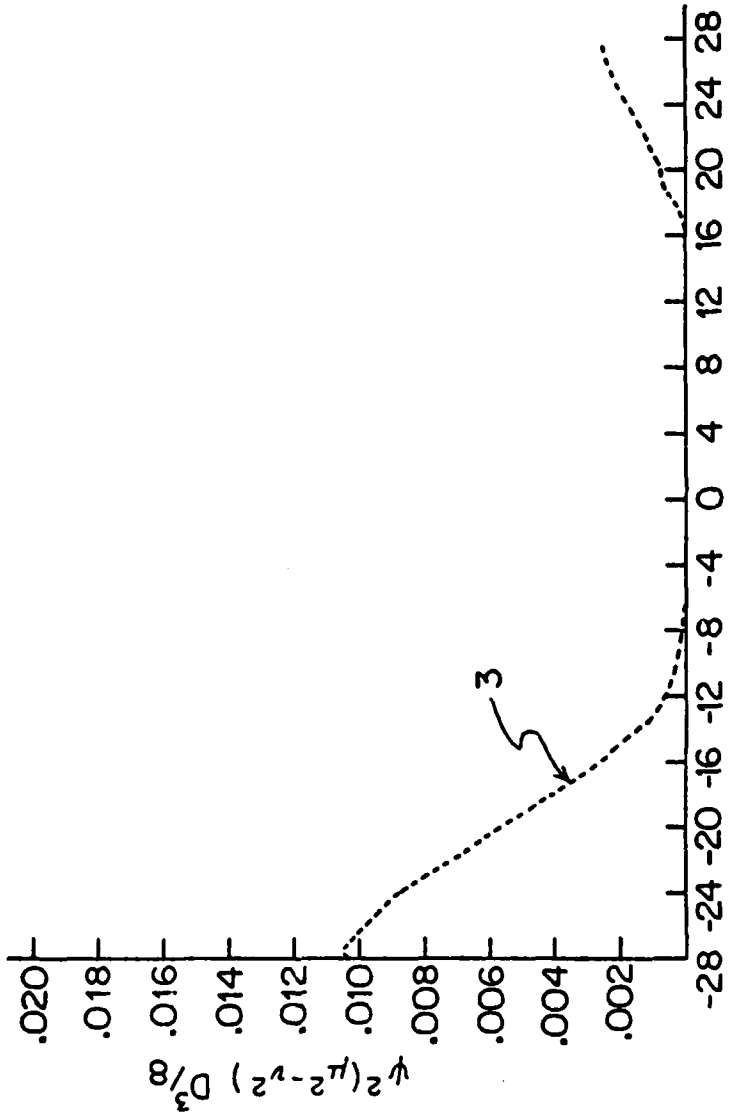

Fig. IV-9--New M.O. 2 -- Basis Set 3

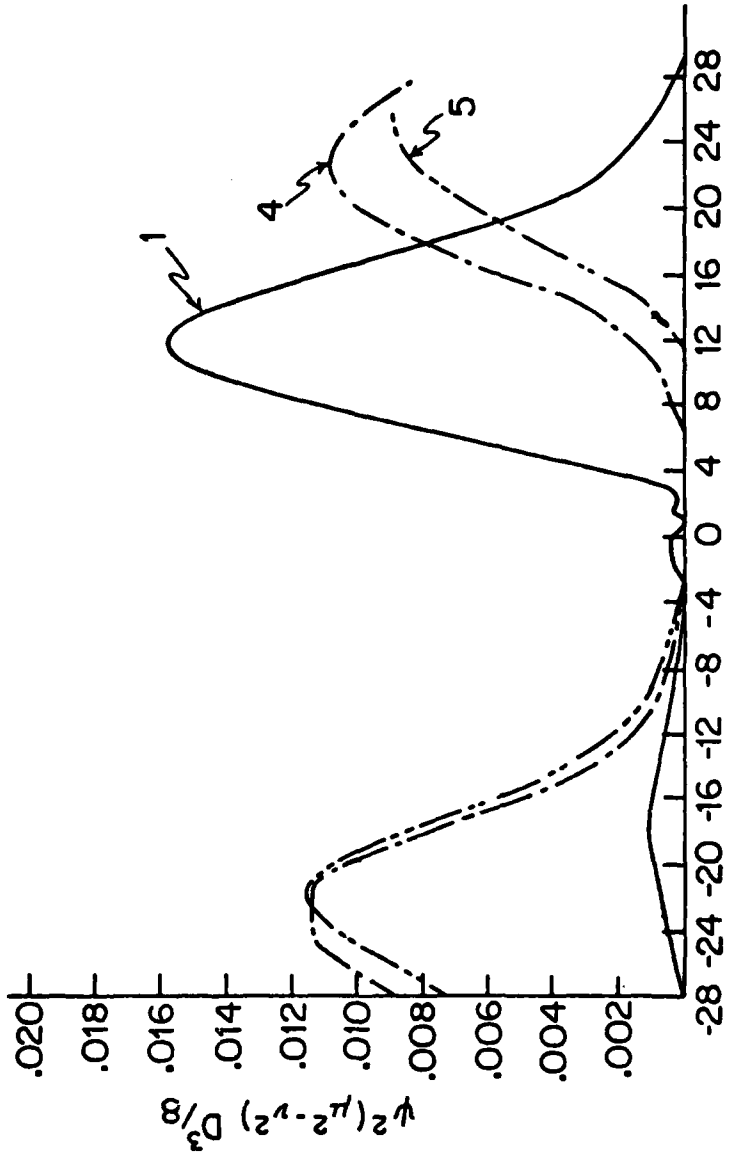

Fig. IV-10--M.O. 6 -- Basis Sets 1, 4 and 5

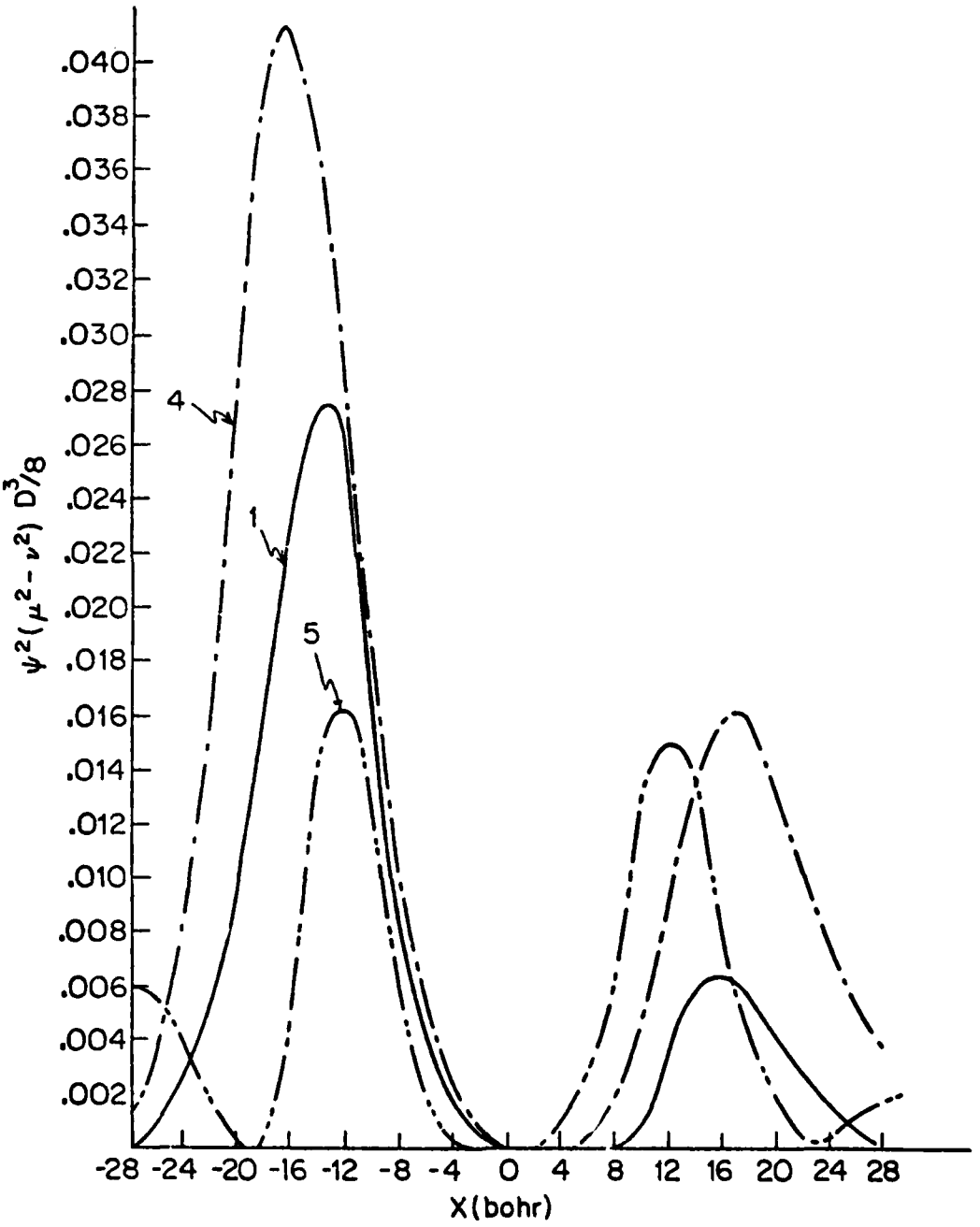

Fig. IV-11--M.O. 9 -- Basis Sets 1, 4 and 5

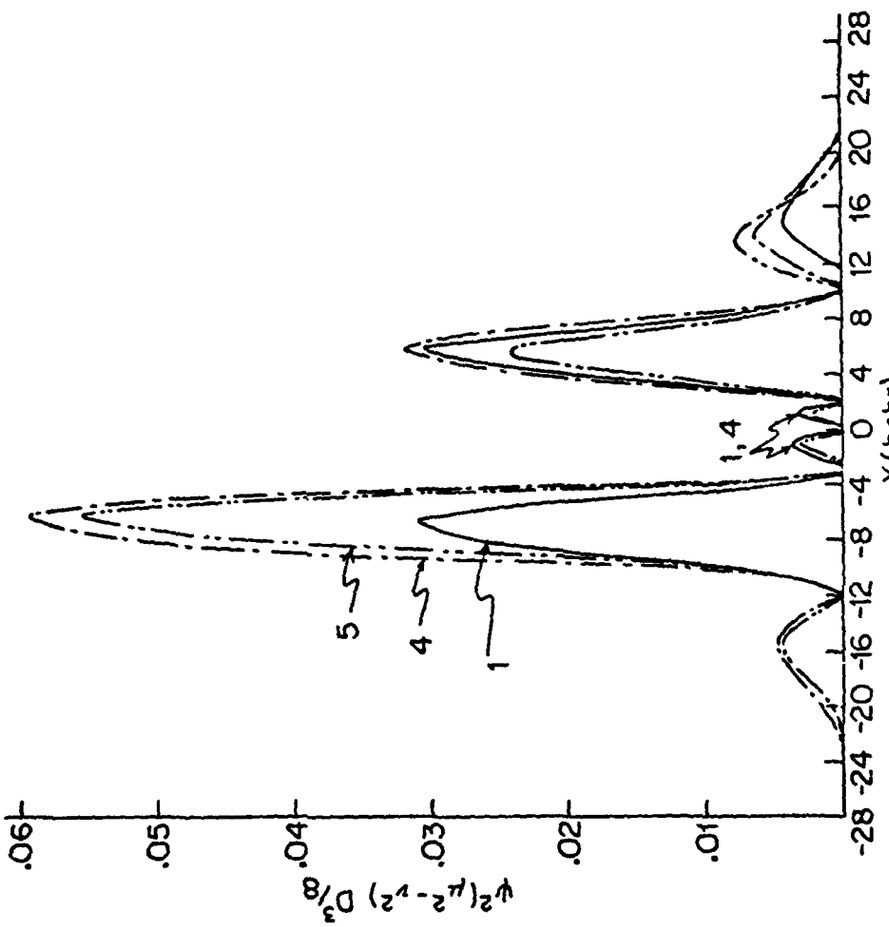

Fig. IV-12--M.O. 10 -- Basis Sets 1, 4 and 5

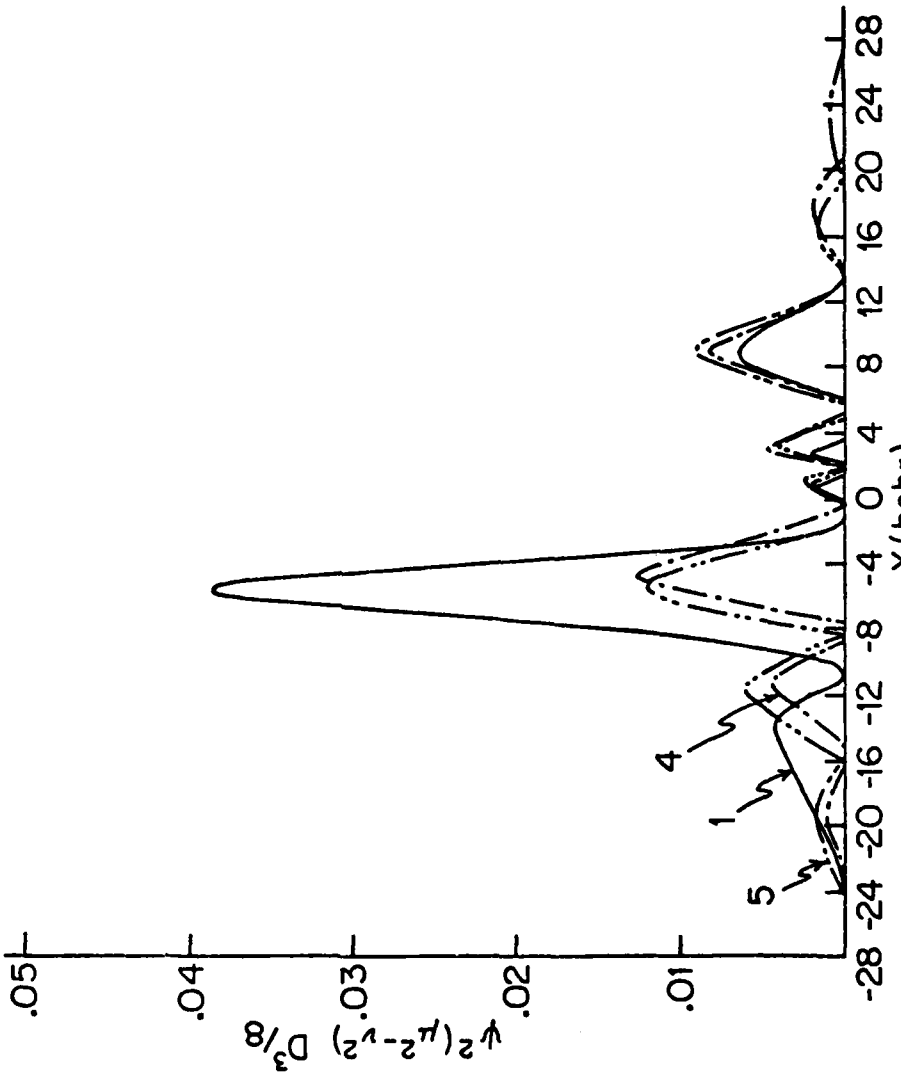

Fig. IV-13--M.O. 13 -- Basis Sets 1, 4 and 5

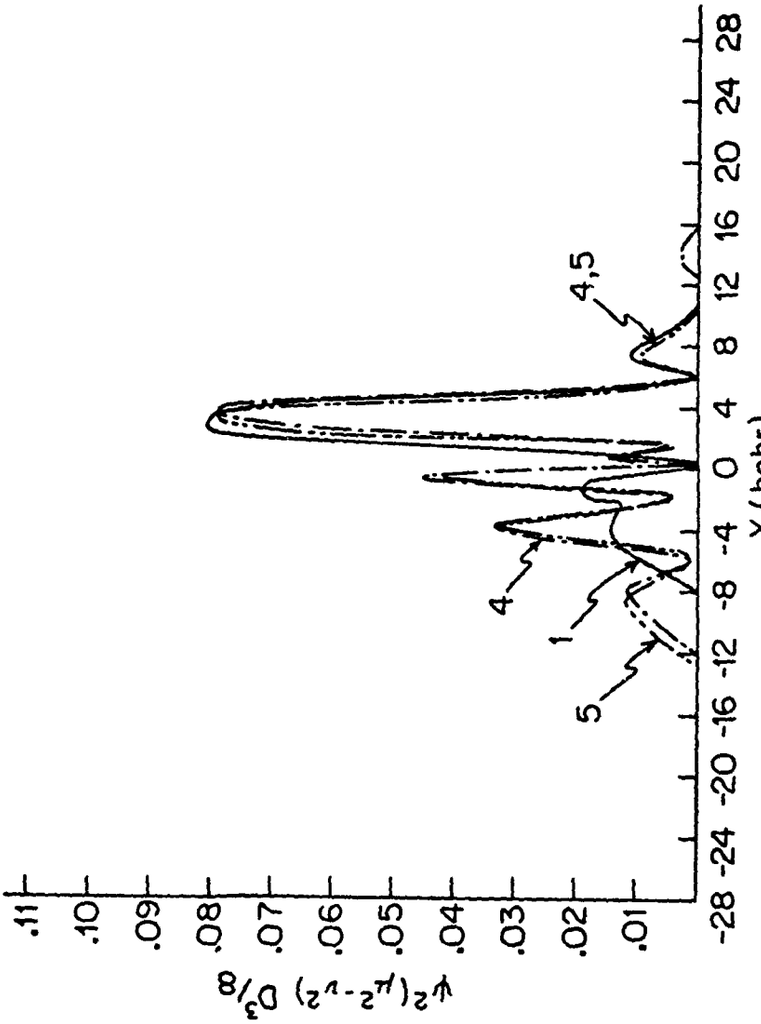

Fig. IV-14--M.O. 14 -- Basis Sets 1, 4 and 5

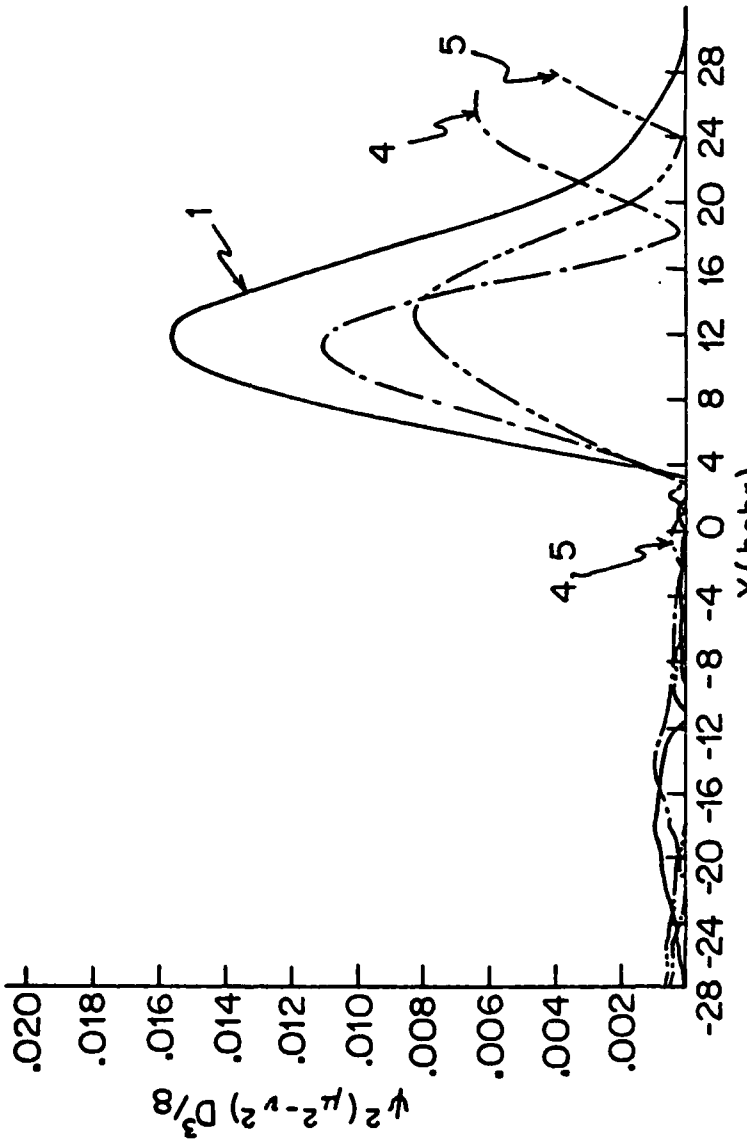

Fig. IV-15--Alternate M.O. 6 -- Basis Sets 1, 4 and 5

CHAPTER V

CONFIGURATION INTERACTION CALCULATIONS ON THE RYDBERG STATES OF HF AND THE FESHBACH STATES OF HF^-

Introduction

In Chapter III, a background discussion of the nature of core-excited resonances was presented. Before describing our work in this area, we briefly review the relevant concepts. Resonances in electron scattering can be classified into two general categories. The first type of resonance, called either a temporary negative ion or simply a resonance, is formed when an incident electron is temporarily captured in the region of a target molecule. The second type of resonance, referred to as a core-excited resonance, is characterized by a "hole" in a normally occupied orbital and two "particles" in normally unoccupied orbitals.[1] The neutral Rydberg electronic state associated with a particular resonance is called the parent state, while the positive ion core is called the grandparent state. The second type of resonance, commonly known as a Feshbach state is the subject of this chapter.

Core-excited resonances can lie either above or below the parent. Feshbach Type I resonances, with which we are concerned here lie below the parent state and thus exhibit a positive electron affinity. These resonances have lifetimes that are long compared to a vibrational

period. This characteristic is manifested through bands with vibrational structure similar to the grandparent. Since the two electrons trapped by the ion core reside in Rydberg orbitals located far from the core, it is not unreasonable to expect the negative ion and the positive ion to show similar vibrational progressions.

Resonance spectra in the rare gases have been studied in great detail.[2] Feshbach states have also been detected and examined for various diatomic molecules, including H_2, CO, N_2, NO, and O_2.[2] Because of the general interest in electron scattering from polar diatomic molecules, experimental investigations on the Feshbach states of HF^- have recently been performed.[3,4]

The purpose of this chapter is to present the results of configuration interaction calculations on the Rydberg states of HF and the Feshbach resonances of HF^-. Before discussing the results of the study, we briefly review the pertinent experimental data on this subject and give a description of the methods employed in our calculational procedure.

Background

HF.

In spite of the corrosive nature of the vapor, the excited states of the HF molecule have been the subject of some experimental investigations. The lowest energy

excited state of HF, the so-called $B^1\Sigma^+$ state, has been studied the most widely. Johns and Barrow first found evidence of the state in 1959 through a vacuum ultraviolet absorption experiment.[5] Through observation of the first six vibrational levels, values for ω_e of 0.145 eV, and r_e of 2.09 Å (3.95 bohr) were determined. DiLonardo and Douglas later reexamined the $B^1\Sigma^+$ state both through absorption[6] and emission,[6,7] and detected vibrational structure through about v=73. The v=0 level was found to lie 83,305 cm^{-1} (10.33 eV) above the HF $^1\Sigma^+$ ground state. According to DiLonardo and Douglas, the vibrational levels are well behaved up to v=26, which lies at an energy of 103,880 cm^{-1} (12.9 eV). Above v=26, severe perturbations are observed as the bands of the B state become mixed with other Rydberg bands. DiLonardo and Douglas have detected a $^3\pi$-$X^1\Sigma^+$ band in the region of the v=27 level of the $B^1\Sigma^+$ state which they hypothesize as being responsible for the perturbations. They also suggest the possibility of perturbations beginning as low as v=24, and speculate that lower unobserved vibrational levels of the $^3\pi$ state may be the cause.

The $B^1\Sigma^+$ state has also been observed through electron energy loss.[8] In this study, Salama and Hasted place the v=5 vibrational level at 11.3 eV, the v=11 level at 12.2 eV, and report an ω_e of 0.15 eV. This is in disagreement with the data of DiLonardo and Douglas which

shows v=5 at about 11.0 eV.

Other excited states of HF have also been observed below about 14 eV. Salama and Hasted identified two Rydberg series superimposed upon a dissociation continuum which commences at 11.15 eV.[8] The first series, assigned as an s Rydberg series, is reported to originate at 11.72 eV with the 3s member. An ω_e of 0.35 eV and an r_e of 1.207 Å (2.28 bohr) for this member were determined. The second series, tentatively classified as a p series, is reported to originate at 12.82 eV with the 3p member. The quantum defect of this state is rather high for a p series (0.95), and Salama and Hasted do not rule out an alternative assignment as an s series. The ω_e for this series was determined to be 0.30 eV.

DiLonardo and Douglas have also observed three singlet Rydberg states which lie above a continuum in the 1400 A (8.9 eV) region.[7] Between about 12.9 and 14.4 eV, they find evidence of two strong $^1\Sigma^+$-$X^1\Sigma^+$ bands as well as a strong well-behaved $^1\pi$-$X^1\Sigma^+$ system.[6] Although these states have not been analyzed in detail, the $^1\pi$ state is reported to originate at 13.03 eV with vibrational spacing of 2656 cm^{-1}(0.33 eV).[7]

The $B^1\Sigma^+$ state of HF appears to be well characterized, and there is good agreement in all respects among the reported experimental results. This does not hold true for the Rydberg excited states of HF. There is clear

disagreement between Salama and Hasted, who report two series commencing at 11.72 eV and 12.82 eV, and DiLonardo and Douglas who observe no Rydberg states below 12.9 eV. The results of our calculations, which are discussed shortly, clearly support the findings of DiLonardo and Douglas and put into question those of Salamar and Hasted.

$\underline{HF^+}$.

The characteristics of the positive ion states of HF are important in the study of the negative ion Feshbach resonances. The nature of the core excited HF^- states can be better understood by identification with their grandparent HF^+ states. Two ionization potentials of HF have been identified, both through photoelectron spectroscopy.

The lowest energy ionization potential is the $HF^+ {}^2\pi$ which is observed at about 16 eV.[9,10] The ω_e and r_e of this state are reported by Berkowitz to be 3016 cm^{-1} (0.37 eV) and 1.026 Å (1.94 bohr) respectively.[10] There appears to be some disagreement regarding the location of the second ionization potential, a $^2\Sigma^+$ HF^+ state. Lempka et al. place its origin at 18.6 eV,[10] while Berkowitz reports it to originate at 19.1 eV.[9] The vibrational spacing of the $^2\Sigma^+$ state is 1550 cm^{-1} (0.19 eV), about half that of the 2 HF^+ state.[9] Berkowitz reports a value of 1.20 Å (2.3 bohr) for r_e.[10]

$\underline{HF^-}$.

The Feshbach states of HF^- have been the subject of two experimental studies, both of which utilized the technique of electron transmission spectroscopy. Spence and Noguchi find evidence of a Feshbach state originating at 12.825 eV.[3] Four vibrational levels with a spacing of 0.355 eV are analyzed. Because of the excellent agreement of the vibrational spacings with those of the $^2\pi$ ionization potential, the state is assigned as $^2\pi$. Spence and Noguchi also report a severe perturbation on the first vibrational level of this state and provide two alternative explanations for the cause. First, depending upon the probabilities for transition, they speculate that perferential decay to the $B^1\Sigma^+$ state of HF may occur from one or more of the vibrational levels of the observed $^2\pi$ state. Indeed, this explanation appears to be reasonable in light of the perturbations detected in the HF $B^1\Sigma^+$ state spectrum discussed earlier. The second explanation put forth is that the state may be crossed by a second negative ion state. The interaction of the two states would persumably cause a perturbation in the transmission spectrum. Although Spence and Noguchi analyzed the spectrum from about 11.5 to 15.5 eV, they found no evidence of any other HF^- Feshbach states.

In a second experimental study, Mathur and Hasted observe a sharp dip in the transmission spectrum at

10.05 eV.[4] Although no vibrational structure is apparent, it is tentatively classified as a $^2\Sigma^+$ state. According to Mathur and Hasted, the lack of vibrational structure can possibly be explained by an avoided crossing between two states of the same symmetry. The vibrational progression would end after one level with the opening of a new channel, that of a repulsive negative ion state.

Mathur and Hasted also report a distinct Feshbach resonance at higher energy. This state originates at 12.388 eV, and based on an analysis of five vibrational levels is stated to have an ω_e of 0.132 eV. Mathur and Hasted discuss the fact that the vibrational spacing does not agree well with that of the first ionization potential, the $^2\pi$ HF^+ state. Although it is not mentioned, neither does the spacing agree with the spacing of the first excited ionization potential, the $^2\Sigma^+$ HF^+ state. Nevertheless, the state is tentatively classified as a $^2\Sigma^+$ HF^- Feshbach state.

Mathur and Hasted discuss the disagreement of their results with those of Spence and Noguchi. Mathur and Hasted, who performed their measurements at a later date, analyzed the spectrum in the region between 12.8 and 13.5 eV. They found it only marginally possible to detect structure in spite of the fact that Spence and Noguchi find clear evidence of a resonance in that energy range. Alternatively, in Spence and Noguchi's investigation,

performed earlier, no structure is reported between 12.3 and 12.8 eV, the region in which Mathur and Hasted detect a Feshbach state.

In light of the experimental data, we have attempted to provide some insights on the interpretation of the experimental observations between 9 and 14 eV through configuration interaction calculations on the excited states of HF and the Feshbach states of HF^-. Before describing our results and comparing them with the experimental observations, we provide a brief summary of the method used in our calculations.

Method

Although some aspects of the method used in the calculations described here are the same as those given in Chapter IV, they will be repeated for convenience. The atomic orbital basis set was chosen to be sufficiently flexible to represent both HF and HF^- for a range of internuclear distances. A Dunning basis, the (9s/5p) primitive gaussian basis of Huzinaga,[11] contracted to (3s/2p)[12] was adopted, while the hydrogen was represented by the Dunning (2s) basis.[12] In addition to these functions, uncontracted Gaussian Rydberg s functions of exponent 0.036 and 0.0066, and p functions of exponent 0.074, 0.029 and 0.0054 were added to F. Finally, a p type polarization function of exponent 0.9 was added to

hydrogen and a d type, of exponent 1.15, to F. The complete atomic orbital basis set is shown in Table V-1.

The SCF wavefunction and energy for HF were calculated within this basis set. Of the 30 molecular orbitals comprising the basis, only one, that of lowest energy, was dropped from consideration in the CI calculations. Table V-2 provides a list of the molecular orbitals and their eigenvalues as well as the energy of HF at its equilibrium internuclear distance. The SCF total energy of -100.04905 a.u. can be compared with the near Hartree Fock energy of -100.0705 a.u.[13]

The SCF virtual orbitals of HF were assumed to form an adequate basis for performing CI calculations on HF^-. Previous work on HCl[13] confirms that this assumption is justified. The SCF virtual orbitals of HF are eigenfunctions of the full n electron HF potential including its permanent dipole moment. Since, in a case of this type, the scattering is long range, the target molecule is relatively little perturbed by the scattering event. Consequently, the HF virtual orbitals are assumed to be a good representation of the natural orbitals of HF^-.

Configuration Interaction calculations were performed on the ground state of HF, the excited states of HF, the $^2\pi$ positive ion state, and the core-excited states of HF^-. The latter states were derived by populating the appropriate HF virtual orbital with two electrons. In general,

a few seed configuration were selected to represent the given state of interest. Then all single and double hole particle excitations relative to those few seed configurations were generated to form the total CI space. Solution of the CI problem was accomplished by the partitioning technique which was discussed in Chapter II and elsewhere.[15-17]

Results and Discussion

Full CI calculations on the states of HF and HF^- lying between about 9 and 14 eV were performed at a number of internuclear distances. The equilibrium internuclear separation of the HF molecule is 1.732 bohr, and we consider 7.0 bohr as representative of the dissociation limit. Before providing the results of our calculations, we present a brief description of our M.O. notation system, which should considerably simplify the discussion that follows.

The values of the second column in Table V-2 number the M.O.'s of the same symmetry sequentially, and each degenerate pair of π and Δ M.O.'s is assigned one number. We will refer, in the following discussion, for example, to M.O. number 3 as the 3σ and M.O.'s number 4 and 5 as the 2π. Although the M.O.'s have the order shown in Table V-2 at the equilibrium internuclear separation, at distances larger than 2.5 bohr the order has altered.

Table V-3 presents the M.O. notation system for two separations, 1.732 bohr (equilibrium), and 4.0 bohr, for reference purposes. In the CI calculations, all single- and double-hole particle excitations were generated from more than one base. In each case, these generating bases were identified by their strong contribution to the final wavefunction. For each state, we will present the occupations of the bases in the notation described above.

HF.

Table V-4 provides the details of the calculated potential curves for the HF ground and excited states. Figure V-1 displays these data pictorially. The generating bases for each HF state considered here, together with the weighting of the configuration in the final wavefunction for a few appropriate internuclear separations are presented in Table V-5. We will discuss the characteristics of each HF state in turn.

The potential curve for the $1^1\Sigma^+$ HF ground state is identical to that presented in Chapter IV. We will therefore not repeat the analysis except to reiterate that the calculated dissociation energy of 6.02 eV compares well with the experimental value for D_e of 6.1 eV.[18]

The $2^1\Sigma^+$ state indicated in Figure V-1 is the so-called B state of HF. Its minimum, at 3.96 bohr is calculated to lie approximately 10.62 eV above the ground state of HF. This is only slightly higher than the

experimental value for T_e of 10.51 eV.[5] Through a parabola fit, we obtain an ω_e of 0.15 eV which also agrees well with the experimental value of 0.14 eV.[7] At long internuclear distances, near the equilibrium distance for this state, the $2^1\Sigma^+$ B state is clearly valence in character. In this region, it is apparently quite ionic in nature and lies close in energy to the $H^+ + F^-$ limit of 16.07 eV.[7] At shorter distances, however, the state is Rydberg in character and represents the first member of an s Rydberg series leading to the first excited ionization limit $HF^+(^2\Sigma^+)$ at 19.1 eV. This change in nature can be understood more easily by referring to the data of Table V-5. The configurations contributing most strongly at 2.3 bohr are those representing a positive ion core with one electron populating successively higher, Σ^+ M.O.'s. At 4.0 bohr, the dominant configuration is $1\sigma^2 2\sigma^2 1\pi^4 3\sigma 4\sigma$. At this longer distance, the 4σ M.O. has become valence in character. The fact that the $2^1\Sigma^+$ B state is the first member of a Rydberg series leading to the $^2\Sigma^+$ ionization limit at shorter internuclear distances raises the question of the higher members. In exploratory CI calculations, we do identify higher members. Since all lie well above 14 eV in energy in the Franck Condon region, we have not investigated them further.

The $3^1\Sigma^+$ state is a Rydberg state leading to the $HF^+(^2\pi^+)$ ionization limit. As Table V-5 indicates, it is

represented by the $^2\pi$ positive ion core plus an electron occupying successively higher Rydberg π M.O.'s. Its minimum lies 13.75 eV above the HF ground state at about 2.0 bohr separation. This state is likely to be one of the $^1\Sigma^+$ states observed by DiLonardo and Douglas between 12.9 and 14.4 eV. Although the perturbations observed in the higher vibrational levels of the B $1^1\Sigma^+$ state may be a result of the interaction of the B state with the $3^1\Sigma^+$, it is unlikely that this could be the case. Figure V-1 shows the crossing of the $1^1\Sigma^+$ and the $3^1\Sigma^+$ to occur at about 13.7 eV. This is significantly higher than the energy where the perturbations begin (12.9 eV). Even assuming the calculated potential curves to be too high by a few tenths of an eV, it does not seem reasonable that the $3^1\Sigma^+$ is responsible for the perturbations in the region of the v=27 level of the $B^1\Sigma^+$ state.

The $1^1\Delta$ HF state is identical in orbital occupation to the $3^1\Sigma^+$ state just discussed. The two states parallel one another and the minimum of the $1^1\Delta$ at 13.66 eV is only slightly lower than that of the $3^1\Sigma^+$ state. To our knowledge, this state has not yet been detected experimentally.

According to Figure V-1, the $1^1\pi$ HF state is repulsive. This state corresponds to the dissociation continuum reported by DiLonardo and Douglas to occur in the region of about 1400 Å (8.9 eV).[6] At short

internuclear distances, the $1^1\pi$ is the first member of an s Rydberg series leading to the ionization limit $HF^+(^2\pi)$. The energy of this state at its minimum, together with the location of the ionization limit, leads to a quantum defect of 1.55, which seems reasonable for an s Rydberg series. At longer distances, this state, like the B $2^1\Sigma^+$ state, becomes valence in character. The $1^1\pi$, together with the $1^1\Sigma^+$ HF ground state leads to the limit $H(^2S) + F(^2P)$.

The $2^1\pi$ is probably the first member of a p Rydberg series leading to the ionization potential $HF^+(^2\pi)$. The minimum energy of this state given the minimum energy of the ionization limit results in a quantum defect of 0.74, a value not unexpected for a p Rydberg series. Its dominant contributions again come from configurations representing an HF^+ core and one electron occupying higher energy Σ^+ M.O.'s. The minimum of this state lies at 1.978 bohr, 13.40 eV above the HF ground state. We calculate an ω_e of 0.26 eV. DiLonardo and Douglas speculate that the cause of the perturbations above the v=26 vibrational level in the $B^1\Sigma^+$ state are due to a crossing of the B state by a $^3\pi$ state. They observe this perturbation at 12.9 eV. The results of our calculations support DiLonardo and Douglas' interpretation. the $2^1\pi$ crosses the B state at about 13.4 eV according to Figure V-1. Assuming the $^3\pi$ state lies a few tenths of an eV below the $2^1\pi$, it would indeed be in the proper energy range to explain the

perturbations. Indeed, there appear to be no singlet states in the energy region of the perturbations. Our calculated curve for the 2^1 state lies about 0.25 eV above the experimental value for T_e of 13.15 eV.[6]

The $2^1\pi$ state might also be the state observed by Salama and Hasted at 12.82 eV.[8] Since our ab initio procedure generally produces results that are too high by a few tenths of an eV when compared with experimental values, this is certainly possible. The location of our calculated state, however, seems to agree more closely with the experimental data of DiLonardo and Douglas who placed the observed π state slightly higher in energy.

The $3^1\pi$ state is probably the second member of the s Rydberg series leading to the $HF^+(^2\pi)$ ionization limit. Its dominant contributions to the final wavefunction illustrate this fact. At the calculated minimum of 1.977 bohr, the state lies 13.96 eV above the ground state of HF. Through a three point parabola fit, we calculate an ω_e of 0.37 eV. This state has apparently not been observed experimentally.

We have calculated the potential curves for the ground state and six excited states of HF below 14 eV. The $1^1\pi$, and the $3^1\pi$ in the Frank Condon Region are likely to be successively higher members of a Rydberg s series leading to the first ionization limit $HF^+(^2\pi)$. The $2^1\pi$ is probably the first member of a p Rydberg series leading

to the same limit. The $2^1\Sigma^+$ state at short internuclear distances is the first member of a Rydberg s series leading to the excited ionization limit $HF^+(^2\Sigma^+)$. At longer internuclear separations, this state is valence in character and leads to the limit $H^+ + F^-$. The $3^1\Sigma^+$ and the $^1\Delta$ states are each the first member of a Rydberg p π series leading to the ionization limit $HF^+(^2\pi)$.

Our calculated potential curves agree in all major respects with the experimental results of DiLonardo and Douglas[6,7] and find some disagreement with the results of Salama and Hasted.[8] We are convinced that no states other than those we have claculated lie within the energy range of about 11 to 14 eV. We do not find the Rydberg series reported by Salama and Hasted at 11.72 eV.

$\underline{HF^+}$.

In the course of this study, we found it useful to perform what are probably the first configuration interaction calculations on the $HF^+(^2\pi)$ state. We find its minimum at 1.92 bohr at an energy 16.05 eV above the ground state of HF ($1^1\Sigma^+$). We calculate an ω_e of 3211 cm^{-1} (0.398 eV) through a three point fit to a parabola. These calculated data agree exceptionally well with the experimental data which place the state at 16.05 eV with r_e = 1.94 bohr, with an ω_e of 3016 cm^{-1} (0.37 eV).[10]

$\underline{HF^-}$.

For convenience, we will present the results of the

results of HF^- potential curves for two separate energy regions: 9 to 12 eV, and 12 to 14 eV. First, however, a few general comments on the HF^- state calculations will be useful.

Each of the HF^- states has a parent HF excited state and a grandparent HF^+ state. The grandparent state is readily identified by the "hole" in the normally occupied M.O.'s. Although in the discussion of the states of HF, we presented results only for singlet states we can presume that each has a corresponding triplet state where the electrons occupy the same spatial M.O.'s but have unpaired spins. By adding an extra electron to one of the other M.O.'s of each HF state, we can produce an HF^- Feshbach state. Thus each singlet HF state is the parent of one HF^- state, and each triplet HF state is the parent of one HF^- state. For every singlet state considered in the last section, there are therefore two corresponding HF^- states, one of which has a singlet HF parent and one of which has a triplet HF parent. Because of this "doublying" effect, the spectrum of the HF^- states is extremely dense in the region of 9 to 14 eV. In addition, most of the HF^- states that lie in this energy range are repulsive at all internuclear distances. This is not unexpected, particularly at lower energies, where the binding energy to the grandparent positive ion core is very large.

We have calculated the potential curves of all HF^- Feshbach states between 9 and 14 eV that are formed when an extra electron is added to the calculated singlet HF excited states and their corresponding triplet states. We do not present the detailed potential curves of the states that are repulsive except where they are important to the interpretation of the experimental data.

9-12 eV.

Table V-6 presents the calculated energy results for the HF^- potential curves that are displayed in Figure V-2 for this energy range. Table V-7 lists the configurations used as bases in the calculations for excitation generation together with their final percentage weighting in the wavefunction for various pertinent internuclear distances.

The $7^2\Sigma^+$, the $8^2\Sigma^+$ and the $9^2\Sigma^+$ HF^- states are all repulsive Feshbach states. The $6^2\Sigma^+$ HF^- state which crosses these repulsive $^2\Sigma^+$ states is a resonance HF^- state comprised of a fully occupied HF core with the extra electron occupying a valence Σ^+ M.O. The states in this energy region are of interest solely because of the dip observed at 10.05 eV in the transmission experiment of Mathur and Hasted.[4]

The $6^2\Sigma^+$ HF^- valence state is formed by occupation of the HF core with the extra electron in M.O. #17. We have not attempted to examine the characteristics of this

state further since it is important only because it crosses the other $^2\Sigma^+$ Feshbach states.

The $7^2\Sigma^+$ HF^- state is formed by adding two electrons to the normally unoccupied Σ^+ M.O.'s of the $^2\Sigma^+$ HF^+ core. At longer distances this state crosses the $5^2\Sigma^+$ state which leads, together with an HF^- $^2\pi$ state to the limit $H^-(^1s) + F(^2p)$. A detailed discussion of the 5 and 7 $^2\Sigma^+$ states was presented in Chapter IV. At short internuclear distances, the $7^2\Sigma^+$ HF^- state descends rapidly and crosses the 8 and 9 $^2\Sigma^+$ states at about 2 bohr. These latter states are formed by the addition of two electrons to the normally unoccupied π M.O.s of the $^2\pi$ HF^+ core. The parent of the $7^2\Sigma^+$ state is the triplet corresponding in orbital occupation to the B $2^1\Sigma^+$ HF state. The parent of the $8^2\Sigma^+$ state is the triplet corresponding to the $3^1\Sigma^+$ HF state while the parent of the $9^2\Sigma^+$ HF^- state is the $3^1\Sigma^+$ state of HF. The grandparent of all three states is the $^2\pi$ HF^+ ionization limit.

The left hand side of Table V-6 displays the diabatic curves for the four $^2\Sigma^+$ HF^- states. On the right hand side, the adiabats that might produce the observed dip in transmission are illustrated. We have shown the $8^2\Sigma^+$ state to cross the 9 and $7^2\Sigma^+$ states diabatically at about 2.0 bohr. At approximately 2.2 bohr, the $8^2\Sigma^+$ state begins to interact with the $6^2\Sigma^+$. It follows the $6^2\Sigma^+$ state curve for a short distance, then dissociates

and adiabatically follows the curve of the $8^2\Sigma^+$ state.

Whether or not the complex adiabatic interaction of the four $^2\Sigma^+$ states actually occurs must remain speculative. The calculated energy where the interaction occurs agrees with the experimental value of 10.05 eV.[4] It also appears from the adiabats of Figure V-6 that only one vibrational level is excited before the dissociative channel is open, which also confirms the experimental data. Although this type of interaction might explain the dip in transmission observed by Mathur and Hasted, there is at least one strong reason for it to be unlikely. The main problem with the assignment of this avoided crossing as the experimentally observed feature is that it would occur at about 2.2 bohr. This is well outside the Franck Condon region, and it seems reasonable to assume that it would therefore not be detected in a transmission experiment. Thus, although we do not believe the crossing to correspond to the experimental data, we have raised the possibility here for completeness.

12 to 14 eV.

In Table V-8, we present data for three potential curves shown in Figure V-3 for the HF^- states within this energy range. Table V-9 lists the generating configuration bases and their percentage weightings in the final wavefuntion at 1.732, 2.0, and 2.5 bohr. As discussed earlier, there are numerous HF^- states in this energy region.

It is noteworthy indeed, that only one of these states, the $6^2\pi$, appears to be bound, and only two other states, the 5 and $7^2\pi$ cross it. The details of most of the other states are not presented since they complicate the spectrum and are not relevant to the explanation of the experimental data.

The 5, 6, and 7 $^2\pi$ HF^- states of Figure V-3 are formed by adding two electrons to higher energy Σ^+ M.O.'s of the HF^+ ($^2\pi$) core. The grandparent of the three π states is therefore the $^2\pi$ HF^+ ionization limit. The parent of the $5^2\pi$ is the $3^1\pi$ HF state shown in Figure V-1; the parents of the $6^2\pi$ and $7^2\pi$ states are a singlet and a triplet state of HF lying at about 15 eV. Although the singlet HF state is not shown in Figure V-1, it is the $5^1\pi$ state of HF. Table V-10 gives the energy and weighting of the configurations contributing most strongly to the final wavefunction of the $5^2\pi$ HF^- state and its parent, the $3^1\pi$ HF state. Table V-11 provides the same information for the 6 and $7^2\pi$ HF^- states and the $7^2\pi$ parent, the $5^1\pi$ HF state.

Identification and assignment of the HF^- Feshbach states is an extremely complicated exercise for two primary reasons. First, it is frequently difficult to follow a negative ion state from point to point across the potential curve because of the density of states of the same symmetry. Second, parentage assignment is often

not straightforward both because we have only obtained results for the singlet HF states and because these HF states are themselves interacting with other neutral excited states across the surface. Given the information of Tables V-10 and V-11, however, we will attempt to clarify the techniques we used for identification. We emphasize that these methods are somewhat qualitative in nature.

The $5^2\pi$ HF^- state described in Table V-10 is one of the two HF^- states that crosses the bound $6^2\pi$ HF^- state. At all three internuclear distances, its largest contribution to the final wave function arises from the configuration $1\sigma^2 2\sigma^2 3\sigma^2 1\pi^3 4\sigma^2$. This contribution, however, diminishes as we move to longer internuclear distances. Alternatively, at the equilibrium internuclear distance, the contribution from the last listed configuration, $1\sigma^2 2\sigma^2 3\sigma^2 4\pi^3 8\sigma$ is minimal, but becomes singificant at 2.5 bohr. We thus conclude that the state is losing the character of the first configuration and picking up the character of the last configuration as we move across the surface.

One of the methods we use to "recognize" this state at the three distqnces is by noting its largest contributing contributions. We have just seen, however, that the large contributions change somewhat from point to point. The other method we use to identify the state at

each point is by the constancy in the signs of the spin functions of the configurations. From 1.732 bohr to 2.0 bohr, the signs of the third configuration and one spin function of the fifth configuration of the $5^2\pi$ HF^- state have changed. It may be that the first spin function of the third configuration has "gone through zero" between the calculated points. It is more obvious that the second spin functions of the third and fifth configurations have indeed "gone through zero". These become larger and opposite in sign between 1.732 and 2.0 bohr.

At 1.732 bohr, the $3^1\pi$ HF state has its largest contribution from the configuration $1\sigma^2 2\sigma^2 3\sigma^2 4\pi^3 4\sigma$. At longer distances, the weight of this configuration diminishes while the contribution of the configuration $1\sigma^2 2\sigma^2 3\sigma^2 1\pi^3 7\sigma$ increases. The $3^1\pi$ HF state interacts strongly with another state, the $2^1\pi$ HF state shown in Figure V-1. The largest contribution to this latter state at 1.732 bohr is the configuration that attains increasing weight in the $3^2\pi$ HF state.

Parentage assignment of Feshbach states is extremely qualitative in nature. It is important to emphasize here that the HF parent state and the corresponding HF^- state need not retain identical character across the potential surface. One must keep in mind that the HF states interact with other HF states, while the HF^- states interact

with other HF^- states of different character. The parentage assignment is based largely on the character of the states of 1.732 bohr. In addition, there is one other important identifying characteristic. The signs of the spin functions of a particular HF^- states are either in phase or out of phase within a particular spin function and should ideally mimic those of the parent HF state at all internuclear distances. In conjunction with this observation, it should be kept in mind that the sign of the first spin function of a particular state is arbitrary and it is only the signs of the other configurations relative to the sign of the first configuration that is important.

We observe that the largest contributions to the wavefunction of the $5^2\pi$ HF^- state are the configurations $1\sigma^2 2\sigma^2 3\sigma^2 1\pi^3 4\sigma\ n\sigma$, where $n \geq 4$. The parent state of the $5^2\pi$ state should thus be expected to have a large contribution from the configuration $1\sigma^2 2\sigma^2 3\sigma^2 1\pi^3 4\sigma$. Indeed, we note that the $3^1\pi$ HF state fulfills this requirement. It is primarily on this basis that we believe the $3^1\pi$ HF state to be the parent of the $5^2\pi$ HF^- state.

In Table V-11, we show the energy and the contribution to the final wavefunction of the $6^2\pi$ HF^- state, the bound state, and the $7^2\pi$ HF^- state which crosses it. We illustrate the same data for the assigned parent $5^1\pi$ HF state. We think it probable that the parent of the

$6^2\pi$ HF^- state is the triplet counterpart to the $5^1\pi$ HF state simply because triplet states generally lie lower in energy.

At the equilibrium internuclear distance, the $5^1\pi$ HF state is dominated by the configuration $1\sigma^2 2\sigma^2 3\sigma^2 4\pi^3 8\sigma$. The same configuration, with the extra electron occupying the 4σ M.O. also dominates the two HF^- states. We note also that the relative signs of the spin functions of the HF^- states mimic those of the parent $5^1\pi$ HF state reasonably well. Because of the heavy mixing among the 5, 6, and $7^2\pi$ states, however, this requirement does not hold exactly. Another significant observation is that the relative signs of the spin function within a particular configuration are in phase for the $6^2\pi$ HF^- state and out of phase for the $7^2\pi$ HF^- state. In our experience, this is the expected behavior for two HF^- states arising from the same singlet and triplet parent HF state.

It was already noted that the character of the $5^2\pi$ HF^- state shown in Table V-10 changes between 1.732 bohr and 2.0 bohr. The contribution of the first configuration decreases while that of the last configuration $1\sigma^2 2\sigma^2 3\sigma^2 4\pi 4\sigma 8\sigma$ increases. Exactly the reverse behavior is observed for the 6 and $7^2\pi$ HF^- states. This can be understood readily with the aid of Figure V-3. Both the 5 and $7^2\pi$ states cross the $6^2\pi$ bound HF^- state just beyond 2.0 bohr. It is therefore expected that all three states,

which are of the same symmetry, begin to interact strongly at 2.0 bohr. This is indeed the reason for the change in character of all three HF^- states between 1.732 and 2.0 bohr.

The Feshbach state observed experimentally by Spence and Noguchi at 12.825 eV[3] clearly corresponds to the $6^2\pi$ state of HF^- which has a calculated energy of 12.795 eV at 2.0 bohr. The reported perturbation on the first vibrational level of the bound state is undoubtedly due to the interaction of the $6^2\pi$ HF^- state with the 6 and $7^2\pi$ HF^- states. At 2.0 bohr, the $5^2\pi$ and $7^2\pi$ states lie about 0.2 and 0.4 eV above the $6^2\pi$ states respectively. The vibrational spacing of the state observed by Spence and Noguchi is reported to be 0.355 eV.[3] It is therefore reasonable to assume that one or both of the interacting states are responsible for the perturbation. Through a three-point parabola fit, we have calculated a vibrational spacing of 0.61 eV for the $6^2\pi$ HF^- state. This is much larger than the experimental value of 0.355 EV. We believe che poor agreement with experiment to result from the wide spacing of the three calculated points. The good agreement with experimental obtained for some of the HF states could be because the calculated energy points were more closely space; it might also be that the agreement was simply fortuitous. In any case, we do not believe that the $6^2\pi$ HF^- state is the Feshbach state observed by

Mathur and Hasted at 12.388 eV.[14] The authors themselves admit that the vibrational spacing of the state, 0.132 eV, does not agree with the vibrational spacing of the grandparent HF^+ ($^2\pi$) state. Our calculated spacing is much higher than 0.132 eV, and at least is closer to the experimental value reported by Spence and Noguchi.

In summary, we find ourselves in good agreement with the HF^- experimental results of Spence and Noguchi, but in disagreement with those of Mathur and Hasted. We do not believe the complicated set of adiabats displayed in Figure V-2 explains the resonance observed by Mathur and Hasted at 10.05 eV. We do not find the attractive state reported to occur at 12.388 eV. On the other hand, we do find an attractive state in the region of 12.8 eV with characteristics that agree in all major respects with the results of Spence and Noguchi. It should be noted that we also find disagreement with the HF results of Salama and Hasted which were apparently obtained in the same laboratory as the HF^- results of Mathur and Hasted.

Binding Energies.

As discussed earlier, the binding energy of a negative ion state is defined as the difference between the experimentally observed energy of the negative ion state and the energy of the positive ion state, or the ionization limit. The binding energies of two $3s\sigma_g$ electrons to

the positive ion core have been determined for several diatomic molecules. They have all been found to be about 4 eV. The binding energy of the $6^2\pi$ HF^- state given in Figure V-3 is approximately 3.3 eV, calculated at the energy minimum. This binding energy is lower than that of any of the resonances of the diatomic molecules given by Schulz in reference 19. This implies that the two outer electrons in our calculated state are held less strongly to the positive ion core than they are in the other diatomic molecules that have been investigated.

The $3s\sigma_g$ M.O. in these diatomic molecules corresponds to the 4σ M.O. in HF^- at short internuclear distances. In HF^-, one of the configurations contributing to the final wavefunction is certainly that of the position ion core with two electrons occupying the 4σ M.O. However, the contributions to the final wavefunction also include other configurations. The parent state of the HF^- $6^2\pi$ Feshbach state is the third member of an s Rydberg series (n=5) leading to the $^2\pi$ HF^+ ionization potential. We can therefore assume that, on average, at least one of the additional electrons in the HF^- state occupies an M.O. for which n=5. That this electron is held more loosely to the core than would be an electron in a $3s\sigma_g$ M.O. is reasonable. We thus expect the binding energy to be less than for the diatomic molecules reported by Schulz.

The electron affinity of a detected resonance can be calculated by taking the difference in energy of the HF^- state and the corresponding HF parent state. The parent of the $6^2\pi$ HF^- state is the $5^3\pi$ HF state which we did not calculate. However, asuming the triplet to be a few tenths of an eV below the corresponding singlet state, we would expect an electron affinity of about 2 eV at 2.0 bohr.

Conclusions

We have reported the potential curves for the ground state of HF, several excited states of HF, and some of the Feshbach states of HF^-. Our calculated potential curves for the states of HF, though slightly high in energy, give good agreement with the experimental observations of DiLonardo and Douglas[6,7] and poor agreement with those of Salama and Hasted.[8]

The results of the HF^- calculations clearly illustrate the utility of applying ab initio techniques to the study of negative ion states. We identify a complicated set of adiabats in the region of 10 eV which could conceivably be the cause of an observed dip in transmission observed by Mathur and Hasted.[4] Because of the location of the crossing of the states on the potential curves (> 2.0 bohr), however, we believe that the interaction is too far from the Franck Condon Region to be detected.

Neither do we find an attractive HF^- state in the energy range of 12.388 eV also reported by Mathur and Hasted.[4] In contrast, we do identify a Feshbach state at 12.8 eV with characteristics that agree in all major respects with a state detected by Spence and Noguchi.[3]

References

1. G.J. Schulz, Rev. Mod. Phys. 45, 424 (1973).
2. G.J. Schulz, Rev. Mod. Phys. 45, 378 (1973).
3. D. Spence and T. Noguchi, J. Chem. Phys. 63, 505 (1975).
4. D. Mathur and J.B. Hasted, Chem. Phys. 34, 29 (1978).
5. J.W.C. Johns and R.F. Barrow, Proc. Roy. Soc. (London), A 251, 504 (1959).
6. D. DiLonardo and A.E. Douglas, Can. J. Phys. 51, 434 (1973).
7. D. DiLonardo and A.E. Douglas, J. Chem. Phys. 56, 5185 (1972).
8. A. Salama and J.B. Hasted, J. Phys. B: Atom. Molec. Phys. 9, L333 (1976).
9. H.J. Lempka, T.R. Passmore, and W.C. Price, Proc. Roy. Soc. A, 304, 53 (1968).
10. J. Berkowtiz, Chem. Phys. Lett. 11, 21 (1971).
11. S. Huzinaga, J. Chem. Phys. 42, 1293 (1965).
12. T.H. Dunning and P.J. Hays, "Modern Theoretical Chemistry", Volume 3, H.F. Shaefer, Ed., Plenum Press, New York, N.Y. (1977).
13. A.D. McLean and M. Yoshimine, J. Chem. Phys. 47, 3256 (1967).
14. E. Goldstein, G.A. Segal and R.W. Wetmore, J. Chem. Phys. 68, 271 (1978).

15. G.A. Segal and R.W. Wetmore, Chem. Phys. Lett. 32, 556 (1975).

16. R.W. Wetmore and G.A. Segal, Chem. Phys. Lett. 36, 478 (1975).

17. G.A. Segal, R.W. Wetmore, and K. Wolf, Chem. Phys. 30, 269 (1977).

18. J. Berkowitz, W.A. Chuptea, P.M. Guyon, J.H. Holloway, and R. Spohr, J. Chem. Phys. 54, 5165 (1971).

19. G.J. Schulz, Rev. Mod. Phys. 45, 423 (1973).

Table V-1

Gaussian Basis Set

Fluorine		Hydrogen	
ξ_s	[5s]	ξ_s	[2s]
9995.0	0.001166	13.36	0.032828
1506.0	0.008870	2.013	0.231024
350.3	0.042380	0.4538	0.817226
104.1	0.142929		
34.84	0.355372	0.1233	1.000000
12.22	0.462085		
4.369	0.140848		[1p]
12.22	-0.148452	1.000000	1.000000
1.208	1.05527		
0.3634	1.000000		
0.036	1.000000		
0.0066	1.000000		
ξ_p	[5p]		
44.36	0.020876		
10.08	0.130107		
2.996	0.396166		
0.9383	0.620404		
0.2733	1.000000		
0.074	1.000000		
0.029	1.000000		
0.0054	1.000000		
ξ_d	[1d]		
1.15	1.000000		

Table V-2

SCF Results for HF (R = 1.732 bohr)

M.O.	Text Notation	Symmetry	Eigenvalue (a.u.)
1	1σ	Σ^+	-26.29879
2	2σ	Σ^+	-1.60169
3	3σ	Σ^+	-0.76886
4	1π	π	-0.65063
5		π	-0.65063
6	4σ	Σ^+	0.00696
7	2π	π	0.01335
8		π	0.01335
9	5σ	Σ^+	0.01511
10	6σ	Σ^+	0.06850
11	3π	π	0.07965
12		π	0.07965
13	7σ	Σ^+	0.09187
14	8σ	Σ^+	0.26703
15	4π	π	0.30504
16		π	0.30504
17	9σ	Σ^+	0.32973
18	10σ	Σ^+	0.92540
19	11σ	Σ^+	1.33003
20	5π	π	1.34772
21		π	1.34772
22	12σ	Σ^+	1.71036
23	6π	π	1.84189
24		π	1.84189
25	13σ	Σ^+	2.75879
26	1Δ	Δ	2.91399
27		Δ	2.91399

Table V-2 (continued)

M.O.	Text Notation	Symmetry	Eigenvalue (a.u.)
28	7π	π	3.35095
29		π	3.35095
30	14σ	Σ^+	4.17831
31	15σ	Σ^+	5.65648

Total Energy: -100.04905 a.u.

Nuclear Repulsion Energy = 5.19630 a.u.

Total Electronic Energy = -105.24535 a.u.

Table V-3

SCF Molecular Orbital Designation

M.O. #	1.732		4.000	
	Order	Symmetry	Order	Symmetry
1	1σ	Σ^+	1σ	Σ^+
2	2σ	Σ^+	2σ	Σ^+
3	3σ	Σ^+	1π	π
4	1π	π		π
5		π	3σ	Σ^+
6	4σ	Σ^+	4σ	Σ^+
7	2π	π	5σ	Σ^+
8		π	2π	π
9	5σ	Σ^+		π
10	6σ	Σ^+	6σ	Σ^+
11	3π	π	3π	π
12		π		π
13	7σ	Σ^+	7σ	Σ^+
14	8σ	Σ^+	8σ	Σ^+
15	4π	π	4π	π
16		π		π
17	9σ	Σ^+	9σ	Σ^+
18	10σ	Σ^+	10σ	Σ^+
19	11σ	Σ^+	11σ	Σ^+
20	5π	π	5π	π
21		π		π
22	12σ	Σ^+	12σ	Σ^+
23	6π	π	6π	π
24		π		π
25	13σ	Σ^+	13σ	Σ^+
26	1Δ	Δ	7π	π
27		Δ		π

Table V-3 (continued)

M.O. #	1.732		4.000	
	Order	Symmetry	Order	Symmetry
28	7π	π	14σ	Σ^+
29		π	1Δ	Δ
30	14σ	Σ^+		Δ
31	15	Σ^+	15σ	Σ^+

Table V-4

Calculated CI Energy Points for HF [a]

State	Internuclear Distance (bohr)										
	1.5	1.732	2.0	2.3	2.5	3.0	3.8	4.0	4.2	5.0	7.0
1 $^1\Sigma^+$	0.761	0	0.336	--	2.046	3.624	5.187	5.384	5.552	5.922	6.015
2 $^1\Sigma^+$	--	14.482[b]	13.637[b]	13.021	--	--	10.658	10.617	10.634	--	12.5[c]
3 $^1\Sigma^+$	--	13.843	13.746	--	14.779	--	--	--	--	--	--
1 $^1\Delta$	--	13.739	13.661	--	14.566	--	--	--	--	--	--
1 $^1\pi$	--	10.797	9.586	8.519	--	7.017	--	--	--	--	--
2 $^1\pi$	--	13.524	13.398	13.614	--	--	--	--	--	--	--
3 $^1\pi$	--	14.220	13.961	14.411	--	--	--	--	--	--	--

[a] Relative to HF at equilibrium, E = -2727.430 eV.

[b] Determined by fitting a parabola to the calculated values at 3.8, 4.0, and 4.2 bohr.

[c] Adjusted to fit experimental data.

Table V-5

Generating Bases for HF Potential Curves

State	Configuration and Weighting (%)					
	1.732 bohr		2.3 bohr	4.0 bohr		
$1^1\Sigma^+$	$1\sigma^2 2\sigma^2 3\sigma^2 1\pi^4$	(.99)	(.99)	$1\sigma^2 2\sigma^2 1\pi^4 3\sigma^2$	(.74)	
	$1\sigma^2 2\sigma^2 3\sigma 1\pi^4 10\sigma$	(.00)	(.00)	$1\sigma^2 2\sigma^2 1\pi^4 3\sigma 4\sigma$	(.06)	
	$1\sigma^2 2\sigma^2 1\pi^4 10\sigma^2$	(.00)	(.00)	$1\sigma^2 2\sigma^2 1\pi^4 4\sigma^2$	(.17)	
$2^1\Sigma^+$	$1\sigma^2 2\sigma^2 3\sigma 1\pi^4 4\sigma$	--	(.23)	$1\sigma^2 2\sigma^2 1\pi^4 3\sigma^2$	(.18)	
	$1\sigma^2 2\sigma^2 3\sigma 1\pi^4 6\sigma$	--	(.49)	$1\sigma^2 2\sigma^2 1\pi^4 3\sigma 4\sigma$	(.59)	
	$1\sigma^2 2\sigma^2 3\sigma 1\pi^4 7\sigma$	--	(.14)	$1\sigma^2 2\sigma^2 1\pi^4 4\sigma^2$	(.18)	
	$1\sigma^2 2\sigma^2 3\sigma 1\pi^4 8\sigma$	--	(.06)			
$3^1\Sigma^+$	$1\sigma^2 2\sigma^2 3\sigma^2 1\pi^3 2\pi$	(.34)	--			
	$1\sigma^2 2\sigma^2 3\sigma^2 1\pi^3 3\pi$	(.62)				
$1^1\pi$	$1\sigma^2 2\sigma^2 3\sigma^2 1\pi^3 4\sigma$	(.17)	(.14)			
	$1\sigma^2 2\sigma^2 3\sigma^2 1\pi^3 6\sigma$	(.38)	(.48)			
	$1\sigma^2 2\sigma^2 3\sigma^2 1\pi^3 7\sigma$	(.22)	(.10)			
	$1\sigma^2 2\sigma^2 3\sigma^2 1\pi^3 8\sigma$	(.17)	(.23)			

Table V-5 (continued)

State	Configuration and Weighting 1.732 bohr		2.3 bohr	4.0 bohr
$2^1\pi$	$1\sigma^2 2\sigma^2 3\sigma^2 1\pi^3 4\sigma$	(.02)	(.44)	
	$1\sigma^2 2\sigma^2 3\sigma^2 1\pi^3 6\sigma$	(.22)	(.01)	
	$1\sigma^2 2\sigma^2 3\sigma^2 1\pi^3 7\sigma$	(.55)	(.12)	
	$1\sigma^2 2\sigma^2 3\sigma^2 1\pi^3 8\sigma$	(.13)	(.35)	
$3^1\pi$	$1\sigma^2 2\sigma^2 3\sigma^2 1\pi^3 4\sigma$	(.72)	(.18)	
	$1\sigma^2 2\sigma^2 3\sigma^2 1\pi^3 6\sigma$	(.01)	(.04)	
	$1\sigma^2 2\sigma^2 3\sigma^2 1\pi^3 7\sigma$	(.12)	(.67)	
	$1\sigma^2 2\sigma^2 3\sigma^2 1\pi^3 8\sigma$	(.08)	(.01)	
$1^1\Delta$	$1\sigma^2 2\sigma^2 3\sigma^2 1\pi^3 2\pi$	(.30)	--	
	$1\sigma^2 2\sigma^2 3\sigma^2 1\pi^3 3\pi$	(.65)	--	

Table V-6

Calculated Ci Energy Points for HF^- -- 9 to 12 eV [a]

State	Internuclear Distance (bohr) 1.732	2.0	2.5	4.0
$6^2\Sigma^+$	--	8.811	10.324	--
$7^2\Sigma^+$	13.601	11.328	8.716	5.809
$8^2\Sigma^+$	11.887	11.258	9.379	6.362
$9^2\Sigma^+$	12.657	11.521	9.923	6.506

[a] Relative to HF at equilibrium, E = -2727.430.

Table V-7

Generating Bases for HF^- Potential Curves -- 9 to 12 eV

State	Configuration and Weighting (%) 1.732 bohr		2.5 bohr		4.0 bohr	
$6^2\Sigma^+$	--		$1\sigma^2 2\sigma^2 3\sigma^2 1\pi^4 9\sigma$	(.90)	--	
			$1\sigma^2 2\sigma^2 1\pi^4 6\sigma 9\sigma$	(.00)		
$7^2\Sigma^+$	$1\sigma^2 2\sigma^2 3\sigma^2 1\pi^3 4\sigma 2\pi$	(.48)	$1\sigma^2 2\sigma^2 3\sigma^2 1\pi^3 4\sigma 2\sigma$	(.54)	$1\sigma^2 2\sigma^2 1\pi^3 3\sigma^2 4\sigma 2\pi$	(.83)
	$1\sigma^2 2\sigma^2 3\sigma^2 1\pi^3 4\sigma 3\pi$	(.36)	$1\sigma^2 2\sigma^2 3\sigma^2 1\pi^3 4\sigma 3\sigma$	(.00)	$1\sigma^2 2\sigma^2 1\pi^3 3\sigma^2 4\sigma 3\pi$	(.00)
$8^2\Sigma^+$	$1\sigma^2 2\sigma^2 3\sigma^2 1\pi^3 4\sigma 2\pi$	(.59)	$1\sigma^2 2\sigma^2 3\sigma^2 1\pi^3 4\sigma 2\pi$	(.66)	$1\sigma^2 2\sigma^2 1\pi^3 3\sigma^2 4\sigma 2\pi$	(.86)
	$1\sigma^2 2\sigma^2 3\sigma^2 1\pi^3 4\sigma 2\pi$	(.15)	$1\sigma^2 2\sigma^2 3\sigma^2 1\pi^3 4\sigma 3\pi$	(.01)	$1\sigma^2 2\sigma^2 1\pi^3 3\sigma^2 4\sigma 3\pi$	(.01)
$9^2\Sigma^+$	$1\sigma^2 2\sigma^2 3\sigma 1\pi^4 4\sigma^2$	(.23)	$1\sigma^2 2\sigma^2 3\sigma 1\pi^4 4\sigma^2$	(.24)	$1\sigma^2 2\sigma^2 1\pi^4 3\sigma 4\sigma^2$	(.15)
	$1\sigma^2 2\sigma^2 3\sigma 1\pi^4 4\sigma 6\sigma$	(.32)	$1\sigma^2 2\sigma^2 3\sigma 1\pi^4 4\sigma 6\sigma$	(.34)	$1\sigma^2 2\sigma^2 1\pi^4 3\sigma 4\sigma 6\sigma$	(.45)
	$1\sigma^2 2\sigma^2 3\sigma 1\pi^4 4\sigma 7\sigma$	(.22)	$1\sigma^2 2\sigma^2 3\sigma 1\pi^4 4\sigma 7\sigma$	(.06)	$1\sigma^2 2\sigma^2 1\pi^4 3\sigma 4\sigma 7\sigma$	(.00)
	$1\sigma^2 2\sigma^2 3\sigma 1\pi^4 4\sigma 8\sigma$	(.20)	$1\sigma^2 2\sigma^2 3\sigma 1\pi^4 4\sigma 8\sigma$	(.12)	$1\sigma^2 2\sigma^2 1\pi^4 3\sigma 4\sigma 9\sigma$	(.00)

Table V-8

Calculated CI Energy Points for HF^- -- 12 to 14 eV [a]

State	Internuclear Distance (bohr) 1.732	2.0	2.5
$HF^- 5^2\pi$	13.418	13.016	12.642
$HF^- 6^2\pi$	14.203	12.795	14.722
$HF^- 7^2\pi$	14.498	13.229	11.994

[a] Relative to HF at equilibrium, E = -2727.430 eV.

Table V-9

Generating Bases for HF^- Potential Curves -- 12 to 14 eV

State	Configuration and Weighting (%) 1.732 bohr		2.5 bohr	
$5^2\pi$	$1\sigma^2 2\sigma^2 3\sigma^2 1\pi^3 4\sigma^2$	(.59)	$1\sigma^2 2\sigma^2 3\sigma^2 1\pi^3 4\sigma^2$	(.34)
	$1\sigma^2 2\sigma^2 3\sigma^2 1\pi^3 4\sigma 6\sigma$	(.09)	$1\sigma^2 2\sigma^2 3\sigma^2 1\pi^3 4\sigma 6\sigma$	(.10)
	$1\sigma^2 2\sigma^2 3\sigma^2 1\pi^3 4\sigma 7\sigma$	(.12)	$1\sigma^2 2\sigma^2 3\sigma^2 1\pi^3 4\sigma 7\sigma$	(.03)
	$1\sigma^2 2\sigma^2 3\sigma^2 1\pi^3 4\sigma 8\sigma$	(.00)	$1\sigma^2 2\sigma^2 3\sigma^2 1\pi^3 4\sigma 8\sigma$	(.45)
$6^2\pi$	$1\sigma^2 2\sigma^2 3\sigma^2 1\pi^3 4\sigma^2$	(.09)	$1\sigma^2 2\sigma^2 3\sigma^2 1\pi^3 4\sigma^2$	(.06)
	$1\sigma^2 2\sigma^2 3\sigma^2 1\pi^3 4\sigma 6\sigma$	(.10)	$1\sigma^2 2\sigma^2 3\sigma^2 1\pi^3 4\sigma 6\sigma$	(.18)
	$1\sigma^2 2\sigma^2 3\sigma^2 1\pi^3 4\sigma 7\sigma$	(.01)	$1\sigma^2 2\sigma^2 3\sigma^2 1\pi^3 4\sigma 7\sigma$	(.02)
	$1\sigma^2 2\sigma^2 3\sigma^2 1\pi^3 4\sigma 8\sigma$	(.48)	$1\sigma^2 2\sigma^2 3\sigma^2 1\pi^3 4\sigma 8\sigma$	(.22)
$7^2\pi$	$1\sigma^2 2\sigma^2 3\sigma^2 1\pi^3 4\sigma^2$	(.01)	$1\sigma^2 2\sigma^2 3\sigma^2 1\pi^3 4\sigma^2$	(.00)
	$1\sigma^2 2\sigma^2 3\sigma^2 1\pi^3 4\sigma 6\sigma$	(.14)	$1\sigma^2 2\sigma^2 3\sigma^2 1\pi^3 4\sigma 6\sigma$	(.08)
	$1\sigma^2 2\sigma^2 3\sigma^2 1\pi^3 4\sigma 7\sigma$	(.00)	$1\sigma^2 2\sigma^2 3\sigma^2 1\pi^3 4\sigma 7\sigma$	(.01)
	$1\sigma^2 2\sigma^2 3\sigma^2 1\pi^3 4\sigma 8\sigma$	(.72)	$1\sigma^2 2\sigma^2 3\sigma^2 1\pi^3 4\sigma 8\sigma$	(.56)

Table V-10

Energy and Configuration Weighting of the $5^2\pi$ HF^- State and the $3^1\pi$ HF State

State	Configuration	Configuration Weighting		
		1.732 bohr	2.0 bohr	2.5 bohr
HF^- $5^2\pi$	$1\sigma^2 2\sigma^2 3\sigma^2 1\pi^3 4\sigma^2$	-0.77	-0.60	-0.58
	$1\sigma^2 2\sigma^2 3\sigma^2 1\pi^3 4\sigma 5\sigma$	-0.05	-0.18	-0.00
		-0.13	-0.04	+0.01
	$1\sigma^2 2\sigma^2 3\sigma^2 1\pi^3 4\sigma 6\sigma$	-0.14	+0.28	-0.13
		-0.26	+0.01	-0.28
	$1\sigma^2 2\sigma^2 3\sigma^2 1\pi^3 4\sigma 7\sigma$	+0.17	+0.11	+0.10
		+0.31	+0.16	+0.13
	$1\sigma^2 2\sigma^2 3\sigma^2 1\pi^3 4\sigma 8\sigma$	-0.01	-0.50	-0.36
		+0.01	-0.26	-0.56
		(13.418 eV)	(13.016 eV)	(12.642 eV)

Table V-10 (continued)

State	Configuration	Configuration Weighting		
		1.732 bohr	2.0 bohr	2.5 bohr
HF $3^1\pi$	$1\sigma^2 2\sigma^2 3\sigma^2 1\pi^3 4\sigma$	-0.85	-0.61	-0.43
	$1\sigma^2 2\sigma^2 3\sigma^2 1\pi^3 5\sigma$	+0.01	-0.14	-0.21
	$1\sigma^2 2\sigma^2 3\sigma^2 1\pi^3 6\sigma$	+0.09	-0.24	-0.21
	$1\sigma^2 2\sigma^2 3\sigma^2 1\pi^3 7\sigma$	-0.35	-0.68	-0.82
	$1\sigma^2 2\sigma^2 3\sigma^2 1\pi^3 8\sigma$	+0.29	+0.21	+0.08
		(14.220 eV)	(13.961 eV)	(14.411 eV)

Table V-11

Energy and Configuration Weighting of the 4 and 5 $^2\pi$ HF^- States and the $5^1\pi$ HF State

State	Configuration	Configuration Weighting		
		1.732 bohr	2.0 bohr	2.5 bohr
HF^- $6^2\pi$	$1\sigma^2 2\sigma^2 3\sigma^2 1\pi^3 4\sigma^2$	+0.30	-0.40	-0.24
	$1\sigma^2 2\sigma^2 3\sigma^2 1\pi^3 4\sigma 5\sigma$	-0.00	-0.12	+0.04
		-0.02	-0.04	-0.15
	$1\sigma^2 2\sigma^2 3\sigma^2 1\pi^3 4\sigma 6\sigma$	-0.26	-0.28	-0.16
		-0.18	-0.33	-0.39
	$1\sigma^2 2\sigma^2 3\sigma^2 1\pi^3 4\sigma 7\sigma$	-0.04	+0.13	-0.07
		-0.10	+0.13	+0.13
	$1\sigma^2 2\sigma^2 3\sigma^2 1\pi^3 4\sigma 8\sigma$	+0.49	+0.25	+0.27
		+0.48	+0.19	+0.38
	$1\sigma^2 2\sigma^2 3\sigma^2 1\pi^3 6\sigma^2$	+0.39	+0.47	+0.53
	$1\sigma^2 2\sigma^2 3\sigma^2 1\pi^3 6\sigma 7\sigma$	+0.15	+0.19	+0.25
		+0.25	+0.32	+0.05
		(14.203 eV)	(12.795 eV)	(14.722 eV)

Table V-11 (continued)

State	Configuration	Configuration Weighting		
		1.732 bohr	2.0 bohr	2.5 bohr
HF^- $7^2\pi$	$1\sigma^2 2\sigma^2 3\sigma^2 1\pi^3 4\sigma^2$	+0.09	+0.32	+0.03
	$1\sigma^2 2\sigma^2 3\sigma^2 1\pi^3 4\sigma 5\sigma$	-0.07	-0.10	-0.17
		+0.02	+0.05	+0.03
	$1\sigma^2 2\sigma^2 3\sigma^2 1\pi^3 4\sigma 6\sigma$	+0.33	+0.33	+0.27
		-0.19	-0.23	-0.09
	$1\sigma^2 2\sigma^2 3\sigma^2 1\pi^3 4\sigma 7\sigma$	-0.05	-0.09	-0.08
		-0.00	-0.03	+0.03
	$1\sigma^2 2\sigma^2 3\sigma^2 1\pi^3 4\sigma 8\sigma$	-0.66	-0.45	-0.65
		+0.54	+0.57	+0.38
		(14.498 eV)	(13.229 eV)	(11.994 eV)

Table V-11 (continued)

State	Configuration	Configuration Weighting		
		1.732 bohr	2.0 bohr	2.5 bohr
HF $5^1\pi$	$1\sigma^2 2\sigma^2 3\sigma^2 1\pi^3 4\sigma$	-0.18	-0.35	-0.42
	$1\sigma^2 2\sigma^2 3\sigma^2 1\pi^3 5\sigma$	+0.13	+0.09	+0.09
	$1\sigma^2 2\sigma^2 3\sigma^2 1\pi^3 6\sigma$	+0.59	+0.66	+0.65
	$1\sigma^2 2\sigma^2 3\sigma^2 1\pi^3 7\sigma$	-0.09	-0.13	-0.03
	$1\sigma^2 2\sigma^2 3\sigma^2 1\pi^3 8\sigma$	-0.74	-0.61	-0.58
		(15.693 eV)	(14.933 eV)	(15.086 eV)

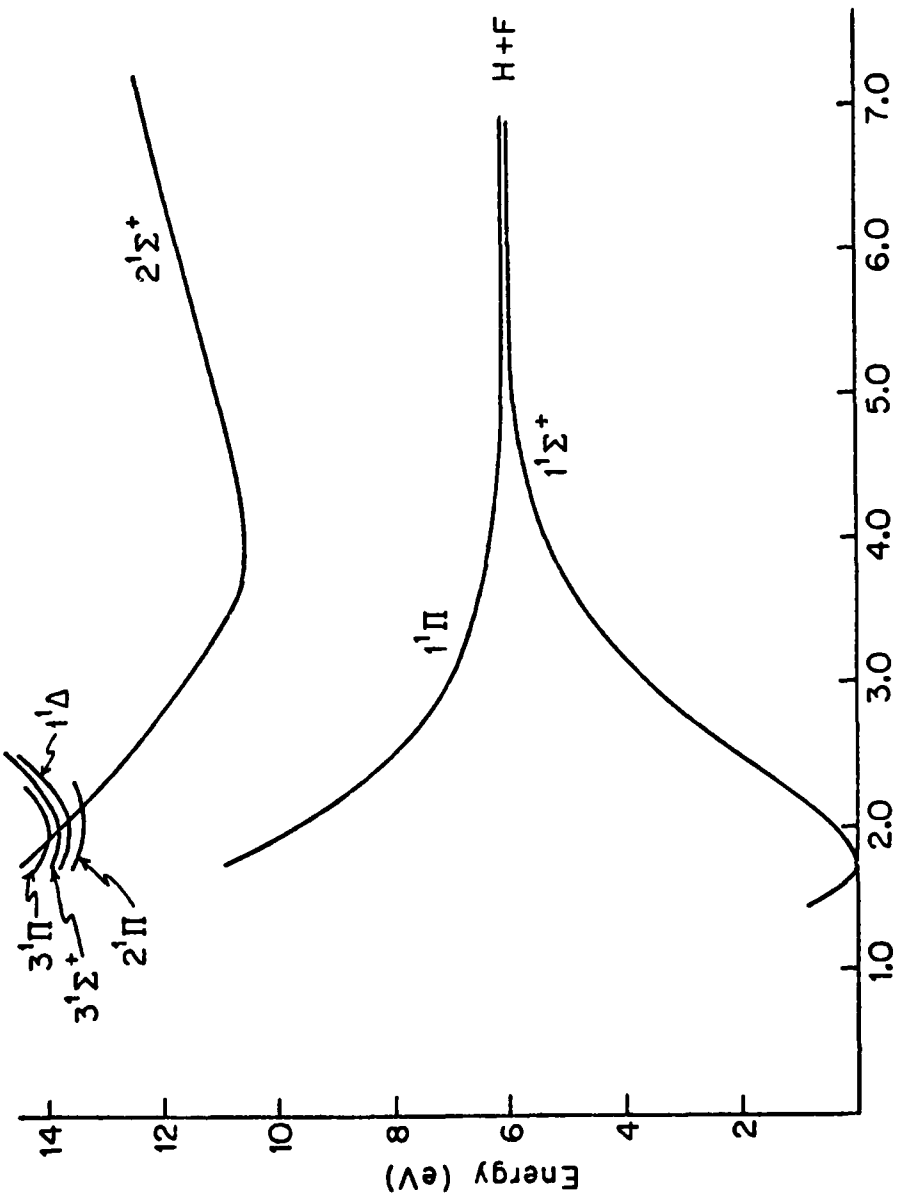

Fig. V-1--Calculated Potential Energy Curves for HF

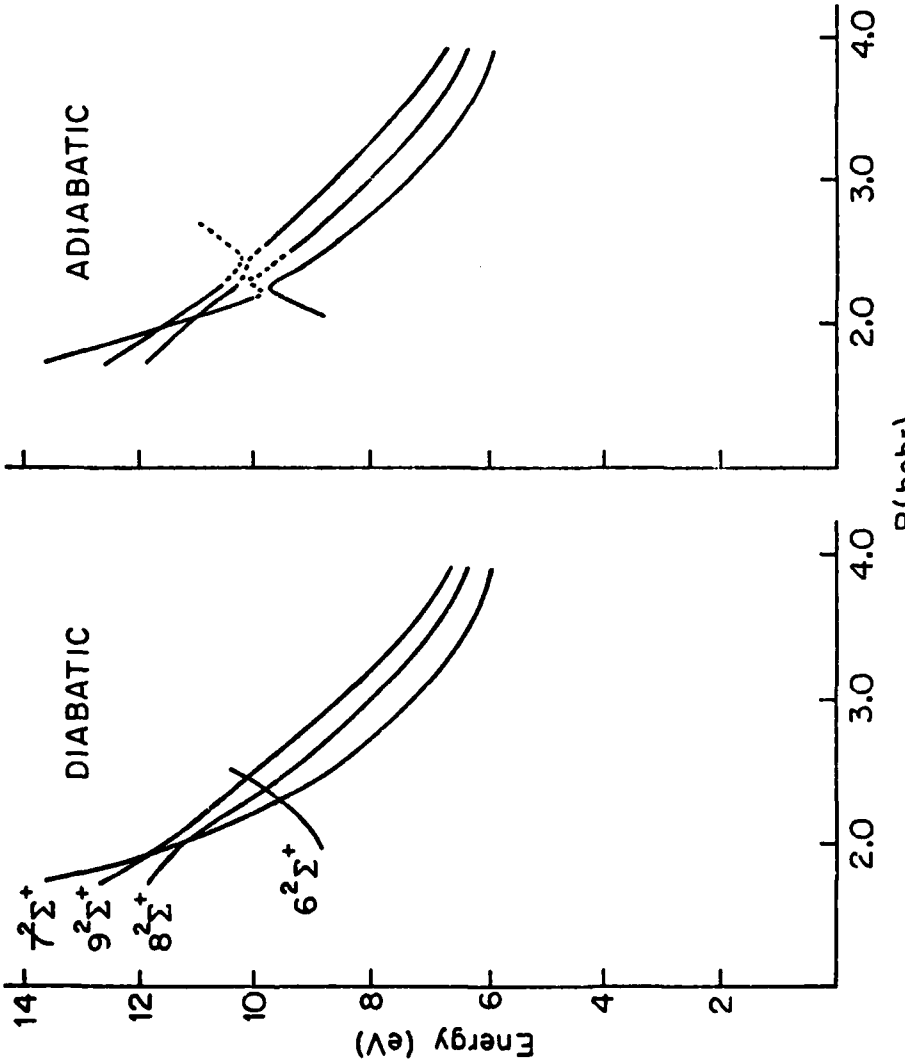

Fig. V-2--Calculated Potential Energy Curves for HF^- -- 9 to 12 eV

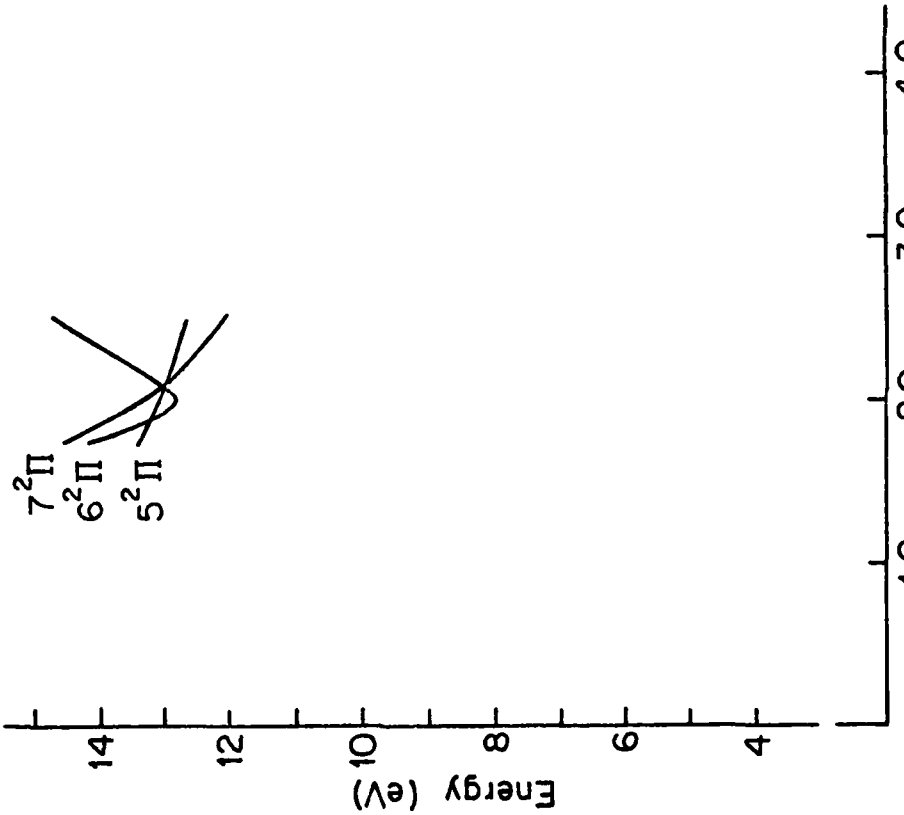

Fig. V-3--Calculated Potential Energy Curves for HF^- -- 12 to 14 eV


D
FI
2